

**Cyanide volatilisation
from
gold leaching operations
and
tailing storage facilities**

by

Nadia Lötter

submitted in fulfilment of the requirements of the degree

Master of Metallurgical Engineering

in the

**Faculty of Engineering, Built Environment and
Information Technology**

University of Pretoria

Pretoria

Republic of South Africa

November 2005

Summary

SUMMARY

In recent years, emissions of hydrogen cyanide from metallurgical operations have received renewed attention by legislative bodies, leading to the need for a reliable quantification method for HCN volatilisation. Subsequently, the purpose of this project, launched by AngloGold Ashanti Ltd. and in collaboration with MINTEK and the University of Pretoria, was to develop a prediction model for cyanide volatilisation from plant operations and tailings storage facilities in South Africa.

The study was done in four stages, the first being a laboratory study of the equilibrium behaviour of hydrogen cyanide. Henry's Law constant (k_H) was determined at different solution cyanide concentrations, salinities and temperatures. A value for k_H was established at 0.082 atm.L/mol, which was found to be independent on the solution cyanide concentration between 10 and 200 ppm cyanide. In addition, the effect of temperature on k_H was found to be negligible at solution temperatures between 20 and 35°C. It was also concluded that high salinities increase k_H and promote volatilisation, but this effect was negligible at the typical salinity levels found in South African process water.

The second stage entailed a detailed study of the mass transfer coefficient, K_{OL} , for hydrogen cyanide from cyanide solutions and pulp mixtures, both in the laboratory and on-site. It followed from this investigation that the most important parameters affecting K_{OL} are the $HCN_{(aq)}$ concentration in the liquid, the wind velocity across the solution or pulp surface, expressed in terms of a Roughness Reynolds number, Re^* , and the moisture content, or solid to liquid ratio, of the pulp. Furthermore, it was concluded that K_{OL} is highly sensitive to $HCN_{(aq)}$ concentrations at low concentrations, while it becomes rather insensitive to $HCN_{(aq)}$ at concentrations above 20 ppm $HCN_{(aq)}$.

The data generated by the laboratory and on-site test work was incorporated into the development of an empirical prediction model, based on the Roughness Reynolds number (Re^*), moisture content (M), and aqueous cyanide concentration ($HCN_{(aq)}$) which may be described by the following equation:

Summary

$$K_{OL} = a Re^{*b} M^c HCN_{(aq)}^d + e$$

The model coefficients were subsequently determined for application of the model to leach tanks, adsorption tanks, tailing storage facility surfaces and return water dams. The calculated model predictions for K_{OL} were in excellent agreement with the measured test work data.

Finally, the prediction model was validated at the leach and adsorption sections of a selected gold plant and a selected tailings storage facility. The model predicted that 9% of the cyanide lost in the leach and adsorption section could be attributed to HCN volatilisation. As for the tailings storage facility, the model assigned 63% of the cyanide lost from the tailings storage facility to HCN volatilisation, of which 95% occurred from the area on the tailings dam surface covered in a thin liquid film.

It is recommended that the current methods available for the determination of $HCN_{(aq)}$ be further improved, due to the sensitivity of the model to the input value of the $HCN_{(aq)}$ concentration, in order to ensure that reliable predictions are made. It is also suggested that additional validation work be done in order to establish the generic applicability of the model to different sites.

Contents

TABLE OF CONTENTS

1. INTRODUCTION	1
2. GOLD EXTRACTIVE METALLURGY	3
2.1 Cyanide in gold processing	3
2.2 Tailings storage facilities	5
2.3 Focus areas of study	6
3. CYANIDE AS REAGENT	7
3.1 History and use of cyanide	7
3.3 Cyanide toxicity	8
3.4 Cyanide management	10
3.4.1 Public perception	10
3.4.2 Process economics	11
3.4.3 Environmental performance	12
3.4.4 Cyanide legislation	13
4. ENVIRONMENTAL FATE	15
4.1 Attenuation mechanisms	15
4.1.1 Volatilisation	15
4.1.2 Ultraviolet degradation (photolysis)	19
4.1.3 Base metal complexation	20
4.1.4 Precipitation	20
4.1.5 Adsorption	21
4.1.6 Oxidation	21
4.1.7 Thiocyanate formation	22
4.1.8 Formation of ammonium formate	22
4.1.9 Bacterial metabolisation	22
4.2 Conclusion	23
5. PROPERTIES AND VOLATILISATION OF HCN	24

Contents

5.1 Chemical and physical constants of HCN	24
5.1.1 Dissociation constant (pK_A) of HCN	24
5.1.2 Henry's constant (k_H)	26
5.2 Volatilisation mass transfer	30
5.2.1 Theoretical models	30
5.2.2 Mass transfer coefficients	35
5.3 Current status of HCN volatilisation estimation methods	46
5.3.1 Step degradation model	47
5.3.2 Roughness Reynolds number model	51
5.3.3 Re-aeration constant model	54
5.3.4 AMIRA models	55
6. PROJECT OBJECTIVES AND SCOPE	59
6.1 Equilibrium study – Henry's Law constant	59
6.2 Volatilisation rate investigation – Mass transfer coefficients	60
6.3 Conceptual Model development	61
6.4 On-site model verification	63
7. EXPERIMENTAL METHODS	64
7.1 Equilibrium test work	64
7.2 Wind tunnel test work	66
7.2.1 Mass transfer coefficient measurements	66
7.3 On-site test work	69
7.3.1 Leach vessel test station	69
7.3.2 Tailings storage facility test stations	71
7.3.3 Sampling methods	72
7.3.4 Surface area estimations	73
8. RESULTS AND DISCUSSION	74
8.1 Equilibrium test work	74
8.2 Wind tunnel test work	81

Contents

8.3 On-site test work	89
8.4 Model development	97
8.5 Model verification	102
9. CONCLUSIONS	110
9.1 Laboratory equilibrium test work	110
9.2 Wind tunnel test work	110
9.3 On-site test work	111
9.4 Model development	113
9.5 Model verification	113
10. RECOMMENDATIONS FOR FUTURE WORK	115
11. REFERENCES	116
12. BIBLIOGRAPHY	120
APPENDIX A – GOLD EXTRACTION PROCESS SUMMARY	122
APPENDIX B – MINTEK CYANIDE SPECIATION APPROACH	131
APPENDIX C – SOLID EXTRACTION STANDARD OPERATING PROCEDURE	133
APPENDIX D – EQUILIBRIUM TEST WORK SUMMARY	138
APPENBIX D – WIND TUNNEL TEST WORK SUMMARY	139
APPENDIX E – SITE TEST WORK SUMMARY	143
APPENDIX F – TAILINGS STORAGE FACILITY GEOGRAPHICAL INFORMATION AND DATA	151

Contents

LIST OF FIGURES

Figure 2.1. Generic flow sheet for gold extraction from ores using aqueous cyanide as lixiviant.	4
Figure 3.1. International use of hydrogen cyanide (www.cyantists.com , 2005).	8
Figure 3.2. Four driving forces for sound cyanide waste management (AMIRA, 1997).	11
Figure 3.3. Legislation for aquatic cyanide in South Africa (www.cyanidecode.org , 2000).	13
Figure 4.1. Attenuation mechanisms for tailing storage facilities (Smith and Mudder, 1990).	16
Figure 4.2. Hydrogen cyanide dissociation curve at 25°C (AMIRA, 1977).	17
Figure 5.1. Dependence of pK_A of HCN on temperature at low salinity (Verhoef et al, 1990).	25
Figure 5.2. pK_A dependence on salinity at 25°C ($I \rightarrow 0$) (AMIRA, 1997).	25
Figure 5.3. Temperature dependence of Henry's Law constant.	28
Figure 5.4. Chemical mass transfer from a stratified lake.	31
Figure 5.5. The two-film model for mass transfer from a water body to the atmosphere.	32
Figure 5.6. Derivation of the two-film model (adapted from Thomas, 1982).	33
Figure 5.6. (continued) Derivation of the two-film model (adapted from Thomas, 1982).	34
Figure 5.7. Temperature dependence of HCN rate constant (k_v) (Broderius and Smith, 1980).	37
Figure 5.8. Effect of rate of aeration on mass transfer rate constant at 29°C (Dodge and Zabban, 1952).	39
Figure 5.9. Effect of activated carbon on the rate of cyanide loss at 20°C (Adams, 1990 a,b).	44
Figure 5.10. HCN volatilisation as a function of total cyanide for different ore types for initial total cyanide in tailings as NaCN: oxide and transition ore 200 ppm; sulphide ore 650 ppm) (Rubo et al, 2000).	45
Figure 5.11. Schematic illustration of conceptual cyanide degradation model for single metal cyanide complex solution (Simovec and Snodgrass, 1985).	47
Figure 5.12. Summary of wind stress coefficient formulas and formulas adopted from Wu (1969).	53

Contents

Figure 6.1. Schematic of adapted conceptual model indicating the individual modules in CN Balance project.	62
Figure 7.1. Experimental set-up used in equilibrium test work.....	64
Figure 7.2. Photo of experimental set-up used in equilibrium test work.....	65
Figure 7.3. Wind tunnel apparatus used to measure mass transfer coefficients.	66
Figure 7.4. Photo of wind tunnel apparatus used to measure mass transfer coefficients.	67
Figure 7.5. Set-up of leach vessel test station.	70
Figure 7.6. Set-up of tailings surface test station.	71
Figure 7.7. Photo of tailings surface test station set-up.....	72
Figure 8.1. Measurement of $\text{HCN}_{(g)}$ evolved from a cyanide solution containing 105 mg/L cyanide as a function of pH (20°C , $\text{S}\rightarrow 0$).	74
Figure 8.2. $\text{HCN}_{(g)}$ as a function of pH at different cyanide concentrations (20°C , $\text{S}\rightarrow 0$).	75
Figure 8.3. Equilibrium distribution of HCN between water and air for different cyanide solution concentrations (20°C , $\text{S}\rightarrow 0$).	76
Figure 8.4. Best graphical trend line fit for pure cyanide solution tests (20°C , $\text{S}\rightarrow 0$). ..	77
Figure 8.5. Salinity tests with added NaCl and CaCl_2 (20°C).	78
Figure 8.6. Effect of salinity on k_H with added NaCl or CaCl_2 (20°C).	78
Figure 8.7. Effect of temperature on k_H at various cyanide concentrations ($\text{S}\rightarrow 0$). ..	79
Figure 8.8. Temperature dependence of k_H for 10 ppm aqueous solutions and data from the literature.	80
Figure 8.9. Velocity profile measurements inside the wind tunnel.	82
Figure 8.10. Mass transfer coefficient (K_{OL}) as a function of $\text{HCN}_{(aq)}$ concentration.	82
Figure 8.11. Correlation for K_{OL} as a function of $\text{HCN}_{(aq)}$ under flow conditions.	83
Figure 8.12. Mass transfer coefficient correlations for flowing solutions at 20°C , 35°C and 5 cm depth.	86
Figure 8.13. Mass transfer coefficient for stagnant trough solutions compared to correlation for flowing solutions.	87
Figure 8.14. Power fit correlation for mass transfer coefficient of stagnant solutions.	87
Figure 8.15. Pulp experiments at different solid to liquid ratios.	88
Figure 8.16. Measured effects of moisture content on K_{OL} (tailings storage facilities).	90
Figure 8.17. Mass transfer coefficients as a function of $\text{HCN}_{(aq)}$ concentration for different tailings surface moisture contents.	91

Contents

Figure 8.18. Measurements of $\text{HCN}_{(g)}$ evolved from different leach tanks at various airflow velocities.....	93
Figure 8.19. Dependence of measured volatilisation rates from leach tanks on Re^*	95
Figure 8.20. Dependence of K_{OL} to Re^* for leach tank tests.....	96
Figure 8.21. Volatilisation prediction model coefficients determined for different scenarios.....	98
Figure 8.22. Measured mass transfer coefficients vs. empirical model predictions for flowing solution laboratory experiments.....	99
Figure 8.23. Measured mass transfer coefficients vs. empirical model predictions for stagnant solution laboratory experiments.....	100
Figure 8.24. Measured mass transfer coefficients vs. empirical model predictions for pulp laboratory experiments.....	100
Figure 8.25. Measured mass transfer coefficients vs. empirical model prediction for leach tank tests.....	101
Figure 8.26. Measured mass transfer coefficients vs. empirical model predictions for tailings storage facility surface tests.....	101
Figure 8.27. Stability constants used for metal complexes in the cyanide speciation model developed by MINTEK.....	103
Figure 8.28. Comparison of predicted HCN loss through volatilisation from tailings storage facilities to the calculated total cyanide loss determined from the mass balance (ISE method).....	104
Figure 8.29. Comparison of predicted HCN loss to volatilisation from tailings storage facilities to the calculated overall cyanide loss determined from the mass balance (MINTEK speciation model method).....	105
Figure 8.30. Comparison of predicted HCN loss from leach tanks to volatilisation to the calculated overall cyanide loss determined from the mass balance.....	107
Figure 8.31. Model predictions for HCN volatilisation from leach tanks compared to predictions made using the AMIRA model.....	108
Figure E-1. Cyanide speciation for tailings discharge stream sample predicted by MINTEK speciation model based on ISE cyanide measurements.....	144
Figure E-2. Cyanide speciation for tailings discharge stream sample predicted by MINTEK speciation model based on WAD cyanide measurements.....	145
Figure E-3. Cyanide speciation for decant pond sample predicted by MINTEK speciation model based on ISE cyanide measurements.....	146
Figure E-4. Cyanide speciation for decant pond sample predicted by MINTEK speciation model based on WAD cyanide measurements.....	147

Contents

Figure E-5. Cyanide speciation for return water dam sample predicted by MINTEK speciation model based on ISE cyanide measurements.	148
Figure E-6. Cyanide speciation for return water dam sample predicted by MINTEK speciation model based on WAD cyanide measurements.....	149
Figure F-1. Map of tailings storage facility used in TSF model validation.	151
Figure F-2. Location of global positioning system data points on TSF map.	152

Contents

LIST OF TABLES

Table 3.1. Human response to various HCN exposure limits (Chamber of Mines of South Africa, 2001).	10
Table 5.1. Summary of reported values for pK_A of HCN.	24
Table 5.2. Summary of Henry's Law constants reported in the literature.	27
Table 5.3 Summary of rate constants for HCN volatilisation.....	36
Table 5.4. Effect of stirring on the volatilisation rate (Lye et al, 2004).	40
Table 5.5. Estimated volatilisation mass transfer coefficients from metal complex solutions containing 200 mg/L cyanide (Simovec and Snodgrass, 1985).....	50
Table 5.6. $(k_V^0)_{env}$ determined for various water bodies (Smith et al, 1980).	55
Table 5.7. Modelling parameter established for AMIRA TSF model (NPI Emission Estimation Technique Manual for Gold Processing, 1999).	58
Table 8.1. Sensitivity analysis of K_{OL} for HCN to k_i and k_g	84
Table 8.2. Moisture content classification of different areas found on talings surfaces.	89
Table 8.3. Comparison of laboratory and on-site K_{OL} measurements with moisture.	92
Table 8.4. Prediction of volatilisation rates from leach tanks.	96
Table D-1. Glass plate tests at ambient temperature.....	139
Table D-2. Glass plate tests at 35°C.....	140
Table D-3. Flowing trough solution tests.....	141
Table E-1. Tailings storage facility surface tests.....	143
Table E-2: Leach tank tests	150

1. Introduction

1. INTRODUCTION

Cyanide is generated by a number of natural processes and organisms (Lorösch, 2001). In spite of this steady production of the highly toxic substance, a naturally occurring cyanide cycle prevents cyanide in the environment from reaching levels that present potential risks to health and the environment. Hydrogen cyanide present in the atmosphere is generally degraded by natural mechanisms such as bio-oxidation to form ammonia and bicarbonate.

However, cyanide is also produced synthetically and used as a reagent in various industries, including gold extraction, leading to increased emissions of cyanide to the environment. Many investigations have attempted to quantify the impact of cyanide emissions generated by processes and activities associated with the gold extraction industry. In general, it has been found that cyanide pollution and control remains controversial and that an improved understanding as to the fate of cyanide in metallurgical operations is needed.

Volatilisation is known to be one of the main attenuation mechanisms for cyanide from tailing storage facilities (Smith and Mudder, 1991; Lye et al, 2001). Despite the existence of a relatively good knowledge base for reactions of cyanide in the liquid phase, recent emphasis on air emissions of HCN by legislative bodies, especially the National Pollutant Inventory in Australia, has led to the need for better knowledge of the processes involved in this loss mechanism. In order to improve accounting of cyanide for control purposes and comply with the new codes and environmental standards, some uncertainties still need to be addressed regarding cyanide emissions, particularly through volatilisation.

Empirical data of HCN volatilisation from tailings dams are scarce and generic models are difficult to develop due to the site-specific nature of the process. Cyanide loss through volatilisation from open air leach tanks are currently being estimated by mass balancing in South Africa, which is not reliable enough to satisfy the requirements of gold companies or regulators.

Consequently, the aim of this project is to derive a means of predicting the cyanide volatilisation rate from pulp solutions in gold plant operations, given the conditions

1. Introduction

and various critical parameters, to within a reasonable accuracy. This tool will take the form of an empirical model that will be based on fundamental theories of mass transfer and combined with extensive experimental data. Ultimately, the aim is to validate the model using practical data from a number of selected sites in South Africa.

2. Gold extractive metallurgy

2. GOLD EXTRACTIVE METALLURGY

2.1 Cyanide in gold processing

In gold extraction, as is the case with the treatment of all ore minerals, the ultimate objective of the metallurgical process is to recover the valuable mineral from the ore gangue minerals in the purest possible form and at the highest possible profitability. Various process design options are available, and are currently in practice across the world. The optimal process design is normally a function of the ore mineralogy and grade.

In order to set the perspective for the discussions that will follow, a general overview will now be presented of the process flow in a typical gold cyanidation plant, a typical example of which is shown in Figure 2.1. Although the diagram captures the essential elements of the gold extraction process, various combinations of the units presented may be used in practice. A more detailed description of each unit operation is given in Appendix A.

The liberation of gold is achieved by size reduction of the ore received from the mines in order to expose the gold minerals from the waste rock, combined with classification and recirculation of the oversized material. The pulp may then undergo various preparation steps before leaching is commenced. During leaching, cyanide is added to the pulp, typically in the form of sodium or calcium cyanide. Potassium cyanide may also be used, but is more expensive and thus normally not economically viable. The gold is dissolved as the auro dicyanide complex, typically using oxygen as oxidant via an electrochemical reaction:



This reaction forms the basis of the cyanidation process. However, according to Lorösch (2001) gold dissolution typically consumes less than 1% of the cyanide added during gold leaching, and is therefore technically only a side reaction. This can be attributed to

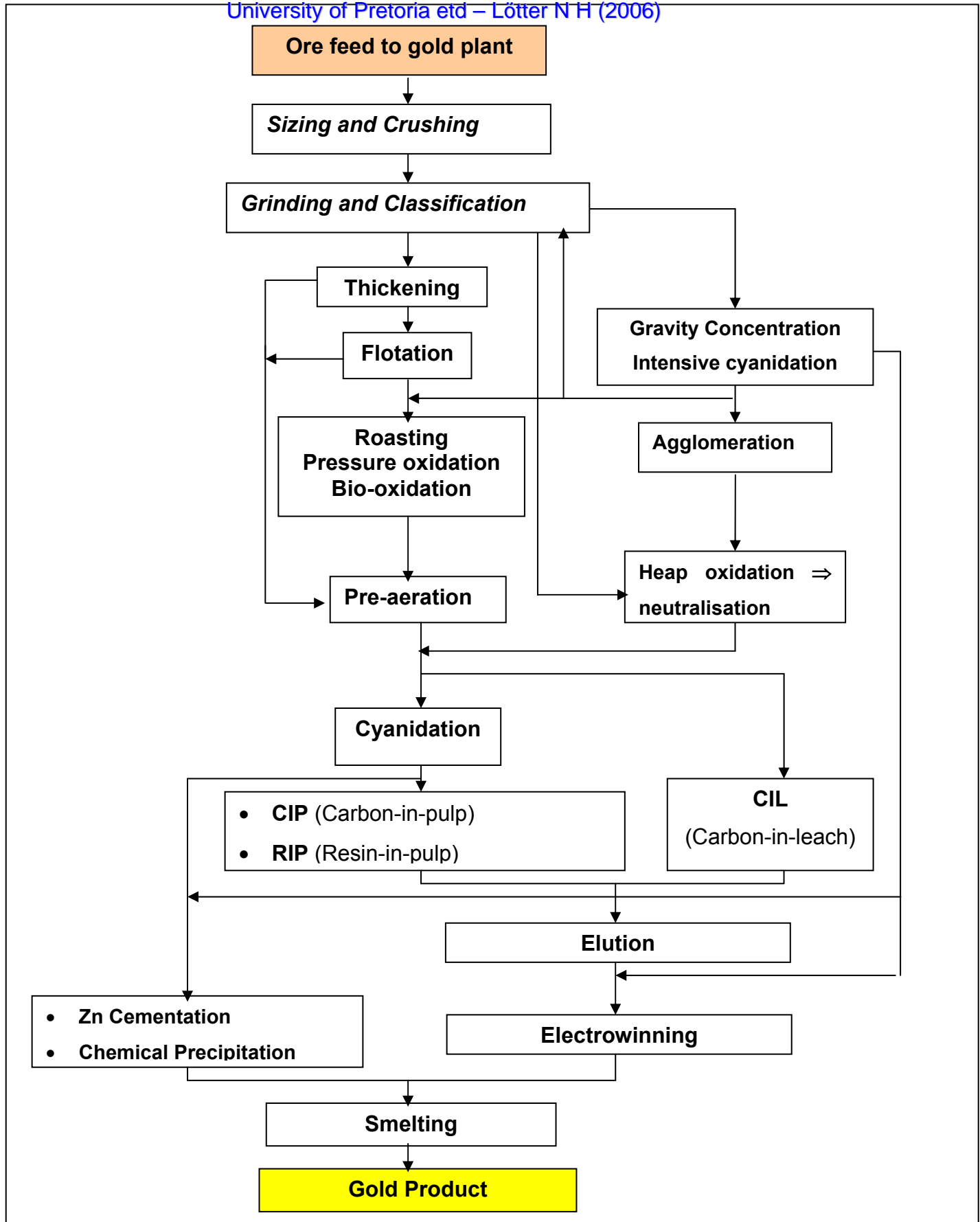


Figure 2.1. Generic flow sheet for gold extraction from ores using aqueous cyanide as lixiviant.

2. Gold extractive metallurgy

the fact that gold competes against other, more abundant metals such as copper, zinc, iron and cobalt for complexation with the available cyanide. The formation of metal ion complexes with metals other than gold and silver is especially significant in ores that contain large amounts of iron and cobalt, since six cyanide ions are consumed for every atom, leading to unavoidable high cyanide consumption in the leaching stage (Adams, 1990a). In addition, cyanide consumption is typically very high in bioleaching circuits, as the pulp often contains labile sulphur species, which readily react with cyanide necessitating high cyanide tenors in the leach. Excess cyanide is also typically maintained during leaching to sustain the rate of leaching at an acceptable level.

The leached gold is subsequently separated from the pulp and recovered from the pregnant solution by one of various precipitation methods. The solid gold precipitate is then smelted and cast into bars on the plant, after which it is refined to remove impurities present to produce fine gold.

2.2 Tailings storage facilities

Tailings storage facilities are used extensively to store tailings pumped from the plant operations, where natural attenuation mechanisms can aid in the reduction of cyanide levels. These include volatilisation, dilution through rainfall, biodegradation, oxidation, photolysis, adsorption onto solids and seepage through the sediments at the base of the impoundment.

The primary function of a tailings storage facility is the safe, long-term storage of process waste with minimal environmental or social impact, as well as the recovery of process water. The design is specific to the mining operation and site conditions (Mining, Minerals and Sustainable Development, 2002).

A return water dam collects and stores decanted water from the decant pond on the tailings dam prior to being pumped back to the plant. In addition, the return water dam serves several functions:

2. Gold extractive metallurgy

1. Collecting seepage recovered by the filter drains.
2. Permitting additional time for suspended solids in the decanted water to settle.
3. Providing reserve water supplies to the plant.
4. Collecting and contain storm runoff as required by the authorities.

High volumes of water is deposited onto the tailings dam every day, of which most is collected in the decant pond as runoff from the fines, excluding the amount that is lost to seepage and evaporation. The degree of evaporation is very dependent on the climatic and seasonal changes, and seepage will depend on the permeability of the tailing storage facility; however, the National Pollutant Inventory (1999) states that a figure of 10% may be used evaporation losses for reporting purposes in Australia.

In addition, rainfall also adds to the volume of water collected in the decant pool. It is important that the decant pond is kept sufficiently small to avoid excessive seepage and subsequent build up of the phreatic surface, which determines the stability of the dam, and should be kept as low as possible to avoid failure of the dam walls. Various designs of tailings dams may be employed, depending on the climatic conditions, as well as operational and design requirements.

2.3 Focus areas of study

From the overview of the gold extraction process that has just been covered, it is clear that cyanide is generally used as lixiviant for gold ore, and several processes may be used for leaching, one popular approach being cyanidation combined with carbon adsorption (CIP or CIL). From the plant operations, the barren pulp is discarded into a tailing storage facility, where the free cyanide concentration is typically significantly reduced by various processes, including losses through volatilisation to the atmosphere.

This study will focus on cyanide volatilisation from two sections in the gold circuit, namely:

1. Leaching vessels and carbon-in-pulp absorption tanks.
2. Tailing storage facilities, including the dry and wet beach areas, decant pond and return water dam.

3. Cyanide as reagent

3. CYANIDE AS REAGENT

Hydrogen cyanide is a colourless substance with a boiling point of 25.7°C (Huiatt et al, 1983; Chatwin and Trepanowski, 1987). It is infinitely soluble in water, but volatilises readily from solutions at ambient temperature due to its high vapour pressure (1 atm at 25.7°C). It is classified as a P-Class hazardous waste, which is the most regulated type of waste (Young and Jordan, 1995).

3.1 History and use of cyanide

Hydrogen cyanide was first discovered in 1782 when the Swedish chemist, Carl Scheele, succeeded in isolating HCN from the dye, Prussian Blue (Bunce and Hunt, 2004). Ironically, this brilliant chemist died four years later as a result of cyanide poisoning, when he accidentally broke a vial of the toxic HCN gas.

Since its discovery, hydrogen cyanide has been used in countless applications, of which some have been highly controversial. Cyanide is a toxic substance generally associated with death; its negative public perceptions date back to World War II, when the Nazis used a form of cyanide called Zyklon B in concentration camp gas chambers. It has also been alleged that Iraqi forces used cyanide in their attacks against Kurdish civilians during the 1980's. In the United States, cyanide has been used for years to enforce the death penalty.

Despite this general negative connotation, cyanide has become a vital element in industry today and the extraction of gold and silver, for one, would be not be economically viable in many cases, had it not been for advancements made in the cyanidation process.

For the last century, cyanide has been used as a lixiviant in the gold processing industry to extract the gold from liberated ores. Before the nineteenth century, no chemical methods for leaching gold from ores had yet been introduced to the extraction of gold, and miners relied on physical separation methods such as panning and sluices, and on

3. Cyanide as reagent

amalgamation. Then, in 1887, MacArthur and Forrest (Habashi, 1970) recognised the economic potential of gold cyanidation for specific application in the recovery of gold from low-grade ores. Their patent revolutionised the gold recovery process, and the same principle is still used today for gold recovery from ores.

According to a survey done in 2001 (www.cyantists.com), about three million tonnes of hydrogen cyanide is produced annually world-wide, of which about 8% is converted into sodium cyanide and used in the metals industries (mining and metal plating). The remaining 92% is used in various other industries, of which the nylon industry is the main consumer as shown in Figure 3.1.

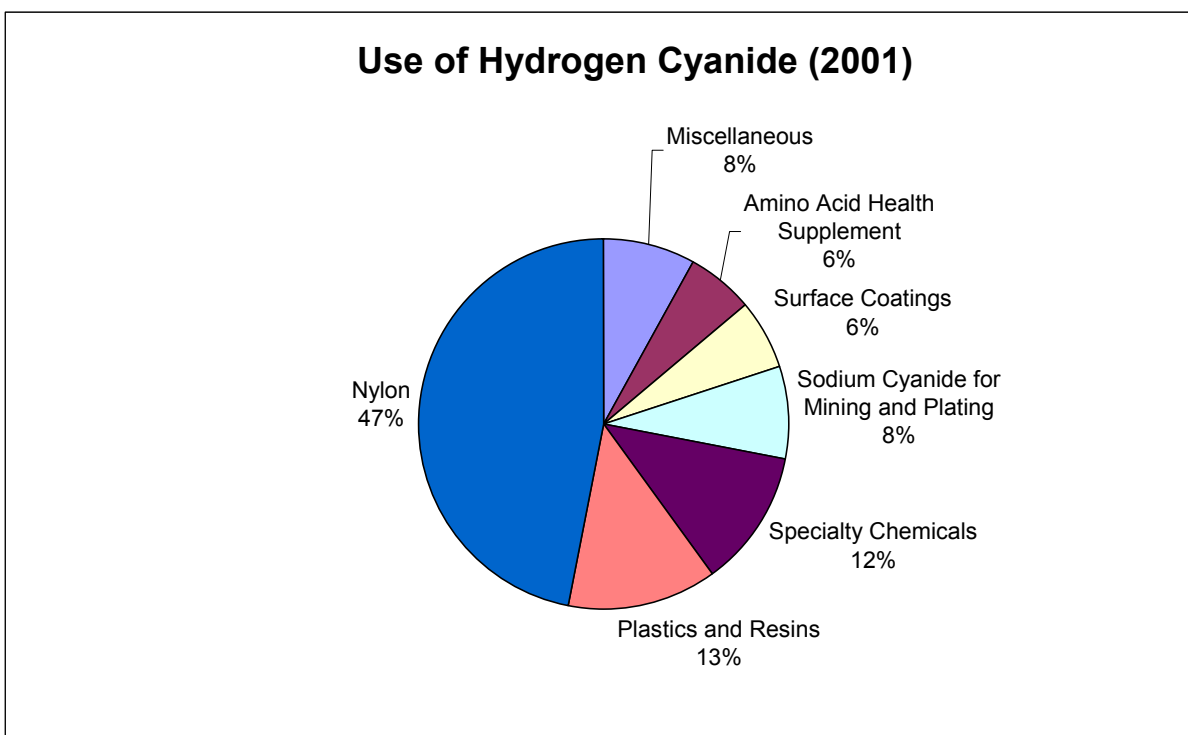


Figure 3.1. International use of hydrogen cyanide (www.cyantists.com, 2005).

3.3 Cyanide toxicity

A number of reviews have examined the toxicological effects of cyanide and its related compounds (Huiatt et al, 1983; AMIRA, 1997). Cyanide is known to be toxic to various species of invertebrates, fish, birds, mammals and humans.

3. Cyanide as reagent

The human body has a natural ability to detoxify small quantities of cyanide, and there is normally a small amount of cyanide and its breakdown products in the body resulting from everyday activities. These activities may include the metabolism of vitamin B12, eating foods that naturally contain cyanide (for example, almonds, lima beans, coffee and table salt), exposure to automobile exhaust gases and smoking cigarettes. In some form or other, humans are exposed to low levels of natural and manmade cyanide every day without risk to health or the environment (Huiatt et al, 1983).

However, cyanide is a toxic substance potentially lethal to mammals and humans. It can enter the body through inhalation, ingestion or adsorption through the skin, followed by adsorption into the blood stream, which distributes the cyanide through the body. Animal tissues have an enzyme called rhodanase which catalyses the conversion of cyanide to thiocyanate, which is then excreted in urine. Thus, cyanide poisoning in humans and animals occurs when these detoxification mechanisms are depleted by the uptake of high levels of cyanide. The hydrogen cyanide molecule inhibits the terminal respiratory enzyme cytochrome oxidase, resulting in respiratory failure of the tissue cells and loss of consciousness. This condition is called hypoxia, and is the ultimate cause of death.

The lethal toxicity of free cyanide for humans is 1-2 mg/kg and 0.028-2.295 mg/L for freshwater invertebrates (Huiatt et al, 1983). Acute exposure to low levels of hydrogen cyanide may cause a variety of symptoms in humans, including weakness, headache, nausea, increased rate of respiration and eye and skin irritation (U.S. Department of Health and Services, 1997). The Chamber of Mines of South Africa (2001) lists various responses of humans to cyanide exposure, as shown in Table 3.1.

In spite of its toxicity, cyanide is a non-persistent chemical that does not accumulate in man or animals, and there is no evidence that it bio-accumulates in ecosystems or the atmosphere (Huiatt et al, 1983).

3. Cyanide as reagent

Table 3.1. Human response to various HCN exposure limits (Chamber of Mines of South Africa, 2001).

HCN concentration in air [ppm]	Human response to exposure
270	Fatal
180	Fatal after 10 minute exposure
133	Fatal after 30 minute exposure
110-135	Fatal after 30 to 60 minute exposure
45-54	Tolerated for 30 to 60 minutes
18-36	Slight symptoms after several hours

3.4 Cyanide management

The four main driving forces for continual improvement of cyanide waste management are public perceptions, process economics, environmental performance, and legislation, as illustrated in Figure 3.4, adopted from AMIRA (1997).

3.4.1 Public perception

In recent years, there has been a growing concern among members of the gold mining industry with regard to cyanide management. The main root of these concerns has been the occurrence of several accidents and environmental incidents (most notably in Europe and Papua New Guinea) that have resulted in a new global debate about the hazards associated with the industrial use of cyanide. This has led to increasing pressure from environmental groups to implement more stringent cyanide controls. In particular, the stability of the cyanide present in large volumes in tailing storage facilities, as well as cyanide emissions across leaching operations, are issues of concern with respect to environmental impacts and health and safety issues, respectively.

3. Cyanide as reagent

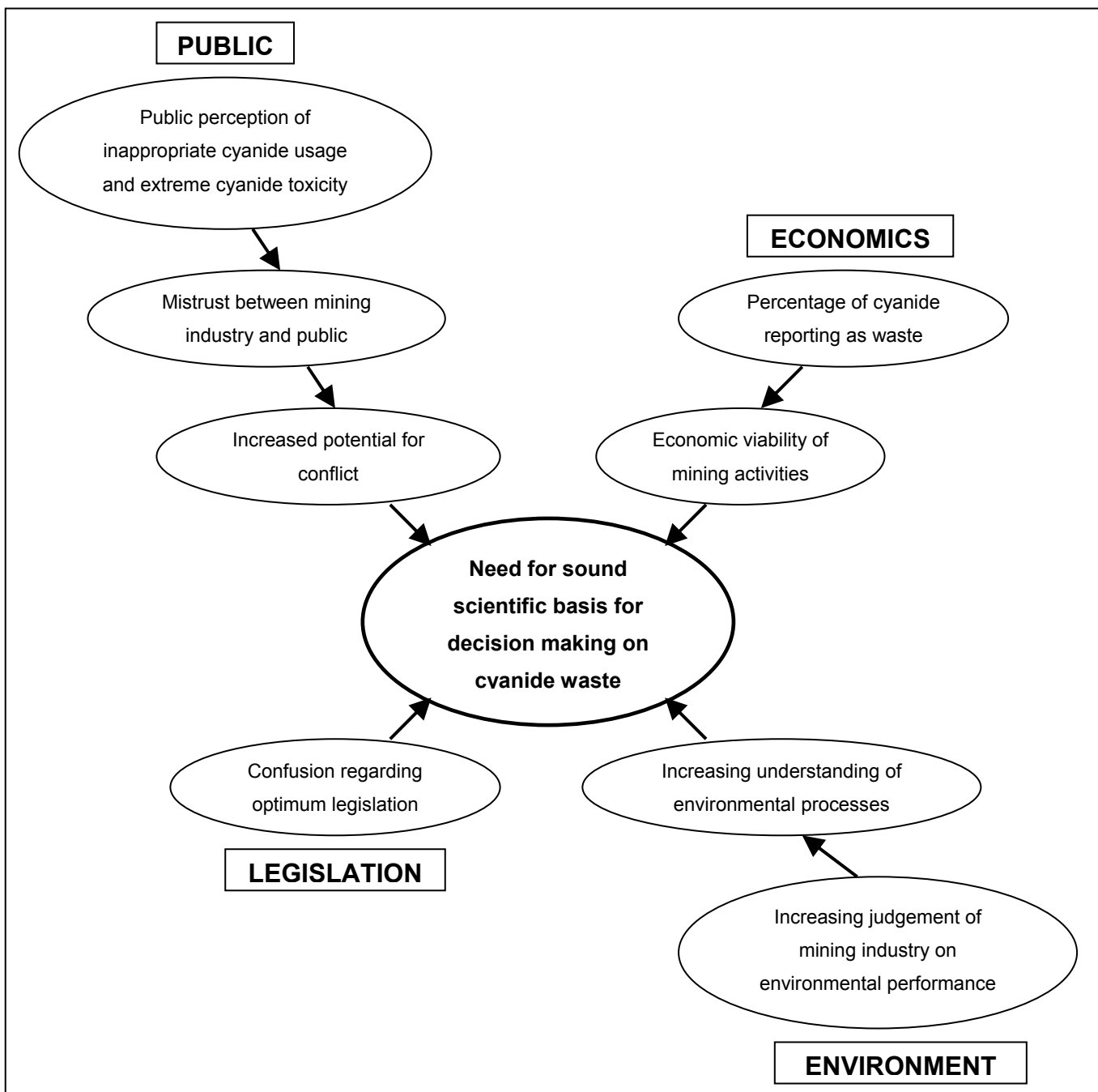


Figure 3.2. Four driving forces for sound cyanide waste management (AMIRA, 1997).

3.4.2 Process economics

From an economic standpoint, the costs attributed to sodium cyanide accounts for a significant portion of the total aboveground costs incurred during gold extraction

3. Cyanide as reagent

(Young and Jordan, 1995). One operational problem faced by the industry is that the majority of sodium cyanide added to the gold ore (typically 0.5 kg/ton) is consumed by unwanted side reactions, as mentioned before.

Continuous attempts have been made to improve cyanide control on gold processing plants; hence, accounting of cyanide has become an important management tool for balancing cyanide consumption and discharges quantitatively. The first step in effective cyanide control should be minimisation of cyanide consumption during leaching operations. This can be achieved to a degree by maintaining the pH at around 10.5 to prevent significant hydrogen cyanide loss by volatilization out of the pulp.

3.4.3 *Environmental performance*

In contrast to the desired situation on gold plants, cyanide volatilisation can be a useful attenuation mechanism for cyanide detoxification purposes across tailing storage facilities, provided the cyanide concentration levels are kept sufficiently low to avoid any potential risks to health or the environment. Due to the slow, continuous nature of volatilisation from an exposed surface such as a tailings dam, and the high diffusion rates of the HCN in air, this has been found to be the case in many studies conducted on atmospheric hydrogen cyanide emissions. Several monitoring surveys reported that no hazardous cyanide levels could be detected near these operations (Devries, 1996; Rubo et al, 2000).

Lye (2004) reviewed the atmospheric chemistry and fate of HCN and estimated the atmospheric concentration of HCN as 243 ± 118 parts per trillion. The global source of HCN was approximated as 1 Tg (N) per annum, resulting predominantly from biomass burning and industry outputs. The mining industry's contribution to this inventory was estimated at between 2.9 and 5.7 %, which could lead to a maximum contribution of 0.06% to the global NO_x gases. Thus, it is safe to assume that the atmospheric impact of hydrogen cyanide released from mining operations is negligible.

3. Cyanide as reagent

3.4.4 Cyanide legislation

Legislation for cyanide management has had a history of non-uniformity amongst countries, and this is currently still the case (Lye, 1999). Although soil contamination can occur through residues from tailings seepage, soil quality is rarely taken into account in legislation. Figure 3.7 represents the current legislation in place with regards to required maximum cyanide levels in aquatic systems in South Africa (Lotz and Wright, 2000).

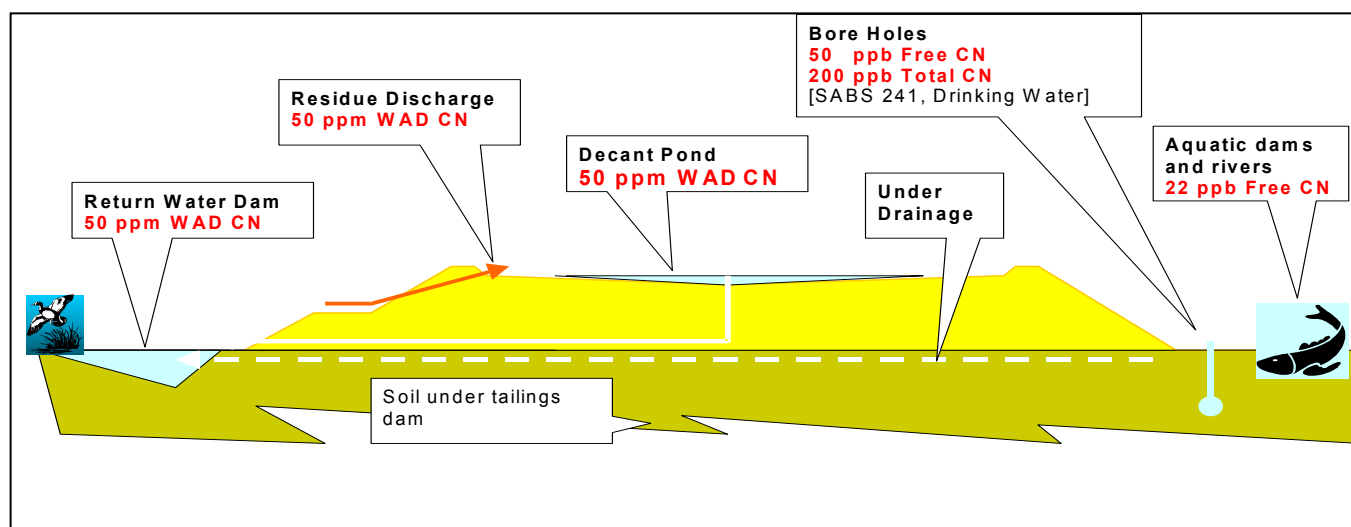


Figure 3.3. Legislation for aquatic cyanide in South Africa (www.cyanidecode.org, 2000).

In South Africa, atmospheric HCN emission monitoring is currently self-regulatory, with the emphasis on safety and health. The Occupational Safety and Health threshold limit value (TLV) for HCN in air is currently set at 10 ppm in South Africa and Australia. New requirements set by the Australian National Pollutant Inventory (NPI) for site personnel, to estimate and report annual cyanide emissions from plant operations as of 1 July 1998, has set a trend for more stringent cyanide control in Australia. At that time, no reliable prediction models were available and AMIRA (Australian Mining Industry Research Association) developed emission models that were implemented in 2002.

Therefore, although the South African government currently only requires reporting of cyanide releases into aqueous systems, it is imperative that a validated, operational system is in place for the prediction of atmospheric releases of cyanide, if and when

3. Cyanide as reagent

local HCN emission legislation is announced, to avoid the dilemma the Australian gold industry faced in 1998.

4. Environmental fate

4. ENVIRONMENTAL FATE

The rare occurrence of free cyanide in nature can be attributed to its high reactivity. The most important mechanisms of cyanide degradation, through interactions with elements in the environment, have been reviewed by various authors (Smith and Mudder, 1991; Huiatt et al, 1983; Lorösch, 2001; Mill, 1993). Figure 4.1 depicts the main attenuation mechanisms playing a role in tailing storage facilities, adapted from Smith and Mudder (1991).

In the following sections, the most relevant cyanide attenuation mechanisms will be discussed, representing a range of competing reactions or processes that often occur simultaneously, depending on the prevailing conditions. However, for the purposes of this particular study, volatilisation is the only loss mechanism that will be investigated and the effects of pulp chemistry, as well as the influence of these other attenuation mechanisms will not be considered in any detail. This section therefore only serves to provide the reader with a 'bird's eye view' of the various interrelated processes encountered in cyanide pulp systems.

4.1 Attenuation mechanisms

4.1.1 Volatilisation

Hydrogen cyanide is a weak acid, and dissociation of the HCN is described by equations 4.1 and 4.2 and by the dissociation curve shown in Figure 4.2.



$$K_A = \frac{[H^+][CN^-]}{[HCN]}, \quad pK_A = 9.21 \text{ at } 25^\circ\text{C} \quad [\text{Eq. 4.2}]$$

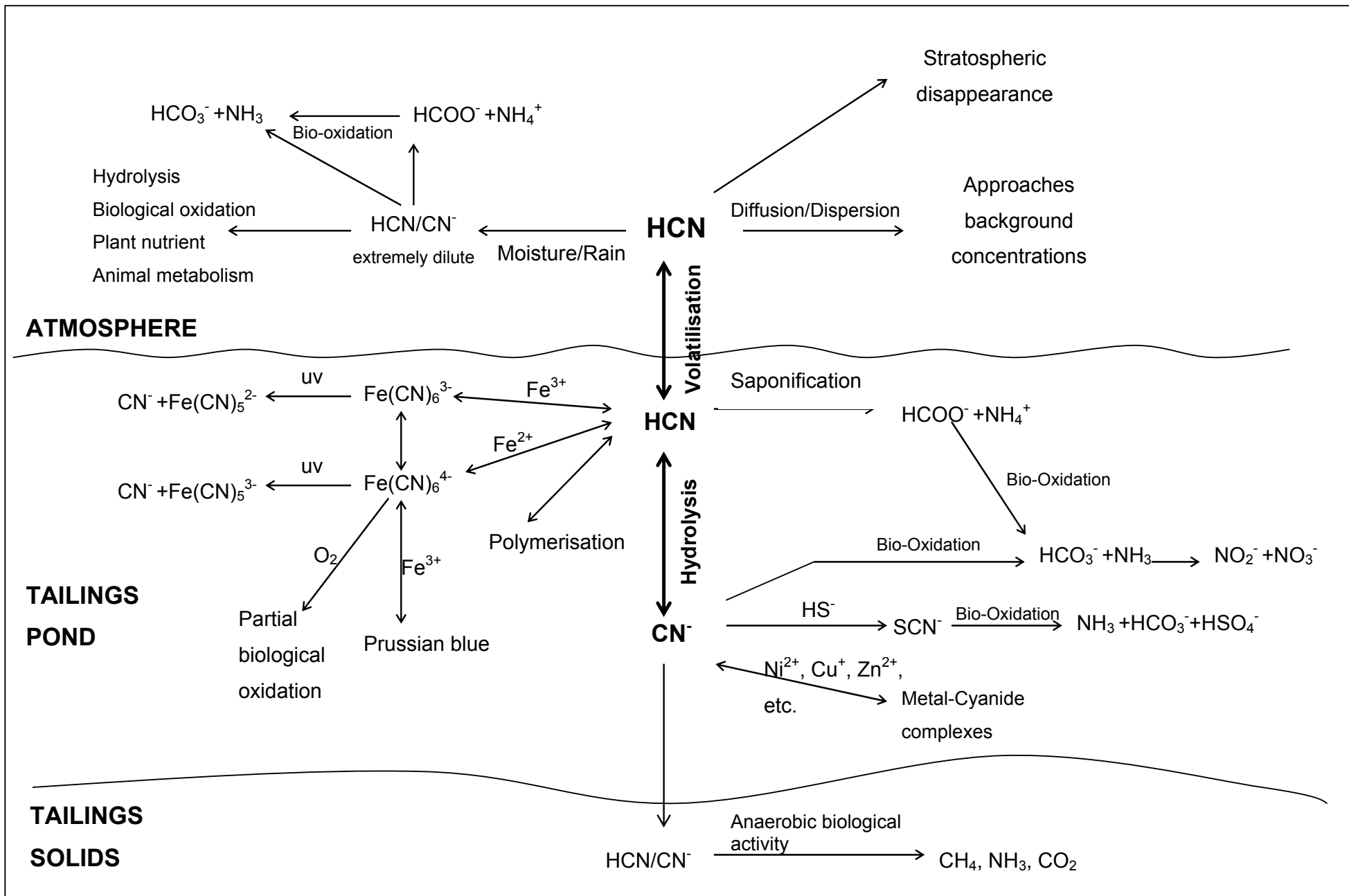


Figure 4.1. Attenuation mechanisms for tailing storage facilities (Smith and Mudder, 1990).

4 Environmental fate

It follows from Figure 4.2 that at a pH value equal to the pK_A value, 50% of the free cyanide in the system will be present as $HCN_{(aq)}$, while at a pH of approximately 7, almost all of the cyanide will be present as $HCN_{(aq)}$, and above 11, almost all the hydrogen cyanide will be dissociated.

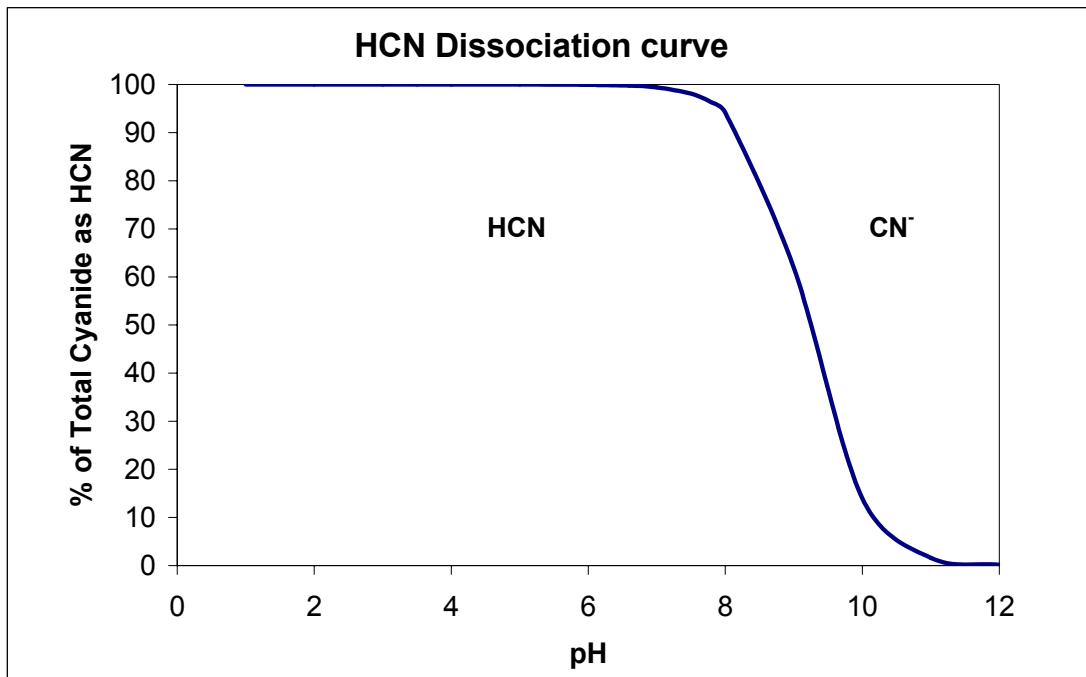


Figure 4.2. Hydrogen cyanide dissociation curve at 25°C (AMIRA, 1977).

As stated before, hydrogen cyanide is a volatile substance and the formation of aqueous HCN would promote volatilisation. The formed $HCN_{(aq)}$ is released to the air in the form of gaseous hydrogen cyanide ($HCN_{(g)}$).

Volatilisation is thus caused by the transfer of a substance (HCN) from an aqueous to a gaseous phase. Henry's Law is typically used to describe the equilibrium behaviour of such systems. Assuming an ideal gas mixture, Henry's Law states:

$$k_H = \lim_{x_{HCN} \rightarrow 0} \frac{P_{HCN_g}}{C_{HCN_{aq}}} \quad [\text{Eq. 4.3}]$$

where k_H = Henry's constant [atm.L/mol]

$P_{HCN(g)}$ = Partial pressure of HCN gas at equilibrium [atm]

4 Environmental fate

$C_{\text{HCN(aq)}}$ = Concentration of $\text{HCN}_{\text{(aq)}}$ at equilibrium [mol/L]

Consequently, Henry's law provides a useful way of predicting the volatility of HCN in a closed system through Henry's constant. However, the rate of volatilisation from a system open to the atmosphere is dependent on the concentration gradient of hydrogen cyanide over the mass transfer boundary layer as well as the value of the mass transfer coefficient, as shown in equation 4.4.

$$N''_{\text{HCN}} = k_{\text{OL}}(\Delta C) \quad [\text{Eq. 4.4}]$$

where N''_{HCN} = Flux of HCN [g/s.cm²]
 k_{OL} = Mass transfer coefficient [cm/s]
 ΔC = Hydrogen cyanide concentration gradient [g/cm³]

These parameters are discussed in more detail in Section 5. Volatilisation is often the main natural mechanism for cyanide attenuation in tailing storage facilities, due to the relatively rapid diffusion of hydrogen cyanide in the air, and the low pH of the tailing solution. Upon entering the tailing dams, the pulp pH is typically in the range of about 10 - 11, but with time the pH of the tailing solution drops significantly as a result of certain environmental interactions. These include dilution effects due to rainfall, which has a natural pH of 5-8 and can decrease the tailing solution pH down to < 9, oxidation of sulfur species and hydrolysis of metal species to generate acid, and carbon dioxide uptake from the air, forming carbonic acid and thus reducing the solution pH.

It is important to note that, although most of the factors affecting volatilisation from both the leach tanks and tailing dams are similar, the leaching conditions are well controlled, whereas conditions on the tailing dams are largely dependent on climatic conditions.

Volatilisation rates from leach tanks are generally low. At an operating pH of 10.5, Adams (1990a) has shown that approximately 6% of the total cyanide loss could be attributed to HCN volatilisation under typical leaching conditions. The CSIRO measured HCN emissions from process tanks in Australia, which are normally operated at a pH of around 9, and estimated the loss of cyanide through volatilisation

4 Environmental fate

as 1% of the total cyanide added to the circuit. On tailings ponds, however, volatilisation is the dominant attenuation mechanism for cyanide, and can account for up to 90% of the total free cyanide loss (AMIRA, 2004, Broderius and Smith, 1980; Simovec et al, 1984).

4.1.2 Ultraviolet degradation (photolysis)

When tailing solutions are exposed to ultraviolet irradiation, CN^- is released from ferrous and ferric cyanides through photochemical degradation, as indicated in Eq. 4.5 and 4.6, and the formation of iron precipitates, such as Prussian blue in acidic solutions, or ferric hydroxide in basic solutions (Broderius and Smith, 1980). The release of one cyanide ion from the complex causes an increase in free cyanide present in the solution during daylight hours.



Decomposition rates of up to 8%/h have been reported. Nevertheless, the turbidity of the solution limits ultraviolet degradation to solution close to the surface, and therefore its impact on attenuation can normally be regarded as minor (Lorösch, 2001).

Photolysis and volatilisation often occur in tandem during daylight hours. Ultraviolet radiation from the sun catalyses the photochemical reaction, liberating free cyanide from the iron cyanide complex ions present in the tailings solution (Huiatt et al, 1983). This free cyanide combines with cyanide released from other metal complexes and free cyanide originally present in the solution to form volatile hydrogen cyanide through hydrolysis. Since this conversion is largely dependent on pH, the pH lowering effect of carbon dioxide absorption, as well as rainfall, promotes the hydrolysis reaction. The formed HCN volatilises into the air and once released, the vapour quickly diffuses to the surrounding atmosphere.

4 Environmental fate

4.1.3 Base metal complexation

Cyanide is also a strong ligand that is capable of complexing with virtually any heavy metal even at low concentrations. Free cyanide reacts with the heavy metal ions found in the ore minerals, forming base metal complexes (Young and Jordan, 1995; Smith and Mudder, 1991). In addition, various cations also react with cyanide to form salts with cyanide removal depending on their solubilities (Young and Jordan, 1995).



Base metal complexation often acts as an intermediate process affecting attenuation, since the cyanide that remains in a complexed form in the solution may dissociate from the weaker metal cyanide complexes (such as $Zn(CN)_4^{2-}$), to release free cyanide, that is then removed through volatilisation, precipitation, ultraviolet degradation, adsorption or oxidation.

4.1.4 Precipitation

Ferrocyanide formed during base metal complexation can combine with several other base metal cations to form insoluble, strong acid dissociable (SAD) cyanide complexes that precipitate from the solution, such as:



Various ferro- and ferricyanide complexes can form in this way depending on the prevailing conditions. These complexes are very stable and therefore regarded as non-toxic, and precipitation is often used in conjunction with other artificial detoxification processes, such as oxidation, to treat cyanide waste. However, exposure to sunlight may cause these complexes to decompose and to again release toxic forms of free cyanide via photolysis.

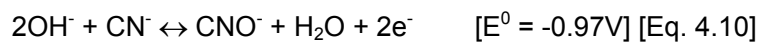
4 Environmental fate

4.1.5 Adsorption

Chatwin and Trepanowski (1987) conducted tests on cyanide attenuation from soils and found that cyanide is significantly adsorbed onto the alumina-containing minerals bauxite and kaolinite, and also on organic matter. Tanriverdi et al (1998) also reported that clay liners have a natural cyanide degradation capacity. Ferric forms of iron present in soil were found to weakly adsorb cyanide. Although Adams (1990b) did not report significant adsorption losses of cyanide in carbon-in-leach tanks compared to other loss mechanisms, the effect of adsorption onto sediments in tailings dams could be significant, depending on the mineralogy and solution chemistry.

4.1.6 Oxidation

Cyanide can be catalytically oxidised in the presence of active inorganic or organic surfaces, e.g. activated carbon or sediment soil, to form cyanogen ((CN)_{2(g)}) and cyanate (CNO⁻) (Adams, 1990a). In practice, cyanogen is formed as an intermediate species that is converted to cyanate.



Copper and nickel cyanide complexes have been reported to specifically enhance oxidation. In the absence of a catalyst, the oxidation of cyanide to cyanate is an extremely slow reaction (Lorösch, 2001). However, in the presence of high oxidant concentrations, e.g. with pure oxygen bubbling, or in the presence of activated carbon, cyanide oxidation could become significant. Adams (1990b) has shown that, for the carbon-in-pulp process, significant losses can be attributed to the formation of cyanate, of which a portion decomposes to form ammonia, carbonate and urea. Additionally, some cyanide is adsorbed onto the carbon. Thus, the presence of carbon (25 g/L) in a typical leach solution, at 20°C and a pH of 10, resulted in an overall increase in cyanide loss of up to 66% over a period of 48 hours.

4 Environmental fate

4.1.7 Thiocyanate formation

It has also been suggested that the formation of thiocyanate, in the presence of thiosulphate or polysulphide, is the main source of cyanide loss in sulphur bearing mineral ore tailings via the following reactions (Rubo et al, 2000):



In the case of oxide ores, where sulphide concentrations are generally low, thiocyanate formation is marginal, and volatilisation should predominate as the loss mechanism from tailings ponds.

4.1.8 Formation of ammonium formate

At high pH values, hydrogen cyanide can undergo a second hydrolysis reaction resulting in the formation of ammonium formate as indicated below. Lorösch (2001) and Smith and Mudder (1991) also refer to this mechanism as saponification.



Due to the slow rate of this reaction, saponification will only become significant as a mechanism for cyanide loss in the absence of rapid processes such as volatilisation, or at high temperatures, where the reaction rate is significantly increased (Dicinoski et al, 1997).

4.1.9 Bacterial metabolisation

Various species of bacteria, fungi, algae, yeasts and plants possess the ability to convert cyanide, which acts as a carbon and nitrogen source, to ammonia and carbonate. The requirement for aerobic conditions plays a major role in the

4 Environmental fate

effectiveness of metabolisation as an attenuation process, as was concluded from a review done by Chatwin and Trepanowski (1987).

4.2 Conclusion

All the attenuation processes discussed are to some extent reversible and could result in fluctuating levels of free cyanide in solution or in the atmosphere depending on the specific circumstances. Volatilisation into open air is by far the most important mechanism by which cyanide is irreversibly removed from aqueous solution. Cyanide removal by precipitation or complex formation is typically reversible, as the products do not leave the solution, and are thus available as sources of cyanide, should the conditions favour the reverse reactions. Photolysis during daylight hours may typically increase the free cyanide by decomposition of cyanide complexes, initiating either the loss of cyanide from solution through volatilisation or by the formation of other cyanide complexes.

Although the attenuation of free cyanide from aqueous solution thus occurs by various and interrelated processes, the dominance of volatilisation as the mechanism for cyanide attenuation on tailings facilities, makes it possible to reasonably predict cyanide attenuation by only considering volatilisation.

5. Properties and volatilisation of HCN

5. PROPERTIES AND VOLATILISATION OF HCN

5.1 Chemical and physical constants of HCN

The properties of relevance to the volatilisation of cyanide are the dissociation constant (pK_A) and Henry's Law constant (k_H) of hydrogen cyanide.

5.1.1 Dissociation constant (pK_A) of HCN

Reporting of the pK_A value for HCN is often inconsistent (see Table 5.1). The value of 9.36 is perhaps the most commonly used. Simovec and Snodgrass (1984) reported pK_A as 9.36 at 25°C, while Huiatt et al (1983) and Smith and Mudder (1991) quoted a value of 9.31, but only the latter specifies the temperature as 20°C. Dodge and Zabban (1952) used a value of 9.14 at 25°C in their calculations.

Verhoefen et al (1990) determined the temperature relationship for pK_A which is shown in Figure 5.1, giving pK_A values at 20°C and 25°C of 9.36 and 9.21, respectively.

Table 5.1. Summary of reported values for pK_A of HCN.

Source	pK_A	Temperature [°C]	Salinity [M NaCl]
Dodge and Zabban, 1952	9.14	25	→0
Simovec and Snodgrass, 1984	9.36	25	Assumed →0
	9.21	20	
Huiatt et al, 1983	9.31	Unspecified	Assumed →0
Verhoefen et al, 1990	9.36	20	→0
Smith and Mudder, 1991	9.31	20	Assumed →0
AMIRA, 1997	9.36	20	→0
	9.21	25	

These values also correlate well with those obtained from a review done by AMIRA (1997). The conclusion here is that caution should be taken when using a pK_A value, since salinity and temperature need to be taken into consideration, as even a slight

5. Properties and volatilisation of HCN

deviance could affect results drastically due to the sensitivity of the CN^-/HCN system to pH values close to pK_A . AMIRA (1997) also showed in Figure 5.2 that the pK_A shifts to significantly higher values at salinities above 2 M NaCl, indicating that higher pH values would be required for safe operation.

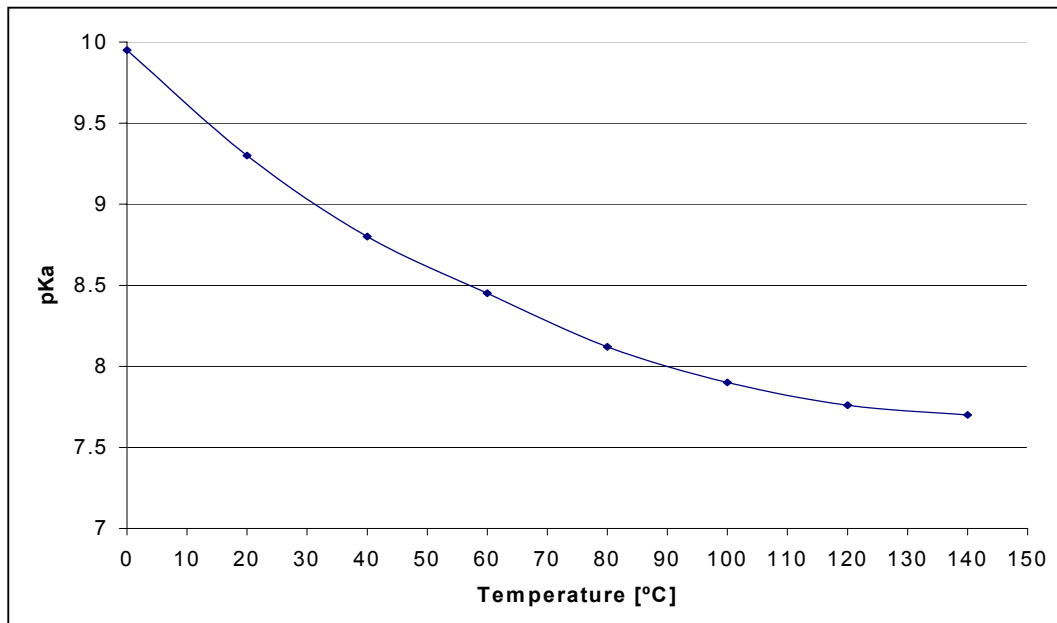


Figure 5.1. Dependence of pK_A of HCN on temperature at low salinity (Verhoefen et al, 1990).

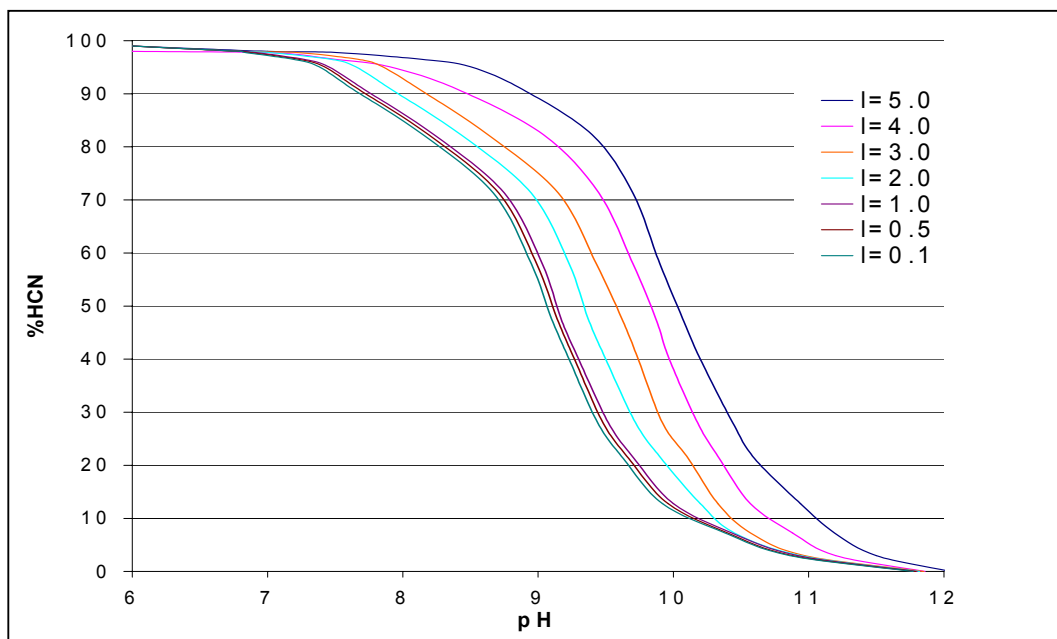


Figure 5.2. pK_A dependence on salinity at 25°C ($I \rightarrow 0$) (AMIRA, 1997).

5. Properties and volatilisation of HCN

From the literature it follows that the most accurate pK_A values for hydrogen cyanide is equal to 9.36 at 20°C and 9.21 at 25°C, at low salinity.

5.1.2 Henry's constant (k_H)

Various investigations have been undertaken to determine the value of Henry's Law constant for hydrogen cyanide, with values reported in the literature summarised in Table 5.2. Almost eighty years ago, some vapour pressure data for hydrogen cyanide was published in International Critical Tables (1928). Extrapolating this data from a total concentration of 7.48 per cent by weight (74 800 ppm) HCN to 4 000 ppm HCN, the value of k_H has been calculated as 0.09 atm.L/mol at 18°C (Dodge and Zabban, 1952). This result is interesting since it correlates particularly well with other values reported for significantly lower HCN concentrations (see Table 5.2), suggesting that Henry's Law is obeyed even at these levels and that Henry's constant is independent of total HCN concentration in this range. Furthermore, experimental work done by the same authors showed that k_H is only slightly influenced by temperature in the range of interest in this work (~10-45°C), but increases rapidly at temperatures above 65°C, as shown in see Figure 5.3. Using their data to calculate the Henry's Law constants, corresponding to the different salinities investigated, gave a value of 0.084 atm.L/mol at low salinity. Equilibration experiments conducted by Patrick (2000) on leach pulp samples taken from three of AngloGold's South African gold plants resulted in a Henry's Law constant value of 0.078 atm.L/mol. All these studies indicate a value between 0.078-0.09 atm.L/mol for k_H at ambient conditions.

Lye et al (2004) also examined Henry's Law constant using two different techniques. The first was the so-called GC headspace technique, which involved sampling of the equilibrium gas phase above a cyanide solution and analysing it using gas chromatography. The second technique made use of a stripping column, where air or nitrogen gas was bubbled through an acidified cyanide solution and the exiting gas was collected into an absorbing column of NaOH, which was in turn analysed for HCN, using a cyanide ion-selective electrode. With both techniques, no significant concentration dependence was observed for Henry's constant, which confirms the findings of Dodge and Zabban (1952) that Henry's Law applies over a broad range of concentrations applicable to typical pulp solutions in gold processing.

5. Properties and volatilisation of HCN

Table 5.2. Summary of Henry's Law constants reported in the literature.

Reference	Henry's Law constant [atm.L/mol]	CN concentration [ppm]	Salinity, I [M NaCl]	Temperature [°C]	Method
Patrick, 2000	0.078	110-130	0	25	Experimental (stripping)
Dodge and Zabban, 1952	0.090	4000	0	18	Extrapolated (based on [HCN _{aq}] with time)
	0.134		0	64	Experimental
	0.332		0	85.5	Experimental
	0.778		0	100	Experimental
Heath et al, 1998	0.084	265	0	Not given (assumed ~ 25)	Calculated from experimental (Sampling of gas phase with syringe)
	0.091		0.75		
	0.112		3		
Chatwin and Trepanowski, 1987	0.1067	Not given	Not given	Not given	Review
Lye et al, 2004	0.132 0.144 ± 0.039 0.173 ± 0.049 0.221 ± 0.067	4.42	0 1 3 5	25	Experimental (GC headspace)
	0.093-0.096		0.26		

Lye et al (2004) states that static techniques, such as the GC headspace technique, are generally known to generate higher k_H values, while dynamic techniques, such as stripping, are generally considered more accurate for compounds with low k_H values, such as HCN. This would explain the 40% higher value obtained from the GC headspace technique compared to the other reviewed data in Table 5.2.

5. Properties and volatilisation of HCN

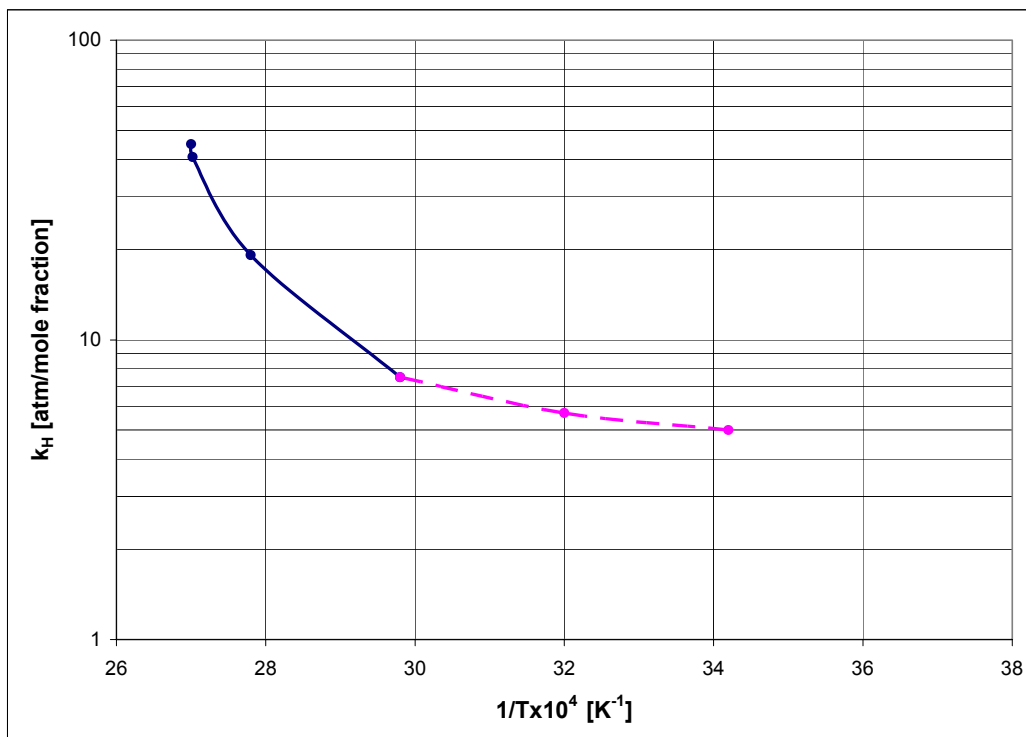


Figure 5.3. Temperature dependence of Henry's Law constant.

(After Dodge and Zabban, 1952. The dashed section was extrapolated from available vapour pressure data.)

The value of k_H is influenced by salinity. Heath et al (1998) showed that a 75% increase in salinity, from 0 to 0.75M NaCl, increased k_H by only 8.3%. In comparison, Lye et al (2004) found that a 100% increase in salinity from nearly 0 to 1M NaCl led to a 9,1% increase in k_H . The results therefore suggest that, although k_H for HCN is dependent on salinity, the effect is relatively small.

Comparison of the findings from these various studies lends some insight into the gas liquid equilibrium of HCN expressed in terms of k_H with respect to concentration, temperature and salinity. The data suggests that

1. A relatively good correlation exists between the reported values of k_H measurements for HCN, with the value of k_H , at ambient temperature and in pure solutions ($I \rightarrow 0$), in the range 0.078-0.1atm.L/mol.
2. Assuming a value for k_H of 0.09 atm.L/mol, which would translate into a k_H value of 5 atm/mol fraction, which indicates that HCN exhibits a strong positive

5. Properties and volatilisation of HCN

deviation from ideality, when one considers that the vapour pressure of pure HCN is 1 atm at 25°C. This illustrates the importance of establishing a reliable value for k_H , as a 500% error would result in equilibrium calculations based on an ideal behaviour, i.e. Raoult's law, resulting in a serious underestimation of the actual gas concentration present in a system.

3. k_H is probably only slightly dependent on concentration, in the range typically used in leaching operations, and also up to concentrations of 4 000 ppm CN. This is significant as it indicates that, although the liquid-gas equilibrium for HCN shows a positive deviation from ideality, this deviation is constant at least up to 4 000 ppm CN.
4. Although k_H is dependent on salinity, the effect is not significant in the range typically used in gold leaching.
5. k_H is temperature dependent, but the effect is only significant at higher temperatures (above 65°C), that are not relevant to the present study. However, this observation is only based on one study, and some additional investigation into this matter might prove to be worthwhile.

Despite the relatively extensive previous work, certain shortcomings in the characterisation of the HCN liquid-gas equilibrium have been identified:

1. There seems to be a discrepancy in the data obtained from different methods. Most of the test work represented here made use of the stripping technique, which is generally preferred for measurement of low k_H values. However, to the author's knowledge, no data for k_H of HCN has been obtained by the use of direct measurement of the gas phase, e.g. by the use of a gas sensor.
2. In addition, none of the investigations mentioned here have reported on the concentration profile of the system during the equilibration period. Knowledge of this time dependence would be useful in revealing the rate at which equilibrium is actually reached in a particular system.

5. Properties and volatilisation of HCN

5.2 Volatilisation mass transfer

5.2.1 Theoretical models

The complexities associated with the modelling of an environmental fate mechanism are no doubt challenging. Mill (1993) states that "...it is often impossible to disentangle the composite effects of several independent processes to learn the role each played in the observed loss". In the case of volatilisation, rates are dependent on thermodynamic and physical-chemical properties of the substance, such as solubility, diffusivity, vapour pressure and deviations from ideality.

In addition, the volatilisation rate would also depend on fluid mechanical regimes existing in the water body and lower atmosphere (Mackay, 1977). In the environment, these are often unpredictable and can change within the hour, which can lead to a change in rate by up to a factor of ten. The presence of contaminants, such as floating or surface-active material, may also affect the interfacial processes and damp turbulence, to create an additional resistance to mass transfer.

However, a modelling strategy that involves combining laboratory measurements of kinetic and equilibrium constants with empirical fitting of data, collected on-site, has been developed. Various studies have attempted to identify a simple model to describe the complex nature of volatilisation of pollutants or other volatile chemicals from water bodies (Thomas, 1982; Smith et al, 1980; Cohen et al, 1978; Mackay, 1977). These will now be briefly discussed.

- Stratified lake model

Depending on the type of water body involved, a number of stages may be involved in the transport of a chemical (Thomas, 1982). In a lake or dam, vertical transport is controlled by direct currents resulting from water flow, and wind and temperature induced currents. Although the first form of current does occur in tailings dams to some extent, the greatest contribution to turbulence originates from the atmosphere, with wind speed the main factor determining the degree of turbulence in the near surface region.

5. Properties and volatilisation of HCN

It has been found in various studies that HCN volatilisation from a liquid body follows first-order kinetics with respect to the concentration of aqueous HCN (Broderius and Smith, 1980; Huiatt et al, 1983; Adams, 1990a). The mass transfer of a chemical across the interface can now be described by the finite difference approximation of Fick's First Law of diffusion. This is based on the assumption that the species within the mixture will move spontaneously from a higher to a lower concentration region to eliminate the concentration gradients that exist in the mixture.

Furthermore, the resistance to mass transfer at the interface between the gas- and liquid phase is typically negligible, and it can therefore assumed that the interface is at equilibrium and that concentration gradients exist in the interfacial boundary layers of each phase only (Thomas, 1982). The rate of volatilisation is dependent on Henry's Law constant, which describes the equilibrium condition at the interface, as well as the gas- and liquid phase mass transfer coefficients, defining the diffusion rates through each layer. Figure 5.5 presents an illustration of the two-film model (Thomas, 1982).

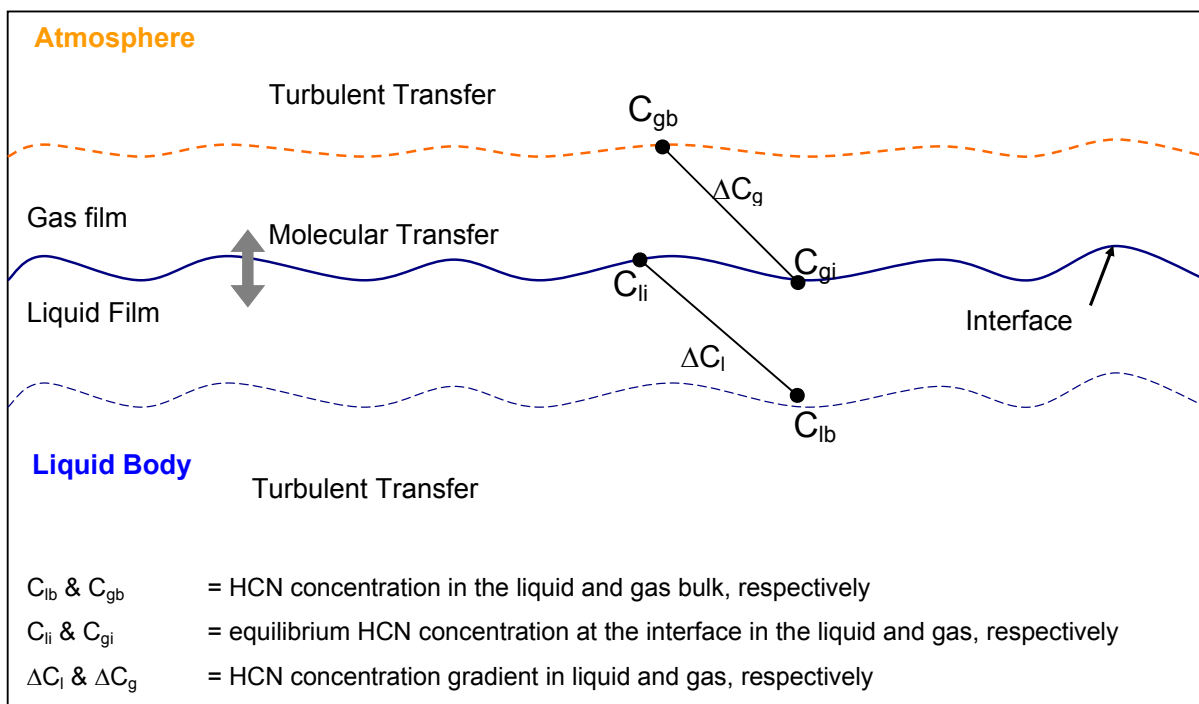


Figure 5.5. The two-film model for mass transfer from a water body to the atmosphere.

5. Properties and volatilisation of HCN

The two-film model allows the phase resistances in the liquid and gas phase to be treated separately. Thus, the reciprocals of the mass transfer coefficients for each phase representing the resistance to mass transfer in that particular phase and with the sum equal to the total resistance. The derivation of the mass transfer coefficients is shown in Figure 5.6.

Assuming first order kinetics, HCN volatilisation may be expressed as

$$-\frac{d[C_{HCN}]}{dt} = k_v [C_{HCN}] \quad [\text{Eq. 5.1}]$$

where $d[C_{HCN}]/dt$ = Rate of volatilisation [g/s.cm³]
 k_v = Volatilisation rate constant [s⁻¹]

The one-dimensional mass transfer across a film can be written according to the finite difference approximation of Fick's Law of Diffusion:

$$N''_{HCN} = k_{OL}(\Delta C) \quad [\text{Eq. 5.2}]$$

where N''_{HCN} = Diffusion molar flux of HCN [g/s.cm²]
 k_{OL} = D/z , mass transfer coefficient [cm/s]
 D = Molecular diffusion coefficient of HCN in water [cm²/s]
 z = Film thickness [cm]
 ΔC = Concentration gradient across the film [g/cm³]

It is assumed here that three consecutive steps determine the mass transfer of HCN from the liquid to the gas phase, i.e.

1. mass transfer of HCN through the liquid film
2. mass transfer of HCN across the interface (assumed to be at equilibrium)
3. mass transfer of HCN through the gas film.

The concentration gradients in the bulk liquid and gas phases are therefore assumed negligible due to the high rate of turbulent mass transfer. Furthermore, assuming steady state conditions, Eq. 5.2 may be written in terms of steps 1 and 3:

$$N''_{HCN} = k_g (C_{gi} - C_{gb}) = k_l (C_{lb} - C_{li}) \quad [\text{Eq. 5.3}]$$

Figure 5.6. Derivation of the two-film model (adapted from Thomas, 1982).

5. Properties and volatilisation of HCN

where k_g = Gas phase mass transfer coefficient in boundary layer film [cm/s]

k_l = Liquid phase mass transfer coefficient in boundary layer film [cm/s]

Assuming that HCN behaves as an ideal gas at the equilibrium conditions, it also follows from Henry's Law that

$$C_{li} = \frac{P_{HCN}}{k_H} \quad [\text{Eq. 5.4}]$$

since C_{li} is the liquid concentration in equilibrium with C_{gi} [g/cm³]

k_H = Henry's Law constant for HCN [atm.cm³/g]

P_{HCN} = Partial pressure of HCN in air [atm]

Eq. [5.3] may now be written as

$$N''_{HCN} = \frac{C_{gb} - k_H C_{lb} / RT}{1/k_g + k_H / RTk_l} = \frac{C_{gb} RT / k_H - C_{lb}}{1/k_l + RT / k_H k_g} \quad [\text{Eq. 5.5}]$$

From the second part of Eq. [5.5], describing the mass transfer in the liquid phase, the overall liquid phase mass transfer coefficient is derived as:

$$\frac{1}{k_{OL}} = \frac{1}{k_L} + \frac{RT}{k_H k_G} \quad [\text{Eq. 5.6}]$$

where R = universal gas constant [atm.cm³/mol.K]

T = temperature [K]

Combining Eq. [5.1], Eq. [5.2] and Eq. [5.6] gives the rate constant for HCN volatilisation from the liquid film:

$$k_V = k_{OL} / Z = \frac{1}{Z} \left[\frac{1}{k_l} + \frac{RT}{k_H k_g} \right] \quad [\text{Eq. 5.7}]$$

Figure 5.6. (continued) Derivation of the two-film model (adapted from Thomas, 1982).

5. Properties and volatilisation of HCN

These mass transfer coefficients are empirical and are dependent on the specific geometry and chemistry of the layers, as well as environmental factors. The reader is cautioned to be mindful of the fact that k_{OL} is only a valid means of expressing the volatilisation rate in the case where the mass transfer across the interface is the rate-limiting step, as the two-film model assumes turbulent mixing in the liquid body. An exception to this may be the case of stagnant ponds, where mass transfer in the bulk liquid may be slow enough to become rate determining.

Thomas (1982) advised that, due to the difficulty of performing in-situ volatilisation experiments from lakes, the volatilisation rates determined could be higher by a factor of ten or lower by a factor of possibly three.

5.2.2 Mass transfer coefficients

Several studies have shown that the rate of volatilisation is mainly affected by the initial free cyanide concentration, pH of the solution, unless most of the free cyanide is already present as HCN, aeration, agitation and temperature (Dodge and Zabban, 1952; Huiatt et al, 1983; Lye et al, 2004). The most important factors affecting volatilisation rates investigated and reported on in the literature, are summarised in Table 5.3, and will now be discussed.

5. Properties and volatilisation of HCN

Table 5.3. Summary of rate constants for HCN volatilisation.

Reference	Rate Constant (k_v) [h^{-1}]	k_{oL} [m/h]	Temperature [°C]	pH	Air flow rate [$m^3/m^3_{\text{solution}} \cdot \text{min}$]	Mechanical stirring [rpm]	CN concentration [mg/L]	
Dodge and Zabban, 1952	0.129	Not given	26	<7	0.83	0	20-500	
Broderius and Smith, 1980	0.0257	Not given	25	7.9	0	0	0.025	
	0.0315						0.200	
Lye et al, 2004	0.525	0.018	25	2	Not given	0	0.26	
	0.340	0.017	25		0			
	0.680	0.034	25		0			160
	0.420	0.021	35		0			0
	1.10	0.037	40		Not given			0
Simovec and Snodgrass, 1984	-	0.0165	20	7	0.05	0	200	
	-	0.0100			0			0

5. Properties and volatilisation of HCN

- Temperature

All the reports cited in this literature survey support the finding that the volatilisation rate of HCN increases with temperature. Broderius and Smith (1980) conducted laboratory and open-air tests on HCN volatilisation from open flasks filled with solutions, containing 25-200 ppb of free cyanide at a pH of 7.9. Their results show that the volatilisation rate constant increases with temperature from 10°C to 25°C by a factor of roughly two, with the exception of the 25 ppb CN run, which returned a factor of over four as shown in Figure 5.7. However, it is assumed here that this can be attributed to an experimental error that might have occurred due to the difficulty in analysing such dilute solutions.

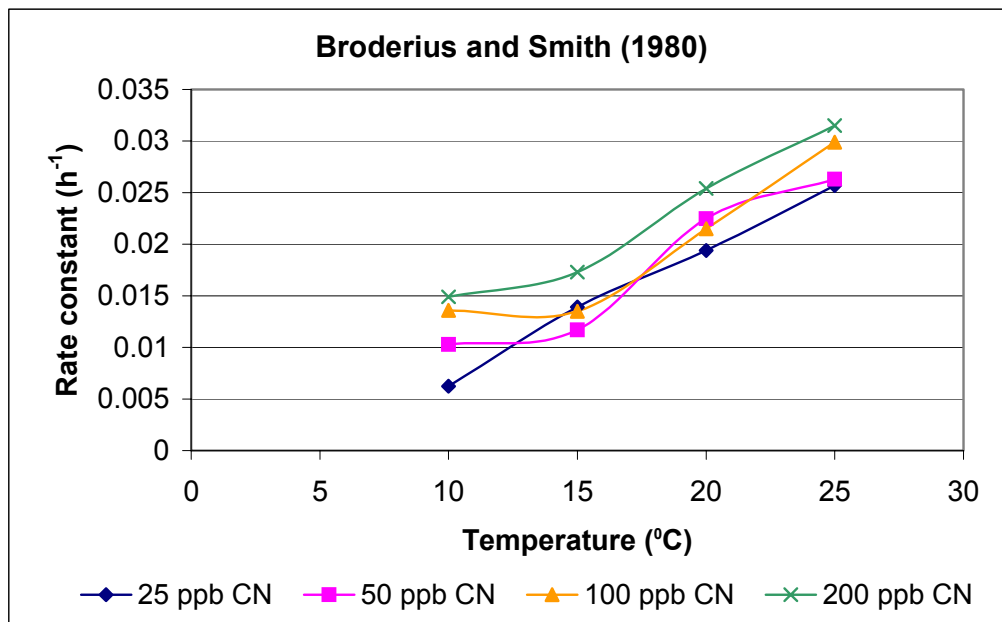


Figure 5.7. Temperature dependence of HCN rate constant (k_v) (Broderius and Smith, 1980).

Although this data is useful in illustrating the influence of temperature on the volatilisation rate, it can unfortunately not be used in a direct comparison with other data sets, as the investigators did not supply values for the corresponding mass transfer coefficients; the rate constants are thus not universal but case-specific. Nonetheless, the trend is clear.

5. Properties and volatilisation of HCN

Lye et al (2004) examined volatilisation rates from a pyrex beaker, placed in a thermostatted bath, and found that a 15°C increase in temperature, from 25-40°C, increased the overall liquid mass transfer coefficient (k_{OL}) by a factor of approximately two, as shown in Table 5.3.

- *Aeration*

There appears to be conflicting evidence as to the effects of aeration on volatilisation rates. Dodge and Zabban (1952) performed batch HCN volatilisation tests on synthesised electroplating waste solutions and investigated the influence of various parameters on the rate constant. The volatilisation rate was found to be directly proportional to the rate of aeration between 0.83 and 23.3 m³ air/m³ solution per minute at room temperature, as shown in Figure 5.8. The hypothesis is that aeration enhances volatilisation due to enhanced mixing effects in the liquid body, as well as by dissolution of HCN gas in the air or oxygen bubbles moving upwards to the surface. In addition, the increased surface area available for mass transfer between the liquid and gas phases, also leads to an overall increase in volatilisation. This postulate seems to be confirmed by Simovec and Snodgrass (1985), who showed that introducing an air flow rate of 0.05 m³ air/m³ solution.min resulted in a 65% increase in the mass transfer coefficient.

However, according to Heath et al (1998), the effect of introducing air to the pulp accounted for less than 10% of the total cyanide lost through volatilisation, in the case of leach tanks. The authors give the maximum air flow rate tested as 43.8 m³/h in a 126.7 m² cylindrical leach tank, for which the tank diameter can be calculated to be 12.7 m, but unfortunately does not specify the exact height of the tank. Assuming a L/D ratio of 1, the volume of the tank would be approximately 1 600 m³, leading to an air flow rate of 0.00045 m³ air/m³ solution.min introduced to the pulp solution, which is significantly lower than the air flow rates tested by Dodge and Zabban (1952).

5. Properties and volatilisation of HCN

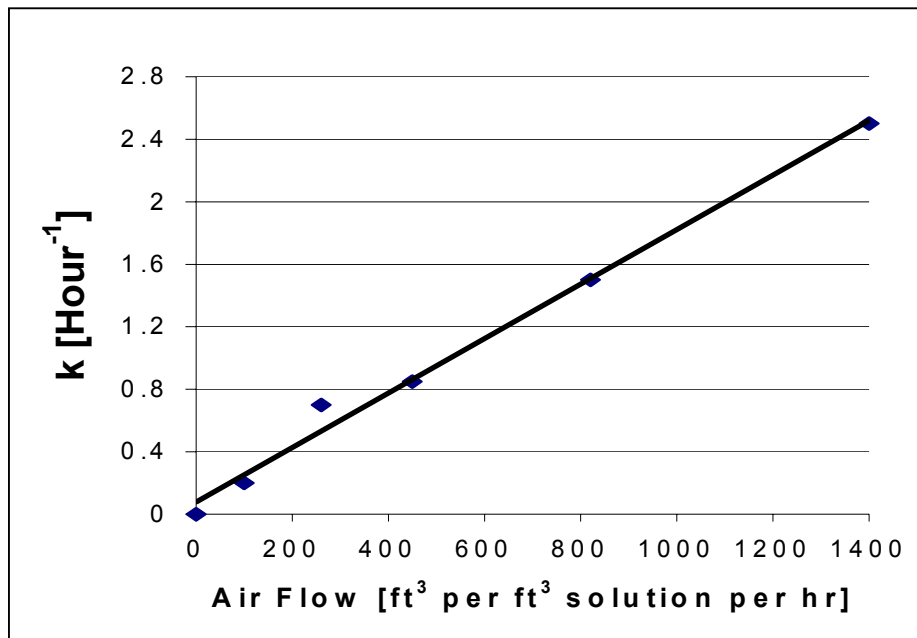


Figure 5.8. Effect of rate of aeration on mass transfer rate constant at 29°C (Dodge and Zabban, 1952).

In order to compare this assumed air flow rate with that of a typical leach operation, data from one of the South African gold plants is used as an example. Taking a conical pachuca tank with a radius of 5.1 m, a conical height of 7.6 m, a cylinder height of 5.4 m and a free board of 1 m, with an applied air flow rate of approximately 125 m³/h per pachuca (obtained from AngloGold Ashanti), one can calculate the total tank volume as 566.5 m³. This translates into a specific air flow rate of 0.0037 m³ air/m³ solution.min. This is approximately ten times higher than the assumed value for the study of Heath et al (1998), and indicates that the rate used by them is rather low, considering that the volume of a conical tank is significantly less than that of a cylindrical tank, and that the residence time of the air would thus be longer. Nevertheless, both these flow rates are evidently much lower than that tested by Dodge and Zabban (1952).

In addition, Lye et al (2004) also reports that air sparging has a negligible effect on volatilisation rate as indicated by the data given in Table 5.3. Although, once again, the air flow rate is not adequately specified, it is reasonable to assume that the value would be in the same order of magnitude as that tested by Heath et al (1998), as it would also apply to leach tanks.

5. Properties and volatilisation of HCN

The evidence presented here, therefore, indicate that, although aeration may have a significant effect on the volatilisation rate, the air flow rates, applied in typical leaching operations, are low compared to those studied by Dodge and Zabban (1952), where a significant effect was found. Nevertheless, some further investigation into this matter would be justifiable.

- Mechanical agitation

The rate constant has also been shown to be strongly dependent on the degree of mechanical agitation, as indicated in Table 5.4 (Dodge and Zabban, 1952; Lye et al, 2004). This effect may be explained by referring back to the stratified lake model described in section 5.2.1, which suggests that the two rate limiting regions in a lake are the interface and the thermocline, respectively. Mechanical agitation will influence both these regions to a degree, by enhancing mixing, and therefore increasing mass transfer in the thermocline, as well as by disturbing and increasing the area of the gas-liquid interface, which will also increase the rate of mass transfer. Mechanical mixing would also enhance the surface renewal of HCN available for volatilisation, thereby effectively preventing the development of a thicker boundary layer over time, as would be the case in an unmixed solution.

Table 5.4. Effect of stirring on the volatilisation rate (Lye et al, 2004).

Rate Constant (k_v) [h^{-1}]	k_{oL} [m/h]	Temperature [°C]	pH	Stirring rate [rpm]	CN concentration [mg/L]
0.34	0.017	25	2	0	0.26
0.68	0.034			160	
0.96	0.048			340	
1.32	0.066			500	

In addition, Dodge and Zabban (1952) found that formation of a vortex, associated with violent agitation, led to a drastic increase in the volatilisation rate (up to 600%).

5. Properties and volatilisation of HCN

- Hydrogen cyanide concentration

As pointed out before, the hydrogen cyanide concentration available for volatilisation is directly dependent on the pH of the solution and the total free cyanide concentration given by the sum of the concentrations of CN^- and $\text{HCN}_{(\text{aq})}$. Knowledge of the pH, pK_A and free cyanide concentration in the solution will thus allow the calculation of the hydrogen cyanide concentration from the hydrolysis curve, as discussed in section 3.2.2. However, since many of the studies included in this review used solutions with low pH values, it may be assumed that the cyanide was fully hydrolysed as $\text{HCN}_{(\text{aq})}$; this would generally apply below a pH of 7.

Dodge and Zabban (1952) derived a correlation for thoroughly agitated and aerated solutions for the rate constant (k_v, h^{-1}), in terms of the air flow rate ($50 < Q < 1400 \text{ m}^3/\text{m}^3 \text{ solution.h}$) and temperature ($26\text{-}62^\circ\text{C}$). The value given in Table 5.3 corresponds to a gentle airflow rate ($50\text{m}^3/\text{m}^3 \text{ solution.h}$ or $0.83\text{m}^3/\text{m}^3 \text{ solution.min}$). Note that, in this work, the rate constant was assumed to be independent of the cyanide concentration. It is also somewhat unrealistic to expect that the rate of volatilisation would be independent of the size and distribution of the air bubbles, and of the height of the container.

More recently, Broderius and Smith (1980) measured the volatilisation rate constant for unstirred solutions at a pH of 7.9. Their results indicate that an increase of 20-30% can be expected with an increase in cyanide concentration from 25-200 ppb. However, comparison of the data shown in Table 5.3 indicates a discrepancy in the perceived concentration dependence of the rate constant. Although Dodge and Zabban (1952) did not consider cyanide concentration in the determination of k_v , it is reasonable to assume that the effect derived by Broderius and Smith (1980), would be even more significant at higher concentrations. However, one should consider that the rate constants derived from and reported in these papers were obtained from agitated and stagnant solutions, respectively. Broderius and Smith (1980) used stagnant solutions at very low concentrations, where the diffusion of hydrogen cyanide from the bulk solution to the interface would probably be the rate-limiting step. It can also be expected that the thickness of the boundary layer would take some time to develop fully. In contrast, the enhanced mixing caused by mechanical agitation and high aeration rates, along with the much higher cyanide concentrations

5. Properties and volatilisation of HCN

used by Dodge and Zabban (1952), eliminated this effect and probably gave rise to the insignificant concentration dependency found in this work. This hypothesis therefore would suggest that, in essence, the process studied by Broderius and Smith (1980) was probably not at steady state, which would further explain the variable rate constants reported.

- Interfacial surface area to volume ratio

Another factor that is once again related to agitation is the liquid-air interfacial surface area to volume ratio. The rate of HCN removal has been shown to be inversely proportional to solution depth (Dodge and Zabban, 1952; Broderius and Smith, 1980; Huiatt et al, 1983), in the case of stagnant solutions.

This effect can be easily understood when one recognises that diffusion in the solution is the dominant mass transfer mechanism in a stagnant solution. Considering that the diffusivity of HCN is ten thousand times smaller in water compared to air ($D = 1.98 \times 10^{-5}$ and 1.72×10^{-9} m²/s @ 20°C, respectively, adapted from Dodge and Zabban (1952)), it follows that the solution will become depleted of HCN to a greater depth, i.e. increasing the thickness of the boundary layer with time.

Thus, diffusion of HCN from the bottom to the top of the solution is typically the rate-determining step for stagnant solutions. This would, however, not be the case for agitated volatilisation, where efficient mixing eliminates the concentration gradients in the bulk liquid and transfer across the interface then becomes rate limiting.

Lye et al (2004) stated that volatilisation rate constants are typically not generally applicable since the shape of the water body is typically unique for every application. Instead, it would be more appropriate to refer to the overall liquid phase mass transfer coefficient (k_{OL} , m/h). This idea is supported by comparing the values of k_v (h⁻¹) and k_{OL} (m/h) that are listed in Table 5.3, indicating relatively good agreement between the k_{OL} values of Lye et al (2004), and Simovec and Snodgrass (1984), despite the significantly different concentrations used for the experiments.

5. Properties and volatilisation of HCN

- Salinity

Increased salinity tends to have a salting-out effect on the solution, decreasing the solubility of HCN gas in the solution and increasing its vapour pressure, thus promoting volatilisation. This effect is especially important at Australian sites, due to the high salinity of Australian process water.

It has however been noted from a study conducted by Heath et al (1998), that an increase in salinity from nearly 0 M to 0.75 M NaCl, only resulted in a minimal increase in HCN volatilisation. Lye et al (2004) also found that, although k_v is dependent on salinity, the effect was negligible in the range studied (1-5 M NaCl).

It is worth noting that the results of Lye et al (2004) were determined at salinities of 1M NaCl, which is applicable to Australian sites where the TDS levels in process water has been reported to reach up to 300 000 ppm. In South Africa, and most other countries, however, levels are more likely to be in the range of 2 000 to 3 000 ppm TDS. Small variations within this range of concentration would thus probably not have a significant effect on cyanide volatilisation.

- Wind velocity

As mentioned before, wind induces an increase in turbulence in the gas phase boundary layer, thereby decreasing the boundary layer thickness and promoting volatilisation. In addition, the gas-liquid interfacial area is increased by the formation of wind-induced waves in the liquid body. Wind currents in the air enable quick mass transfer of the volatilised HCN, thereby maintaining an unsaturated state in the gas phase and preventing equilibrium from being reached. In the work done by Broderius and Smith (1980), it was found that the presence of wind action increased the volatilisation rate constant by as much as 100%.

- Effects of pulp solid particles

The effect of activated carbon particles on the kinetics of cyanide loss in gold extraction was investigated by Adams (1990a,b). He concluded that activated carbon acts as a catalyst for the oxidation of cyanide to cyanate, as shown in equation 5.8,

5. Properties and volatilisation of HCN

and its further decomposition to form ammonium carbonate, leading to increased cyanide loss as shown in Figure 5.8.



Furthermore, at a pH of 10.2, a temperature of 20°C and 25g/L activated carbon, a total of 41% of the cyanide lost was due to cyanate formation, whereas a 25% loss was attributed to adsorption onto the activated carbon. Only 5% of the total cyanide loss was attributed to HCN volatilisation. However, it was found that, in the absence of activated carbon, HCN volatilisation was responsible for the majority of the cyanide loss.

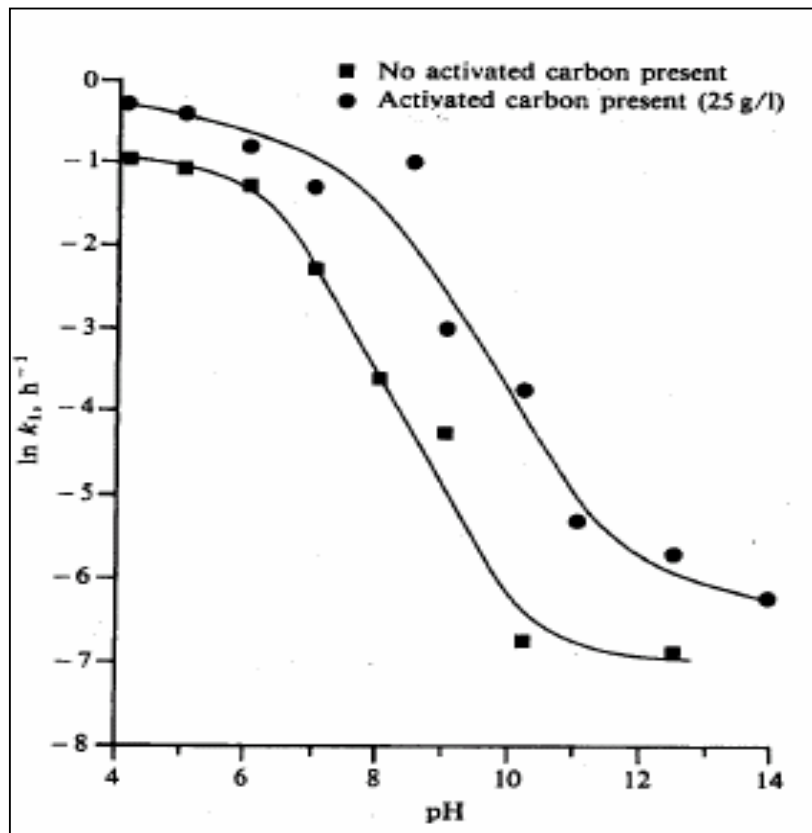


Figure 5.9. Effect of activated carbon on the rate of cyanide loss at 20°C (Adams, 1990 a,b).

In the case of tailings pulp solutions, Rubo et al (2000) reported much higher volatilisation rates from oxide ore tailing solutions than that for transition or sulphide ores. It was shown that the role of volatilisation is greatly reduced by the presence of

5. Properties and volatilisation of HCN

.....

sulphides or base metals in the ore, due to increased formation of cyanate and thiocyanate, as well as copper ferrocyanide precipitation, which would in effect decrease the amount of free cyanide available for volatilisation. However, although the formation of thiocyanate is more prominent in the presence of sulphide ores compared to oxide ores, its contribution to the overall loss of cyanide was found to be relatively low compared to that of volatilisation.

It was shown that 90% of the total cyanide was lost to volatilisation in the case of oxide ores, compared to approximately 40% for transition ore and less than 10% for sulphide ore, as shown in Figure 5.10. In addition, it was shown that, after all the free cyanide present in the tailings solution was depleted, HCN volatilisation was still observed, which must be due to HCN generated from heavy metal complexes. In view of this, they estimated the time frames for the removal of cyanide from tailings through HCN volatilisation as 9 weeks for free cyanide, 6 months for weak acid dissociable cyanide and 1 year for total cyanide.

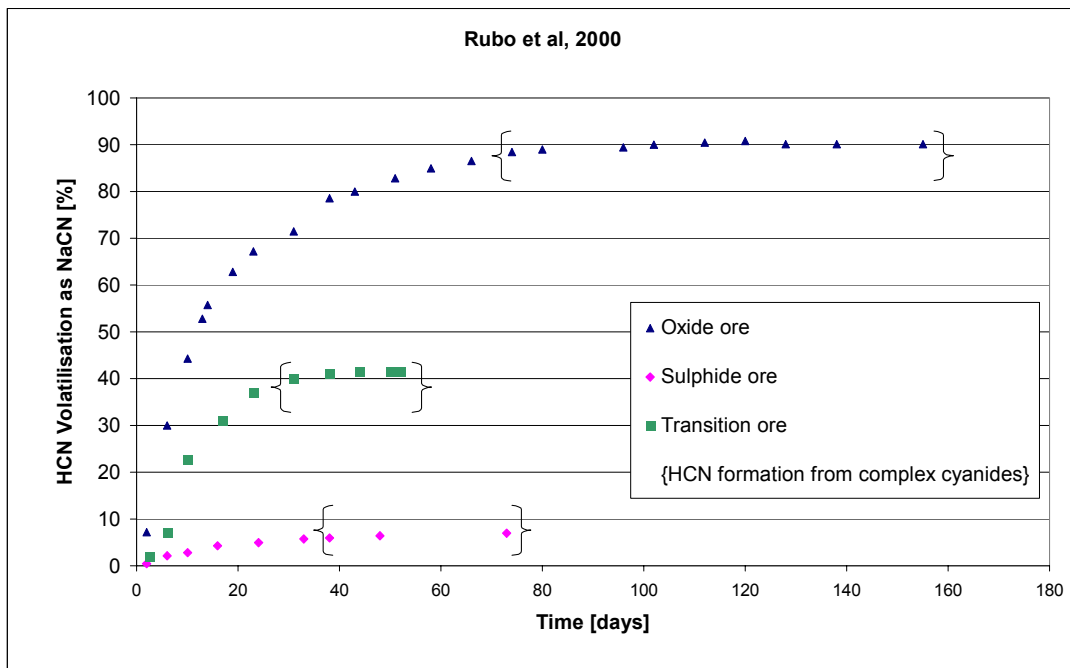


Figure 5.10. HCN volatilisation as a function of total cyanide for different ore types for initial total cyanide in tailings as NaCN: oxide and transition ore 200 ppm; sulphide ore 650 ppm) (Rubo et al, 2000).

5. Properties and volatilisation of HCN

It can therefore be concluded that, in the case of leach processes, the rate of HCN volatilisation is minimal, with the contribution to overall loss becoming even lower in the presence of activated carbon due to additional loss factors. In the case of pulp tailings, however, HCN volatilisation plays the most important role in total cyanide loss over time, especially in the case of oxide ores.

5.3 Current status of HCN volatilisation estimation methods

As stated in section 3.4.4, there is currently no method in use or model available in South Africa for HCN volatilisation predictions. For plant operations, $\text{HCN}_{(g)}$ evolution is being calculated by difference, i.e. by summing the amounts of CN^- , $\text{HCN}_{(aq)}$, SCN^- , CNO^- and metal cyanide complexes entering and leaving the circuit, and by attributing the difference to $\text{HCN}_{(g)}$ volatilisation. Although this currently satisfies for the cyanide legislation and code requirements, a more rigorous method will soon be required with the anticipated changes in cyanide regulations.

Consequently, a prediction model needs to be developed and implemented to provide a reliable quantification method for cyanide losses as a result of HCN volatilisation. This would be an important first step in solving the mass balance for cyanide on operating plants, which is currently incomplete. Additionally, HCN emissions from tailings storage facilities are currently not being recorded due to the absence of a reliable estimation method.

Several other studies have been conducted to develop prediction models for cyanide loss from mining solutions, some with reasonable success. However, the applicability of these models to South African operations is questionable due to the great differences in operating procedures, climate and ore bodies to name but a few. These will now be discussed in order to identify possible hypotheses that might be adopted or combined in the development of a model that will be applicable to typical South African operations.

5. Properties and volatilisation of HCN

5.3.1 Step degradation model

Perhaps the most promising modelling approach found in this literature survey is a study published by Simovec and Snodgrass (1985). They investigated the removal kinetics and natural degradation of cyanide under controlled laboratory conditions, using synthetic solutions containing combinations of metal cyanides (Zn, Fe, Cu and Ni). To simulate typical plant residue and tailings solutions, a 'low mix' and 'high mix' solution was made up for each combination, containing a ratio of metal cyanide to free cyanide of 0.17 and 1.17, respectively. The total cyanide concentration was approximately 200 mg/L.

An initial rapid loss of cyanide, observed during the first 24 hours, was attributed to volatilisation of HCN, followed by a second, less rapid loss through dissociation of the metal cyanide complex and subsequent volatilisation of the formed HCN. The rate of the second loss process was found to be dependent on the dissociation rates of the different metal cyanide complexes.

These observations led to the development of a conceptual model for natural cyanide degradation of a single metal cyanide complex solution. The model is illustrated in Figure 5.11 and is expressed in terms of three separate compartments, each representing a step in the process that could be associated to a transformation of mass.

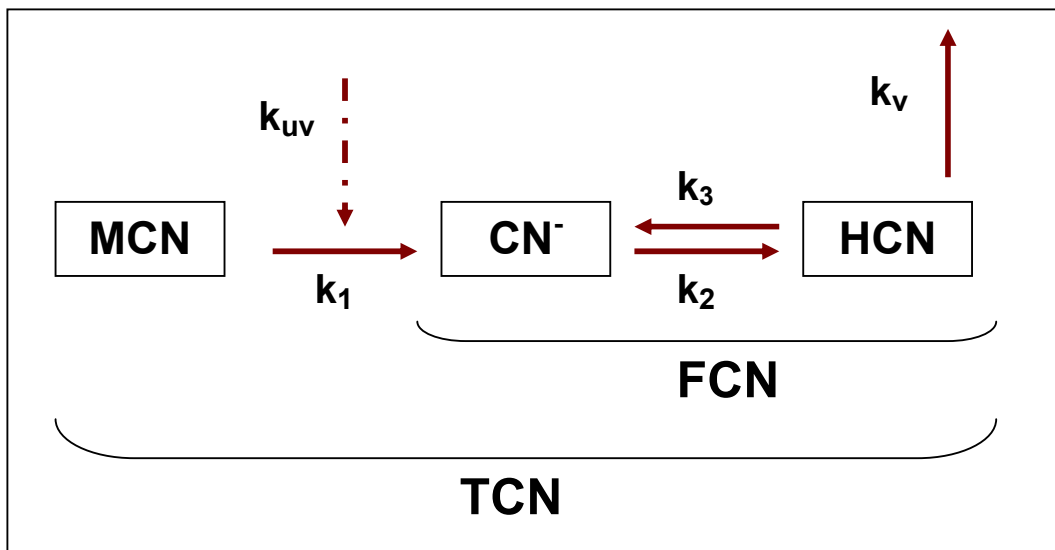


Figure 5.11. Schematic illustration of conceptual cyanide degradation model for single metal cyanide complex solution (Simovec and Snodgrass, 1985).

5. Properties and volatilisation of HCN

The symbols in Figure 5.11 represent the following:

MCN	= Metal cyanide complex
CN ⁻	= Cyanide ion
HCN	= Hydrogen cyanide
FCN	= Free cyanide
TCN	= Total cyanide
k ₁ , k ₂ , k ₃	= Rate constants [h ⁻¹]
k _{UV}	= Rate constant due to ultraviolet irradiation
k _v [*]	= Volatilisation mass transfer coefficient [cm/h]

*: note that this parameter is equivalent to k_{OL} specified in the two film model.

The model thus implies that the cyanide attenuates in three consecutive steps, i.e. the dissociation of the metal cyanide complex into CN⁻ and the metal ion(s), the hydrolysis of CN⁻ to form HCN_(aq), and the volatilisation of HCN_(aq) to HCN_(g).

Since CN⁻ and HCN_(aq) equilibrate rapidly with a change in pH, k₂ and k₃ are not rate limiting. Thus, the rate of cyanide loss can be described in terms of the parameters as:

$$\frac{d[MCN]}{dt} = -k_1[MCN] - k_{UV}[MCN] \quad [\text{Eq. 5.9}]$$

$$\frac{d[FCN]}{dt} = k_1[MCN] + k_{UV}[MCN] - \frac{k_v}{L}[HCN] \quad [\text{Eq. 5.10}]$$

$$\frac{d[TCN]}{dt} = -\frac{k_v}{L}[HCN] \quad [\text{Eq. 5.11}]$$

where [MCN, FCN, HCN, TCN] = Cyanide concentration [g/cm³]

L = Depth of the pond [cm]

The initial test work showed that the effect of ultraviolet radiation was negligible compared to that of volatilisation, and k_{UV} was assumed to equal zero; this assumption might not apply to countries such as South Africa, where the ultraviolet intensity is expected to be high. The dissociation rate constant for each metal

5. Properties and volatilisation of HCN

cyanide complex, as well as the volatilisation mass transfer coefficient, was determined by solving the model equations simultaneously, using the experimental results.

The estimated volatilisation mass transfer coefficients, shown in Table 5.5, vary widely, i.e. over two orders of magnitude range, and could not be adequately explained. It was suggested that the parameter estimation procedure had difficulty resolving values for certain experiments due to their high correlation. Consequently, k_v was removed from the parameter estimation model by assuming an average value of 0.0093 m/h, which was applied in the re-estimation of the metal cyanide decay coefficients. The resulting values were then applied to a plant residue and tailings pond solution, both obtained from a Canadian site, in order to validate the model predictions against actual losses measured over a period.

However, tests done on the residue solution needed further calibration in order to accomplish a satisfactory fit. This was necessary since the model did not account for the possible effect of changes in the pH on the metal decay coefficients, or respeciation of metal complexes, as well as for the variability of metal complexes present in different natural solutions.

An attempt was also made to apply the model to an actual residue solution holding pond, which was operated as a batch system, as well as to a tailings pond, where the continuous in- and out flow of tailings solution were assumed to be at a steady state. The model predictions seems to fit the actual results from the batch residue holding pond well; however, the model predictions for the total cyanide retained in the tailings pond were 60-75% of the actual values. One possible explanation for this could be that the effect of varying wind speeds across the surface of the pond was not taken into account. As discussed before, the presence of wind plays an important role in volatilisation from open-air liquid bodies, and it is possible that the location of the tailings pond was more exposed to wind currents. This could very well have accounted for the additional 25-30 % loss measured.

5. Properties and volatilisation of HCN

Table 5.5. Estimated volatilisation mass transfer coefficients from metal complex solutions containing 200 mg/L cyanide (Simovec and Snodgrass, 1985).

Complex cyanide solution	Air	UV	Mass transfer coefficient	
	[0.05m ³ /m ³ solution.min]		[h ⁻¹]	
	On(+)/off(-)	On(+)/off(-)	4 ^o C	20 ^o C
Cu	+	+	0.56	139.12*
	+	-	0.46	2.02
	-	+	7.85*	0.55
	-	-	2.85*	0.53
Zn	+	+	0.74	0.08*
	+	-	2.14	29.73*
	-	+	1.66	0.74*
	-	-	0.75	0.7
Ni	+	+	0.55	2.97
	+	-	0.91	0.77
	-	+	1.78	0.74
	-	-	1.11	3.33
Fe	+	+	0.29	3.69
	+	-	0.84	0.56
	-	+	42.81*	1.43
	-	-	1.55	0.71

*: Outliers as identified by Simovec and Snodgrass and discussed in text.

The model predicted the degradation of cyanide from the tailings pond solution very closely. Note that the model assumes efficient mixing in the liquid body, which is a reasonable assumption in this case, since the test solutions were continuously aerated, thereby achieving enhanced mixing.

It is therefore evident from this study that, whereas reliable model predictions were attainable from a well defined, controlled system, after recalibration of the experimental data, performing the same task for a solution that was seemingly more

5. Properties and volatilisation of HCN

predictable in experimental terms, proved to be far more complicated in a natural environment. Apart from neglecting the effect of wind, the assumption of a steady state system is also questionable, as filling of a tailings pond is normally done semi-continuously. Furthermore, the effect of the presence of different ore solid particles was not taken into consideration in this study.

Clearly, many variables would have to be considered in the estimation of natural cyanide attenuation. More important, though, is to recognise the valuable contribution from this work, being the conclusion that the mechanism of cyanide loss from residue and tailings solutions may be conceptualised in three separate compartments, where volatilisation is the last step in the process, and which is dependent on the free cyanide formed by the processes preceding it. This idea is essentially the first step in understanding the sequence of events that take place once a tailings solution is discharged into a natural environment.

5.3.2 Roughness Reynolds number model

In a study conducted by Cohen et al (1978), a methodology was proposed to correlate in-situ measurements of environmental data for the volatilisation mass transfer coefficient to laboratory measurements, by assuming a vertical mean logarithmic velocity profile in the gas phase:

$$U = \frac{U^*}{K} \ln \left(\frac{Z}{Z_0} \right) \quad [\text{Eq. 5.12}]$$

where

U	=	Wind velocity [m/s]
U*	=	Friction velocity [m/s]
Z	=	Measured wind velocity height [m]
Z ₀	=	Effective roughness height [m]
K	=	Von Karman constant, taken to be 0.4

The friction velocity and effective roughness height is defined here by an adaptation of the Reynolds number for fluid flow, namely the roughness Reynolds number, Re*, previously developed by Wu (1969):

5. Properties and volatilisation of HCN

$$\text{Re}^* = \frac{Z_0 U^*}{\nu_a} \quad [\text{Eq. 5.13}]$$

and

$$U^* = U_{10} \sqrt{C_D} \quad [\text{Eq. 5.14}]$$

where U_{10} = Wind velocity at a height of 10 m in the environment or 10 cm in the laboratory [m/s]

C_D = Drag coefficient or wind stress coefficient of wind over water

ν_a = Kinematic viscosity of air [m²/s]

Combining these three equations results in an overall expression for Re^* based on the drag coefficient and velocity measurements:

$$\text{Re}^* = \frac{Z_{10} U_{10} \sqrt{C_D}}{\nu_a e^{0.4/\sqrt{C_D}}} \quad [\text{Eq. 5.15}]$$

Wu (1969) also derived formulas for the wind stress coefficient from data presented in thirty independent studies, which he classified into three regimes:

Breeze (0-1 m/s): $C_D = 1.25 \times 10^{-3} / U_{10}^{1/5}$ [Eq. 5.16]

Light wind (3-15 m/s): $C_D = 0.5 \times U_{10}^{1/2} \times 10^{-3}$ [Eq. 5.17]

Strong wind (>15 m/s): $C_D = 2.6 \times 10^{-3}$ [Eq. 5.18]

However, while the formulas for light and strong winds showed good correlations with the compiled data, the expression derived for a breeze results in a sudden increase in the drag coefficient at these very low wind speeds, as illustrated in Figure 5.12. This particular expression was based on data from one study only, as equal weight was assigned to every data point in this study. However, as this trend could not be adequately explained, the decision was made to use the same formula for a light wind to predict the drag coefficient at wind speeds below 1 m/s for the purposes of this study.

5. Properties and volatilisation of HCN

The discontinuity at wind speeds above 15 m/s was found to be the result of an increase in the wind velocity beyond the average wave phase velocity, implying that there exists a critical wind velocity (15 m/s). Below this wind velocity, the waves are responsible for pulling the air mass, but above the critical velocity, the air mass will start to pull the waves instead, leading to a change in the airflow structure and consequently the wind stress coefficient. The wind stress coefficients calculated from the formulas discussed above are also illustrated in Figure 5.12.

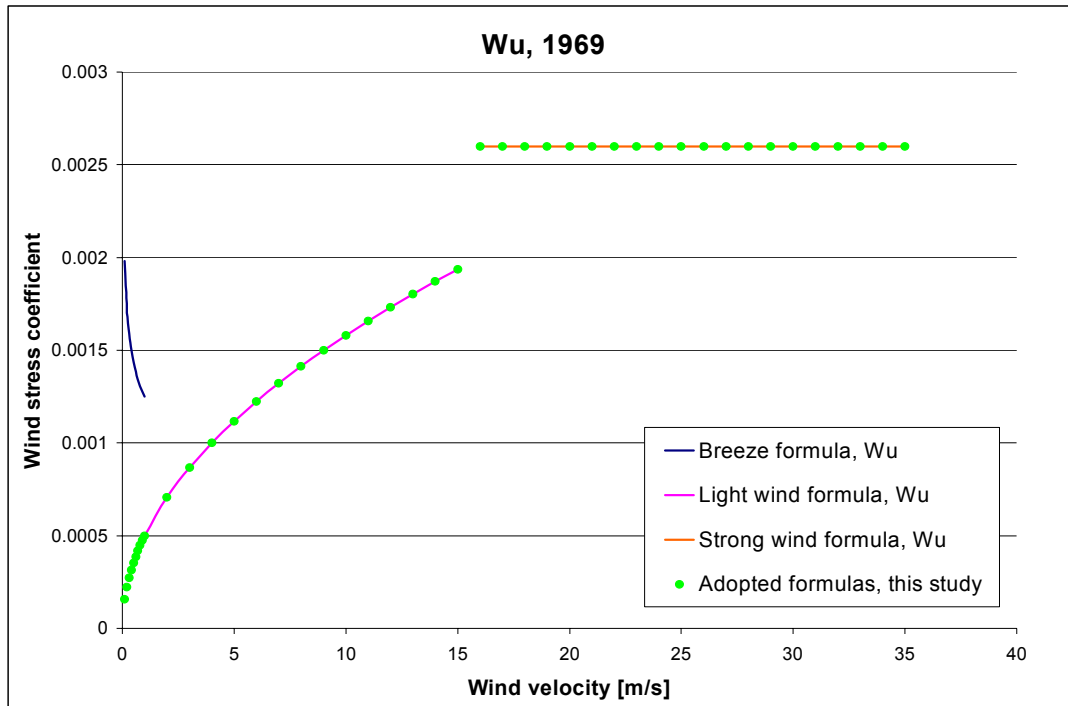


Figure 5.12. Summary of wind stress coefficient formulas and formulas adopted from Wu (1969).

Thus, Cohen et al (1978) suggested that it should be possible to correlate laboratory data for the mass transfer coefficient to Re^* , using the correlation in Eq. 5.15, and applying the drag coefficient formulas adopted from Wu (1969), to within an acceptable degree of accuracy, which could then be applied to environmental conditions. This provides a possible method of accounting for the effects of wind on volatilisation.

5. Properties and volatilisation of HCN

5.3.3 Re-aeration constant model

The re-aeration constant of oxygen $(k_v^O)_{env}$ is commonly used to describe oxygen transfer into various environmental water bodies, including the sea, ponds, lakes and rivers. Due to the reasonable availability of this data, the volatilisation rate constant of a chemical is often correlated to $(k_v^O)_{env}$ (Mackay, 1977, Smith et al, 1980). Since environmental factors such as temperature, turbulence, surface-active organic layers and wind effects may all be incorporated into the determination of $(k_v^O)_{env}$, the environmental volatilisation rate constant for another substance may be estimated by applying

$$(k_v^C)_{env} = \left(\frac{k_v^C}{k_v^O}\right)_{lab} (k_v^O)_{env} \quad [\text{Eq. 5.19}]$$

where k_v^C = Volatilisation rate constant of component C [h^{-1}]

k_v^O = Volatilisation rate constant of oxygen [h^{-1}]

_{env} denotes measurement in the environment

_{lab} denotes measurement in a laboratory

This is a useful tool for extrapolating laboratory measurements to predict environmental volatilisation rate constants. In the case of a lake or pond, though, the flow conditions will be less turbulent than under laboratory conditions and Smith et al (1980) suggested that the correlation be adjusted as follows to improve the accuracy of these predictions:

$$(k_v^C)_{env} = \left(\frac{k_v^C}{k_v^O}\right)_{lab}^{1.6} (k_v^O)_{env} \quad [\text{Eq. 5.20}]$$

Furthermore, they reviewed the published values for $(k_v^O)_{env}$ from various water bodies, as shown in Table 5.6. These values were all based on data obtained before 1920, indicating an obvious need for additional research on this topic. They also did not specify the season or regions for which this data was obtained. In addition, these coefficients were determined for natural water bodies, which one would expect to behave very differently compared to mining solutions, where the influence of chemicals added during processing, and the presence of fine pulp solid particles may play a major role.

5. Properties and volatilisation of HCN

Table 5.6. $(k_V^o)_{env}$ determined for various water bodies (Smith et al, 1980).

Water body	Range for k_V^o [day ⁻¹]	k_V^o correlated to depth [day ⁻¹]	k_V^o correlated to depth [h ⁻¹]	Depth, L [cm]
Pond	0.11-0.23	0.19	0.008	200
River	0.1-9.3	0.96	0.040	300
Lake	0.1-0.3	0.24	0.010	500

Lye et al (2004) used their own data of k_V and k_{OL} to estimate k_G and k_L for HCN as 620 and 25 m/h, respectively. These values correspond to a k_H value of 0.144 atm.mol/L, an agitation rate of 160 rpm, which was considered to be mild agitation, and a temperature of 25°C.

Their value for k_i is comparable with the known value for oxygen in water, at the air-sea interface (20 cm/h) (Liss and Slater, 1974). Using a correlation published in their paper, a value of 245 is calculated for k_g of HCN, which is significantly lower than that estimated by Lye et al (2004). This result indicates that the gas phase resistance to mass transfer predicted by Liss and Slater (1974) is about 2.5 times higher than that estimated by Lye et al (2004). Considering that the work of the former was based on data obtained for air-sea interfaces, it is likely that the additional factors, as mentioned above, do indeed play a role in defining the mass transfer rate. It is therefore suggested here that it would be risky to compare typical oceanic, or other environmental data for volatilisation rates, with a system containing metallurgical process solutions, as these are not natural solutions and therefore would not necessarily behave in a similar way.

5.3.4 AMIRA models

The new requirements of the Australian National Pollutant Inventory (NPI) for site personnel to estimate and report annual cyanide emissions from plant operations as of 1 July 1998, has prompted the development of HCN emission calculators for process tanks and tailing storage facilities (Lye, 2001). These models were developed by a group called AMIRA (Australian Mining Industry Research Association) and are currently being used in Australia to report HCN emissions.

5. Properties and volatilisation of HCN

- Leach tank model

This model relates solution pH, degree of agitation and cyanide concentration to the emission of HCN per hour. The correlation used in the model is

$$E = 1000 \times \left\{ (0.013 \times [HCN_{(aq)}] + 0.46) \times A \times \frac{T}{10^6} \right\} \quad [\text{Eq.5.21}]$$

where E = Emission of HCN [kg]

$$[HCN_{(aq)}] = [NaCN] \times 10^{(9.2-pH)}$$

[NaCN] = NaCN concentration in leach/adsorption tank [mg/l]

pH = pH of pulp

A = Surface area of leach/adsorption tank [m²]

T = Period of emission [h]

The factors 0.013 and 0.46 used in the correlation were the empirically determined correction and degree of agitation factors corresponding to the conditions of the specific units. In addition, this model has since been validated, but only in covered leach tanks, which are sometimes encountered in Australia, and used to prevent excessive losses of cyanide through volatilisation. Further investigations by AMIRA on this model are pending.

Unfortunately, the empirical factor of 0.46, that is applied here to account for the degree of agitation, is specific to the site where this model was tested, and can not be generally applied to leach operations where different stirring rates and tank dimensions are used. Furthermore, the effect of aeration has not been considered here, which is crucial considering that the majority of leach operations in South Africa makes use of aerated pachuca tanks.

Since this model was only applied to closed tanks that are used in Australia, one would expect a semi-equilibrium state to be reached, above the tank surface, whereby further volatilisation would be suppressed. However, in South Africa, only open air leach tanks are currently used, where one would expect much higher losses due to volatilisation, as gaseous HCN is continuously swept away by wind currents,

5. Properties and volatilisation of HCN

and a maximum concentration gradient is therefore maintained above the tank, enhancing volatilisation rates. This effect would also be determined by the effective wind velocity and fetch on the solution surface.

The model developed by AMIRA would therefore not be appropriate to use in current South African operations, as all these additional factors would have to be accounted for.

- Tailing storage facility model

In addition, a TSF emission model has also been developed by AMIRA (Eq. 5.22), which is based on a modelling parameter ($V\%$) that was determined for various pH values. The model was validated through intensive sampling over a 44-hour period, nearly one residence time in their case, at the Marvel Loch gold mine decant pond in Australia. The pond surface area and solution volume was estimated, and the wind speed measured to be an average of 2 m/s. A mass balance was performed for all samples taken and compared to the model predictions for each sample. Comparison of the emission rates measured and calculated (0.065 g CN/h.m^2 and 0.234 g CN/h.m^2) indicates that this model might serve as a reasonable first approximation, but the overestimation of over 300% suggests that more accurate estimations are necessary.

$$\text{HCN}_{(g)} = [\text{CN}_{\text{TSF water}} \times V_{\text{Slurry}}] \times V\% / 100 \quad [\text{Eq. 5.22}]$$

where	$\text{HCN}_{(g)}$	= $\text{HCN}_{(g)}$ released from TSF surface [g]
	$\text{CN}_{\text{TSF water}}$	= Free cyanide concentration in TSF water [g/m^3]
	V_{Slurry}	= Volume slurry to TSF [m^3]
	$V\%$	= Modelling parameter based on pH of slurry, as shown in Table 5.7

5. Properties and volatilisation of HCN

Table 5.7. Modelling parameter established for AMIRA TSF model (NPI Emission Estimation Technique Manual for Gold Processing, 1999).

pH	% of Natural degradation due to volatilisation [V%]
6	90
7	90
8	80
9	60
10	20
11	0
12	0

Although this model is currently being used in Australia for reporting purposes, it is clear that it can only serve as a short-term solution to the inventory problem, as it does not take other important factors, such as temperature, turbulence or degree of mixing, wind effects, presence of solids, etc. into consideration. Furthermore, this model is only applicable to the decant pond, and possibly the return water dam, and therefore the assumption would have to be made that HCN is only emitted from the decant pond, and not the tailings surface surrounding the decant pond. This might be reasonable in Australia, where the decant pond is generally much larger compared to those in South Africa. However, considering that by far the largest surface, on a typical local tailings storage facility, would consist of a combination of so-called dry and wet beach, still containing the various forms of cyanide species in the interstitial solution phase, one would expect the volatilisation of the available free cyanide from this surface to be significant.

6. Project objectives and scope

6. PROJECT OBJECTIVES AND SCOPE

Although the models described in section 5.3 are promising as a first step in the right direction towards reliable prediction of HCN emissions, their current applicability and accuracy is limited and further improvement is required. There is ongoing pressure on industry to develop more reliable methods for these predictions, especially in the light of the international trend to introduce more stringent cyanide legislation. This is largely due to recent events, such as deaths of migratory birds in East and West Africa, Australia and Namibia, as well as ground water contamination.

Consequently, this project was launched as one module of an umbrella project called the CN Balance project, with the goal of broadening knowledge and understanding of cyanide loss mechanisms through research, and ultimately developing methods that can be applied as tools to complete the cyanide mass balance to account for every pathway of cyanide consumption, loss or degradation. The other modules, which are currently being carried out in parallel to the volatilisation module, are ultraviolet degradation, metal speciation (including precipitation) and thiocyanate formation.

The *primary scope* of the project was therefore to investigate the processes by which cyanide losses, through volatilisation, occur from the leaching vessels and tailing storage facilities utilised during gold processing. This includes the environmental and operational factors that are to be considered in the practical determination of hydrogen cyanide emissions from these liquid bodies, with specific reference to pH, free cyanide concentration, temperature, flow configuration, wind velocity, depth and salinity of the solution, and the presence of solid particles.

6.1 Equilibrium study – Henry's Law constant

Although the equilibrium conditions and constants have been investigated before, the first aim of this study was to examine Henry's Law, using a different technique to those mentioned in section 5.1.2 of the literature review, i.e. direct measurement of the $\text{HCN}_{(g)}$ concentration in the gas phase. In addition, continuous data logging was employed to examine the time-dependence of equilibrium development and to establish Henry's constant for various conditions.

6. Project objectives and scope

The goal of this investigation was primarily to clarify the applicability of, or deviation from, Henry's Law under different conditions. The following parameters were investigated individually:

- Free cyanide concentration
- Temperature
- pH
- Salinity

These parameter values were chosen based on their applicability to typical conditions that may be found in South African gold plant operations across the leach circuit and tailings storage facilities, with the exception of the maximum salinity values, for which much higher values, than would typically be found in local process solutions, were investigated. The purpose of this was to confirm the insensitivity of k_H to salinity.

6.2 Volatilisation rate investigation – Mass transfer coefficients

A wind tunnel apparatus was designed to facilitate the determination of the volatilisation rate of hydrogen cyanide from both synthetic and pulp solutions in different flow scenarios and under various controlled conditions, including wind velocity, pH, free cyanide concentration, temperature, solution depth, flow configuration, salinity of the solution and the presence of solid pulp particles. This set-up thus enabled the mass transfer coefficient to be determined and ultimately to be correlated to the various parameters studied. Using this apparatus, the following parameters were studied:

- Temperature
- pH
- Flow configuration
- Free cyanide concentration
- Solution depth
- Pulp solid effects
- Wind velocity
- Presence of bird balls (plastic balls used to cover tailings surfaces)

6. Project objectives and scope

6.3 Conceptual model development

The data generated from the volatilisation experiments was used to develop a mass transfer coefficient prediction model. This model is based on empirical data obtained from a combination of laboratory and on-site measurements.

The two-film model, described in section 5.2.1, formed the theoretical basis for the logic and analysis of the results discussion presented in the section 8. Although it is recognised that this model may not be an accurate description of the conditions in stagnant solutions, which are often found in decant ponds and return water dams, the effect of turbulence was carefully considered in the application of this model by studying different flow regimes, including stagnant liquid bodies, flowing liquid bodies and thin flowing films.

Simovec and Snodgrass (1985) proposed that the loss of cyanide from gold mining solutions occurs in three stages, namely the dissociation of metal cyanide complexes, which may be influenced by ultraviolet irradiation, followed by hydrolysis of the free cyanide ion (CN^-) to form $\text{HCN}_{(\text{aq})}$ which then volatilises as $\text{HCN}_{(\text{g})}$. The focus of the present investigation was on volatilisation of hydrogen cyanide from its free form in solution, i.e. the cyanide anion. Therefore, in terms of the conceptual model of Simovec and Snodgrass (1985), the second stage in their model was taken as a starting point.

In addition, it is recognised that precipitation and thiocyanate formation may also affect the amount of free cyanide available in the second stage. However, referring to the discussion of cyanide attenuation mechanisms presented in section 4, the combined effect of these processes is not expected to be significant in comparison to volatilisation. Nonetheless, these additional mechanisms are currently being studied in other modules of the CN Balance project, and using the free cyanide concentration as a basis for this study still has the advantage that an adjustment to the starting point (CN^-) for the volatilisation model may be made, when adding all these modules to the comprehensive model at a later stage, without changing the volatilisation model. The aim is therefore to develop the volatilisation model, which is expected to account for the majority of cyanide losses, and thereafter refine the prediction model by adding all these additional, probably less significant effects.

6. Project objectives and scope

An adaptation of the conceptual model proposed by Simovec and Snodgrass (1985) is presented in Figure 6.1, indicating all the modules that will make up the final comprehensive model, including the volatilisation module, which is highlighted in red.

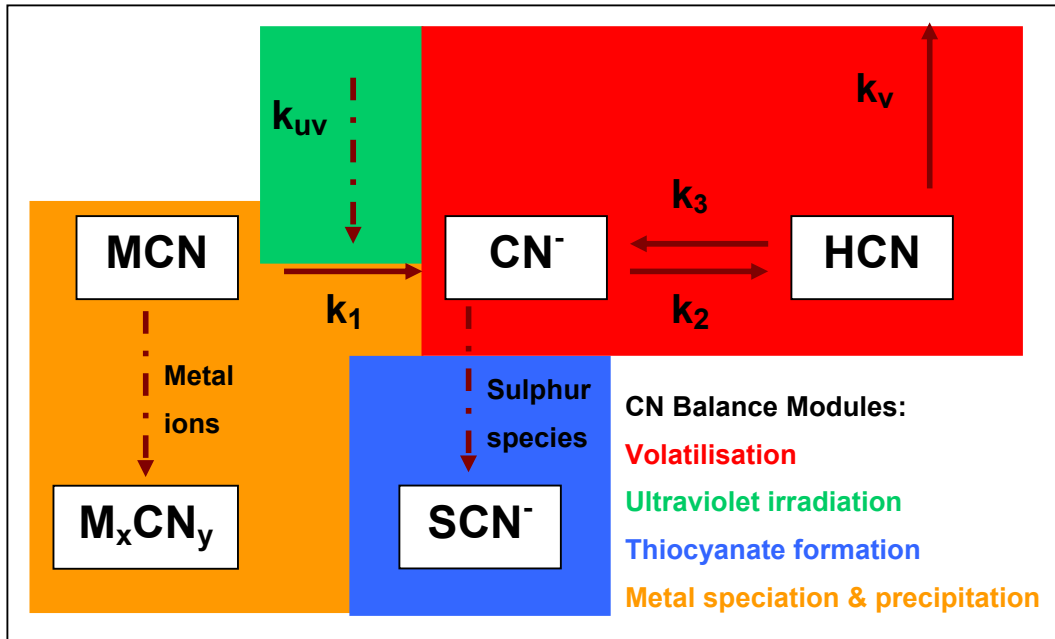


Figure 6.1. Schematic of adapted conceptual model indicating the individual modules in CN Balance project.

For the purposes of this study, a speciation model that has been developed by MINTEK, as discussed in Appendix B, as part of the metal speciation module, was used to calculate the free cyanide concentration of site pulp samples. This model has been shown to provide accurate predictions of the prevailing cyanide speciation chemistry, and has been used locally for site monitoring purposes since 2000. Using the known pK_A value for cyanide, the $\text{HCN}_{(\text{aq})}$ concentration was then calculated. In addition, the volatilisation model reduced to a one-stage mechanism, following the same assumption made by Simovec and Snodgrass (1985), namely that the equilibration between CN^- and $\text{HCN}_{(\text{aq})}$ is rapid, implying that the volatilisation stage would be the rate limiting step.

Furthermore, the methodology proposed by Cohen et al (1978) was used as a means of correlating the influence of wind on the mass transfer coefficient, through the use

6. Project objectives and scope

of the roughness Reynolds number (Re^*) and the drag coefficient formulas derived by Wu (1969).

6.4 On-site model verification

The ultimate purpose of this project was to develop a general, realistic volatilisation model allowing for easy application to a wide range of conditions that may be found on different sites. The final aim was therefore to validate the model predictions by performing an on-site experimental survey and estimating error margins between actual and predicted losses. A preliminary model verification exercise was executed at a local site, discrepancies were identified, and possible corrective methods proposed, for recalibration of the model.

7. Experimental methods

7. EXPERIMENTAL METHODS

7.1 Equilibrium test work

The equilibrium test work was carried out in a closed circuit, through which the cyanide solution was continuously circulated, in order to monitor and control the prevailing conditions, as shown in Figure 7.1. For each experiment, a 2 L batch of cyanide solution was made up, with a NaOH solution of pH above 12, to a specified cyanide concentration and salinity, where applicable. Deionised water and analytical grade reagents were used for all experiments. A 20 mL sample of the test solution was taken at the beginning of each experiment and analysed for cyanide.

A constant water bath was used to adjust and maintain the solution temperature. The water bath was set to the desired temperature and the solution was then introduced to a 10 L round bottomed glass test chamber by means of glass tubes that were specially made to circulate, fill and drain the solution from below the solution level, as indicated in Figure 7.1 and 7.2. A pH electrode, placed inside a glass electrode flow cell, was used to continuously measure the temperature and pH of the solution, while the $\text{HCN}_{(g)}$ concentration was continuously measured and logged using a direct $\text{HCN}_{(g)}$ sensor. An overhead stirrer was used in order to ensure efficient mixing of the gas phase in the sealed round-bottomed chamber.

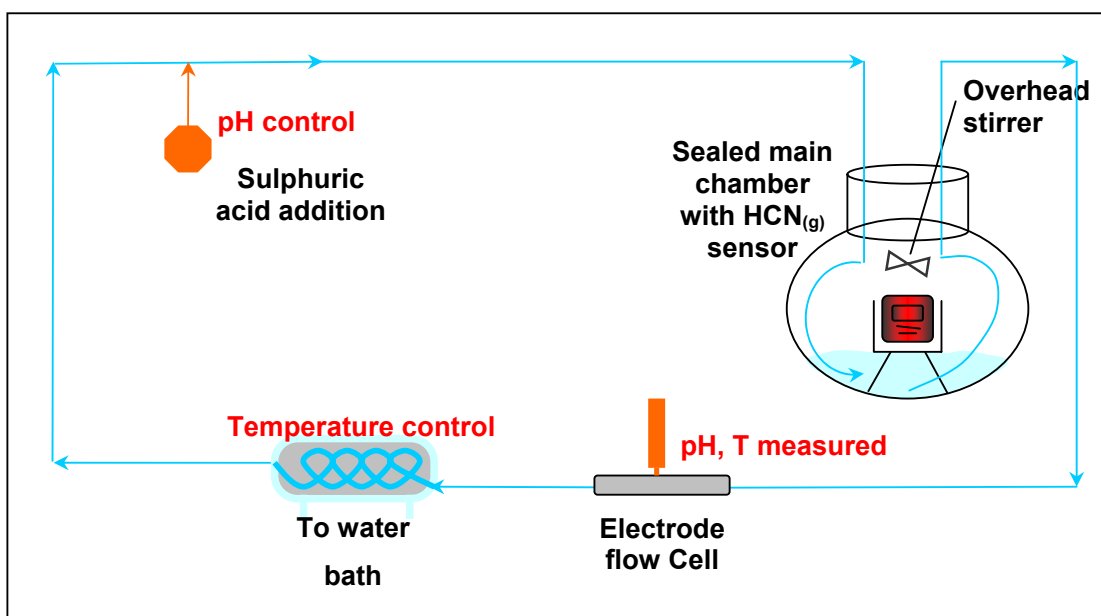


Figure 7.1. Experimental set-up used in equilibrium test work.

7. Experimental methods



Figure 7.2. Photo of experimental set-up used in equilibrium test work.

Once the system was at a steady temperature, the pH was adjusted to 12 by slowly adding 0.1 M sulphuric acid using a micropump. The system was allowed to equilibrate and the response of the $\text{HCN}_{(g)}$ sensor was monitored for a period of 20 to 30 minutes. The sensor was placed inside a glass beaker that was supported on top of the solution, allowing for direct measurements of the gas phase to be made. It was found that the system in the sealed chamber reached steady state after approximately 2 to 3 minutes.

The process was repeated by lowering the pH stepwise, each step resulting in a new, higher $\text{HCN}_{(g)}$ equilibrium concentration being reached, as the $\text{HCN}_{(aq)}$ concentration was effectively increased by lowering the pH, according to the hydrolysis reaction described in section 4.1.1. This was done up to the minimum pH and maximum $\text{HCN}_{(g)}$ concentration detectable by the gas sensor, which was 0-50 ppm $\text{HCN}_{(g)}$. Once the $\text{HCN}_{(g)}$ value approached the upper detection limit of 50 ppm, the experiment was stopped and the pH returned to 12.

7. Experimental methods

The parameter ranges for the investigation were:

- Free cyanide concentration: 10 to 200 ppm CN
- Temperature: 10, 20 and 35°C
- pH: 12 to minimum allowed by gas sensor detection limit
- Salinity: 0 - 1.5 M NaCl; 0 - 0.75 M CaCl₂.

7.2 Wind tunnel test work

7.2.1 Mass transfer coefficient measurements

The mass transfer coefficients were determined using the wind tunnel apparatus shown in Figure 7.3 and 7.4. This set-up was used to conduct laboratory tests using a thin film of solution flowing over a smooth glass plate, a flowing and stagnant solution body and synthetic pulps, for which each method will now be described:

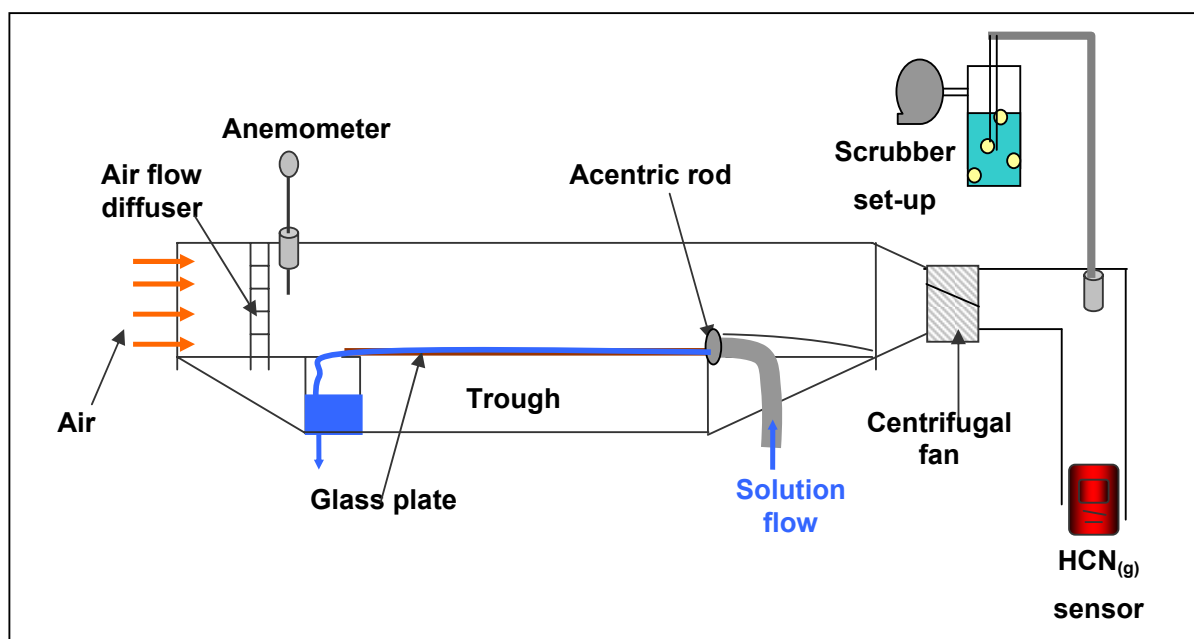


Figure 7.3. Wind tunnel apparatus used to measure mass transfer coefficients.

7. Experimental methods



Figure 7.4. Photo of wind tunnel apparatus used to measure mass transfer coefficients.

- Flowing solution film

A 20L bulk solution was used to ensure a constant cyanide concentration throughout the duration of the test. This solution was made up in a similar manner to that used for the equilibrium test work, by using a pH 12 NaOH solution as base and adding cyanide to the desired concentration. The solution pH was regulated by drop wise additions of 1M NaOH and 1 M H₂SO₄ with the use of a solenoid valve that was connected to a titrator regulation unit and pH electrode. The CN⁻ anion concentration was also constantly monitored using a CN ion specific electrode. The temperature of the bulk solution was maintained at the desired level by the use of a temperature regulator unit connected to a heating rod and thermometer.

Airflow was introduced to the duct at different flow rates using an adjustable centrifugal fan. This flow rate was measured using a thermal wire anemometer. In addition, a polystyrene insert was placed in the top side of the duct in order to achieve higher wind velocities for some tests by effectively decreasing the cross

7. Experimental methods

sectional area of the tunnel. A peristaltic pump was used to pump the bulk solution through a PVC rod, stretching across the width of the tunnel, over a smooth glass plate, in a counter current direction to the airflow. Fine holes drilled on the side of the PVC rod ensured that the solution was spread evenly over the entire width of the glass plate. A second, acentric rod was used to adjust the height of the liquid film.

Once the film was flowing evenly across the entire surface of the glass plate, the pH was adjusted to 11 by manually adding small quantities of 2 M sulphuric acid. A HCN gas sensor was placed in the exit side of the duct, which was fed into a suction head cupboard. Using the HCN sensor to monitor the increase in $\text{HCN}_{(g)}$ concentration resulting from the drop in pH of the flowing solution film, the system was allowed to reach steady state, i.e. until the $\text{HCN}_{(g)}$ concentration in the exit gas stream was constant. Although the gas sensor was used successfully in this test work for monitoring purposes, the $\text{HCN}_{(g)}$ concentrations were generally much lower than those measured during the equilibrium test work, and thus a scrubber set-up was used to more accurately determine these low $\text{HCN}_{(g)}$ concentrations, that were used in the mass transfer coefficient calculations. The scrubber set-up was connected to the exit of the duct and consisted of a scrubbing solution (0.1 NaOH), through which a slip gas stream was drawn with a small vacuum pump with an approximate pumping rate of 2 L/min. The use of the scrubbing solution ensured that all the sampled HCN would be trapped in the solution, which was later analysed for cyanide. In addition, a frit fitting was used to control the size of the gas bubbles in the scrubbing solution, to ensure adequate time and surface area for the transfer of the hydrogen cyanide to the solution.

Once steady state was reached, the scrubber pump was switched on and allowed to run for 15-30 minutes. After this time elapsed, the scrubber solution was changed and the gas stream was scrubbed for another 15-30 minutes. The bulk solution was also sampled in between every scrubbing exercise and analysed for cyanide. This routine was repeated at pH 10 and 9. The scrubber pump was also calibrated before and after every step.

- Flowing solution body

In this case, the glass plate was removed and the trough cavity was filled with the bulk solution once the pH and temperature was at the desired settings. The depth of

7. Experimental methods

the solution was 5 cm and the procedure was identical to that described above for a flowing film, except that the cavity was emptied in between each pH adjustment and refilled.

- Stagnant solution body

Once again, the glass plate was removed and the trough cavity was filled with the bulk solution once all the parameters were at their desired settings. However, once filled, the peristaltic pump was switched off and the scrubber was run for two intervals of 15 minutes, while care was once again taken to sample the trough solution in between each scrubbing to monitor the possible drop in cyanide concentration, as depletion of cyanide was possible due the smaller volume of solution contained in the trough cavity. As described before, the trough was emptied and refilled in between scrubblings.

The effect of so-called bird balls on the solution surface on the mass transfer of cyanide was also evaluated using this set-up. The bird balls were 10 cm diameter plastic balls obtained from an Anglogold Ashanti site in Mali.

- Synthetic pulps

Synthetic pulps were also manually introduced to the trough cavity. The pulps were made up by mixing silica quartz sand, which was ground to 80% +75 μm , and cyanide solutions of a specified concentration, to different solid to liquid ratios. In this case, the pH was not adjusted in between tests and a pH of between 9 and 10 was used. The pulp was sampled at the beginning and end of each test run. These samples were used to determine the interstitial cyanide present as described in Appendix C.

7.3 On-site test work

7.3.1 Leach vessel test station

Site work tests were conducted at two selected sites on aerated pachuca tanks as well a mechanically agitated tank with no aeration. A dome cover device, as shown in Figure 7.5, was used to encapsulate a defined area of the pulp surface, from which the volatilisation rate was measured, as a function of different air flow

7. Experimental methods

velocities, introduced to the encapsulated surface by means of compressed air and an air flow regulator.

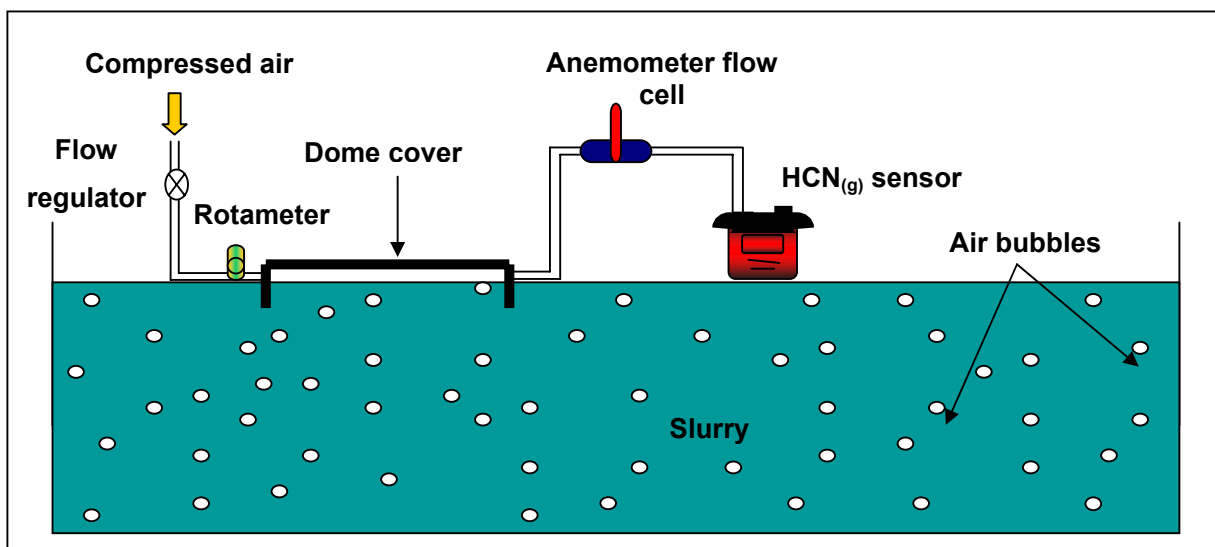


Figure 7.5. Set-up of leach vessel test station.

Measurement of the volumetric airflow rate entering and exiting the device was done by using a rotameter and an anemometer flow cell, respectively, and ensured that no air was lost in the system. The anemometer flow cell consisted of a sealed tube of known diameter containing the measurement probe of a thermal wire anemometer. The $\text{HCN}_{(g)}$ released was measured using a $\text{HCN}_{(g)}$ gas sensor connected to the exiting gas stream.

In the case of both the aerated and mechanically agitated tanks, the $\text{HCN}_{(g)}$ concentration in the device was allowed to reach steady state before introducing compressed air to the system. This would represent a pseudo-equilibrium value resulting from volatilisation from the pulp surface in the absence of air flow. In the case of aerated tanks, $\text{HCN}_{(g)}$ is also introduced by the $\text{HCN}_{(g)}$ in the air bubbles, that equilibrate with the pulp cyanide while travelling to the surface, and then release $\text{HCN}_{(g)}$ as it breaks the surface. For every test, a bucket was filled with the pulp liquor and allowed to stand for approximately 2 hours, after which the clear solution phase was decanted and sampled for a complete cyanide and metal speciation analysis. The aeration rates were also noted where applicable.

7. Experimental methods

7.3.2 Tailings storage facility test stations

Similar to the leach vessel test stations, a dome device was used to cover sections of the tailings surface, chosen to have different moisture contents. The set-up is shown in Figures 7.6 and 7.7. This was done by selecting areas where the tailings surface could be classified as dry, thixotropic, wet sludge, generally covered with a thin solution layer of less than 1 cm, and in areas where a thin film of solution was flowing over a very wet surface. In this case, once again due to the low levels of $\text{HCN}_{(g)}$ detected with these tests, a scrubber set-up was used, analogous to the one described in section 7.2.1. The small vacuum pump was used to introduce airflow across the covered surface through small air inlet holes, and then capture the HCN containing gas in a scrubber solution over a period of 3-4 hours. The scrubber solutions were taken back to the laboratory for cyanide analysis.

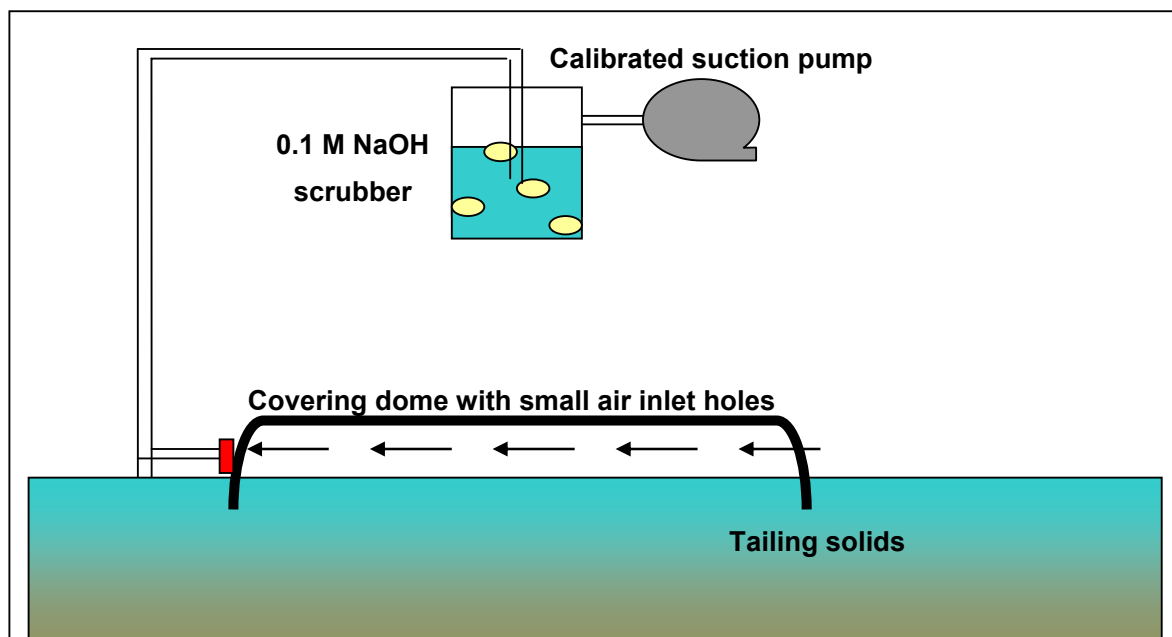


Figure 7.6. Set-up of tailings surface test station.

7. Experimental methods



Figure 7.7. Photo of tailings surface test station set-up.

7.3.3 Sampling methods

During each on-site work campaign, pulp, solution and solid samples were taken in order to perform a mass balance across the different sections, as well as for use in the on-site mass transfer coefficient calculations.

- Leach section sampling

Leach liquor solution samples were taken of the leach tanks where on-site work was performed as explained above. In addition, a complete section sampling exercise was performed on one site across the leach section and CIP circuit. A solution sample of each tank in the train was taken simultaneously and a complete cyanide speciation analysis was performed on each of these samples, in order to perform a complete mass balance across this section.

- Tailing storage facility sampling

7. Experimental methods

In the case of solution samples, grab samples were taken of the discharge stream at the tip point, the decant pond and the return water dam solution. These were sent for a complete cyanide speciation analysis. Solid samples were also taken from each test station location. In the last site work exercise, solid grab samples were taken along the walkable edge of a section of the wet beach area on the tailings surface. Sample lines were chosen in 10 m intervals along the one side of the wet beach. In each sample line, three samples were taken, i.e. one in the dry, hard part, one in the thixotropic region further in towards the wet area, and one in the very wet area, as far in as one was able to walk. Each of the solid samples collected on-site was analysed for interstitial cyanide present in the particular tailings.

7.3.4 Surface area estimations

Information on the total surface areas of the tailings storage facilities was obtained from geographic maps that were supplied by site personnel. In addition, aerial photographs were also obtained, which was used as an aid in the determination of the wet surface area. During the solid sampling exercise explained above, the three sampling points in each sampling line was marked with a flag and the position of each flag was logged using a global positioning system (GPS) instrument. These points were then plotted on the map for the particular tailing storage facility and, using the instrument software, the area covered by the path of the wet, thixotropic and dry lines, as formed by the flag markers, was determined. The shape of the total wet surface in relation to the logged wet path was inferred from the aerial photographs.

Furthermore, as the logged position points, that stretched over approximately 1 km, showed a relatively constant spread in distance between the different moisture content categories (wet, thixotropic and dry), it was assumed that the same spread applied to the opposite side of the wet beach, which was not physically logged. In this way, a reasonable approximation of the total tailings surface areas covered by wet, thixotropic and dry tailings could be determined.

8. Results and discussion

8. RESULTS AND DISCUSSION

8.1 Equilibrium test work

As explained in section 7.1, the equilibrium test work was performed in a closed vessel. A complete summary of all the equilibrium test work as well as sample calculations are shown in Appendix D. Figure 8.1 shows an example of the test results obtained. As illustrated, the test solution was initially kept at a pH of above 12, where only background levels of $\text{HCN}_{(g)}$ were detected by the gas sensor. As the pH was decreased, the CN^- ions present in the solution formed $\text{HCN}_{(aq)}$ according to the reaction in equation 3.1, which became available for volatilisation. As discussed before, the first step in this reaction is known to be relatively rapid and thus the equilibration time should be a function of the volatilisation rate. The time taken for the system to reach equilibrium after a pH change was made, was approximately 2-3 minutes. These results indicate that the equilibration of cyanide species in solution is as expected fast, but also that the mass transfer from the liquid to the gas is also relatively fast.

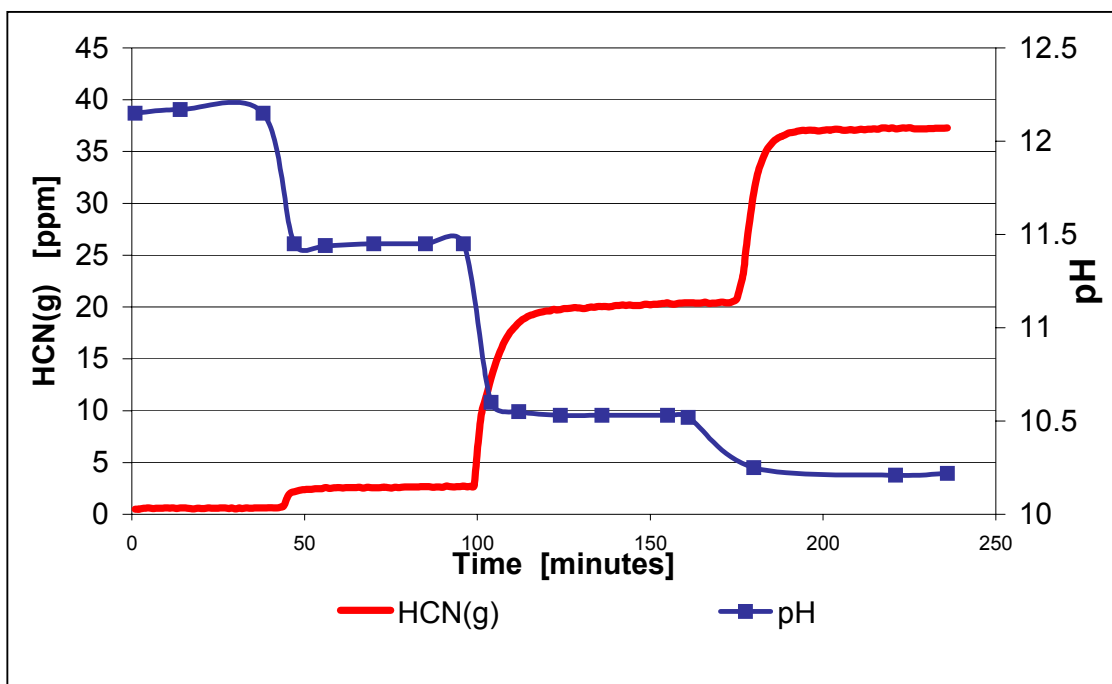


Figure 8.1. Measurement of $\text{HCN}_{(g)}$ evolved from a cyanide solution containing 105 mg/L cyanide as a function of pH (20°C, S→0).

8. Results and discussion

Furthermore, the flat shape of each step in the graph confirms that the system was at steady state, as the $\text{HCN}_{(g)}$ concentration remained at a steady value after equilibration. It was also evident from this observation that the gas phase was thoroughly mixed by the use of the overhead stirrer, otherwise the curves would have slowly drifted upwards during each step change. After completion of each test the pH was adjusted back to 12, and time allowed for the gaseous HCN to go back into solution. A sample was then taken and analysed for cyanide, which was compared to the analysis of the initial solution. No cyanide losses were experienced, confirming that there were no leakages in the system.

The results in Figure 8.2 further illustrate the role played by the two steps in the volatilisation mechanism. Firstly, the curves follow the same shape as the cyanide hydrolysis curve shown in Figure 4.2, because the equilibrium $\text{HCN}_{(g)}$ is directly related to the $\text{HCN}_{(aq)}$ according to Henry's law. The upper limit of the curve is clearly shown in the 10 ppm test run on the far left with the $\text{HCN}_{(g)}$ value limited by the available cyanide in the solution, i.e. the pH was reached where all the cyanide in solution had been converted to $\text{HCN}_{(aq)}$ and hence the $\text{HCN}_{(g)}$ also reached its limit.

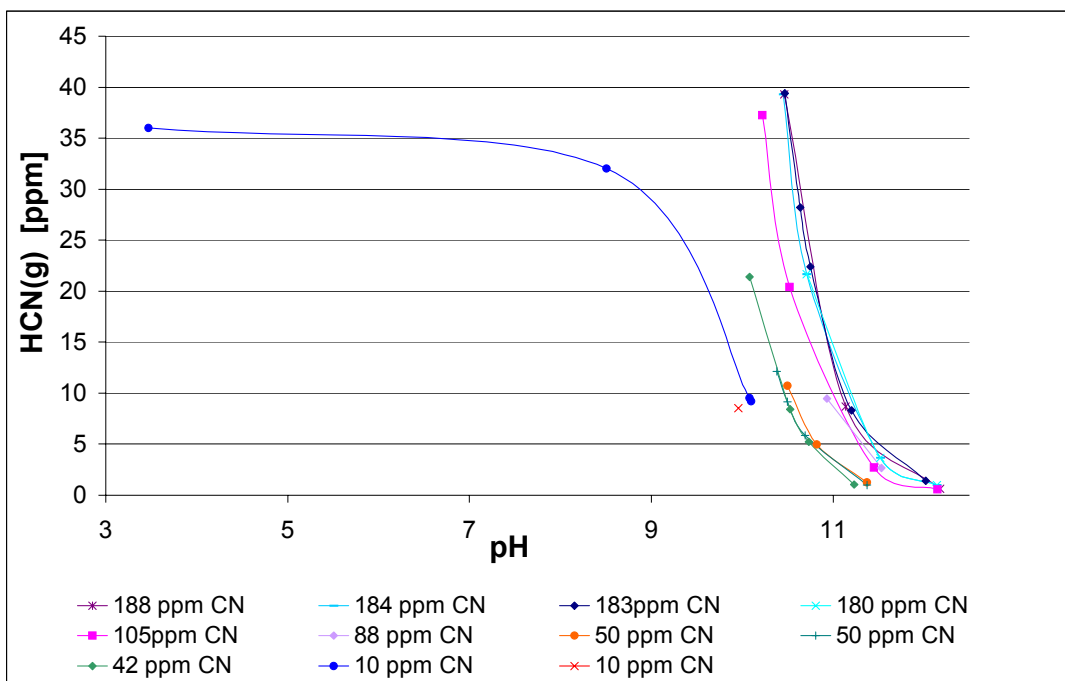


Figure 8.2. $\text{HCN}_{(g)}$ as a function of pH at different cyanide concentrations (20°C , $S \rightarrow 0$).

8. Results and discussion

In addition, it was observed that the position of the curves shifted to the right as the cyanide concentration of the test solution was increased. This was simply due to the higher concentration CN^- present at higher total cyanide concentrations, leading to higher $\text{HCN}_{(\text{aq})}$ and in turn higher $\text{HCN}_{(\text{g})}$ levels. Therefore, the higher the total solution cyanide concentration, the higher the equilibrium $\text{HCN}_{(\text{g})}$ concentration for solutions at the same pH.

The relation of the concentrations of $\text{HCN}_{(\text{g})}$ to $\text{HCN}_{(\text{aq})}$ is depicted in Figure 8.3. The straight lines, representing Henry's Law, show a good correlation, suggesting that k_{H} is independent of the total cyanide concentration. Recalling that the reviewed literature suggested that Henry's Law is obeyed up to cyanide concentrations of 4 000 ppm, this is confirmed by the present results.

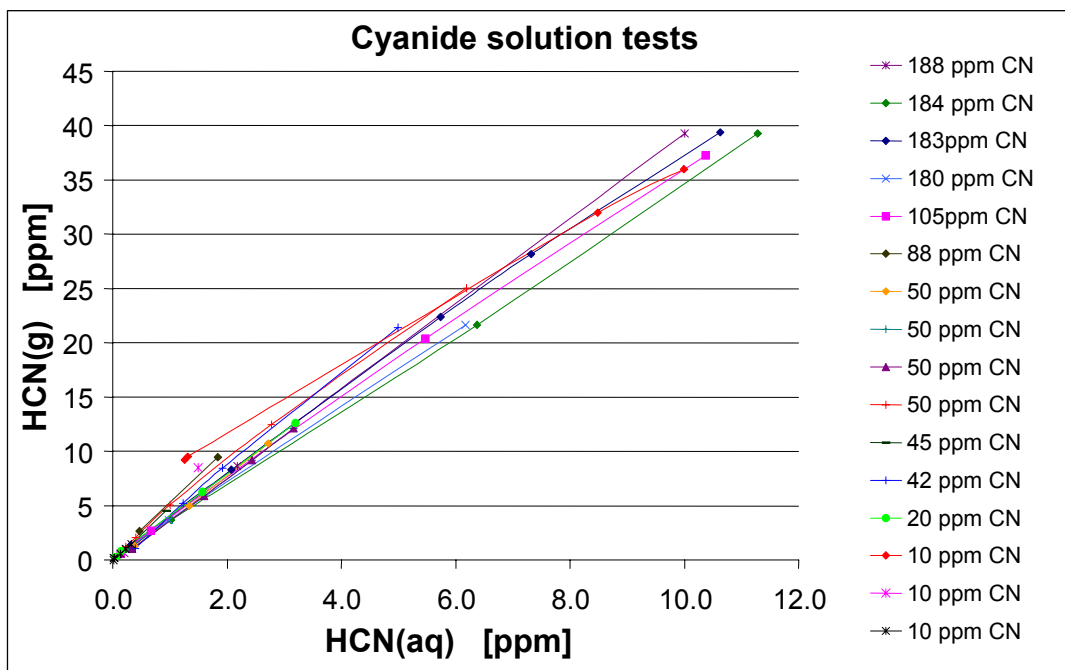


Figure 8.3. Equilibrium distribution of HCN between water and air for different cyanide solution concentrations (20°C, $S \rightarrow 0$).

8. Results and discussion

An average for this data set may be obtained graphically by fitting a straight line that displays the best correlation using a least squares fit. A good trend line fit is obtained ($R^2 = 0.99$), as shown in Figure 8.4, which returns a k_H value of 0.082 atm.L/mol.

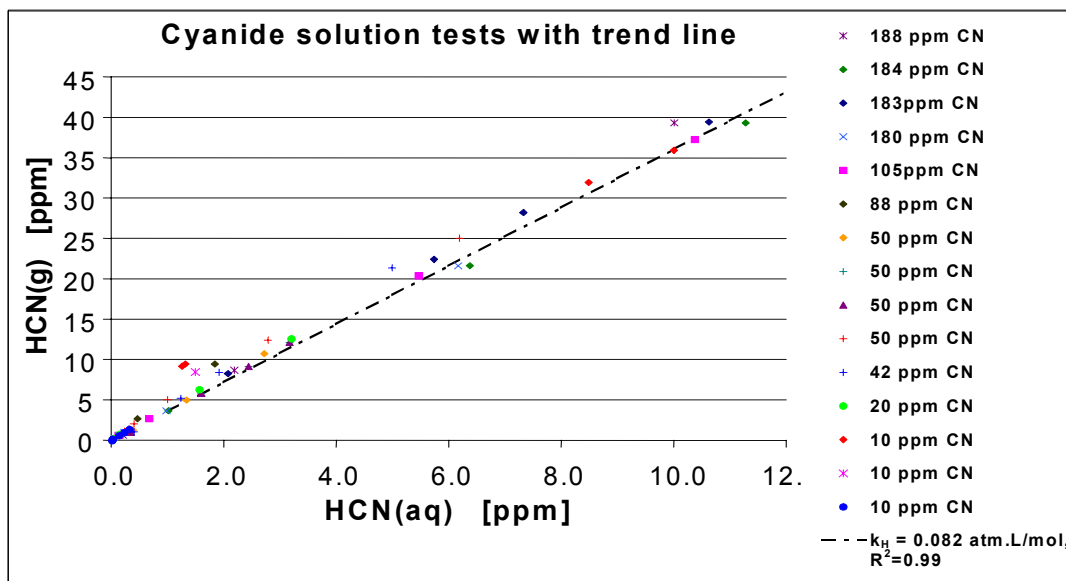


Figure 8.4. Best graphical trend line fit for pure cyanide solution tests (20°C, $S \rightarrow 0$).

The results from the salinity test work are shown in Figure 8.5 and 8.6. Using the hydrolysis curve for cyanide at different salinities, as shown in Figure 5.2, the amount of cyanide present as $\text{HCN}_{(\text{aq})}$ in the solution was calculated for each pH value. It can be seen that the straight-line dependence of $\text{HCN}_{(\text{g})}$ to $\text{HCN}_{(\text{aq})}$ is once again observed, showing that Henry's Law still applies and the slope of the line represents k_H .

Comparing the slopes of the experimental lines for both NaCl and CaCl_2 to the line obtained for the low salinity cyanide solution tests, it follows that the presence of salt in the solution increases the slope by as much as a factor of three. In addition, the higher the salinity the more pronounced this effect. This is often referred to as the 'salting-out' effect, whereby the presence of salt in the solution decreases the solubility of HCN in the solution, and therefore increases the partial pressure in the gas phase.

8. Results and discussion

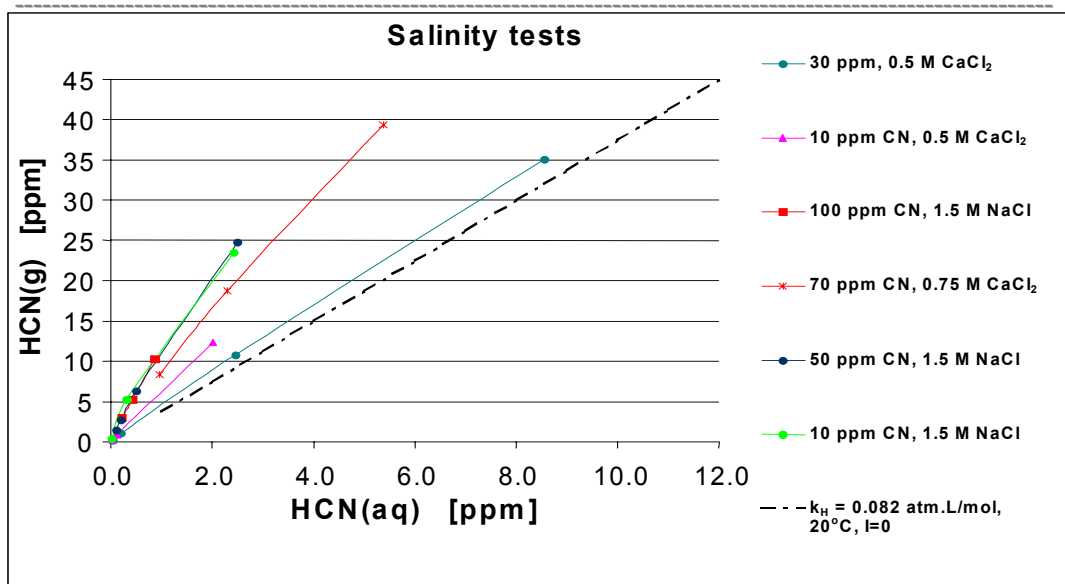


Figure 8.5. Influence of salinity, using NaCl and CaCl₂, on the equilibrium distribution of HCN between water and air for different cyanide solution concentrations (20°C).

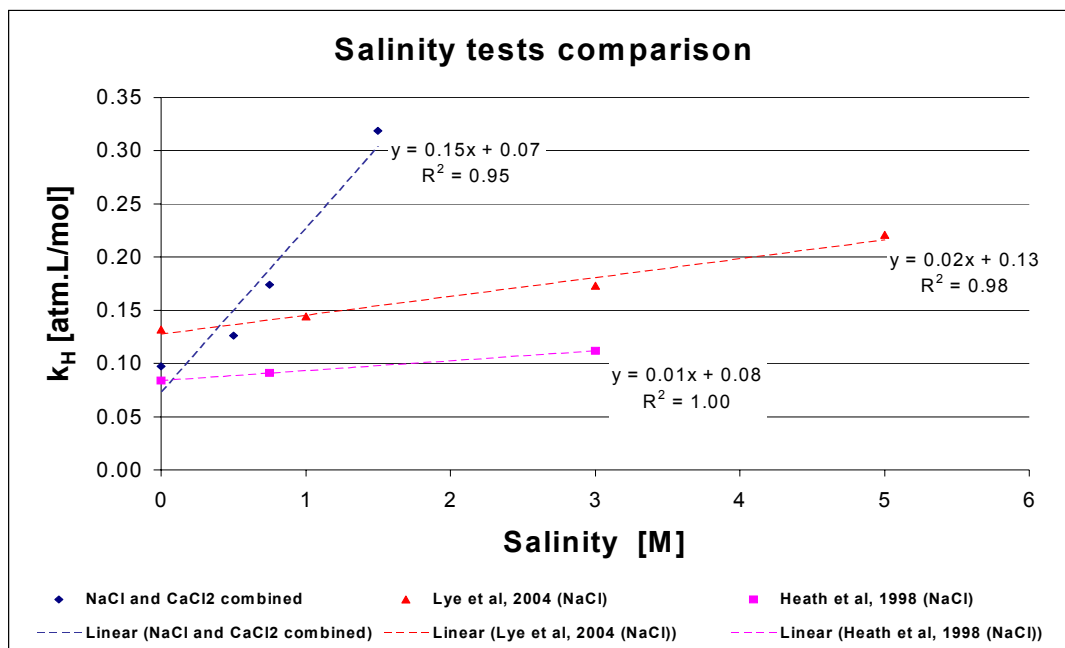


Figure 8.6. Effect of salinity, using NaCl or CaCl₂, on Henry's constant k_H at a temperature of 20°C.

Figure 8.6 illustrates the effect of salinity on k_H , ignoring whether the saline species present in the solution is NaCl or CaCl₂. It is evident that a strong linear correlation exists, which suggests that an increase in approximately 0.15 atm.L/mol can be expected with every 1 M increase in salinity, at least for NaCl and CaCl₂. It is further

8. Results and discussion

observed that the correlation predicts k_H at zero salinity to be 0.07 atm.L/mol, which compares well with the average determined from the low salinity cyanide solution test work (0.082 atm.L/mol).

Comparison of these results to those previously published in literature indicates that the effect of salinity was much more pronounced in this case. This cannot be attributed to the fact that the other studies used only NaCl, as the linear relationship obtained from this work would still have resulted in the same slope, had the two middle data points (CaCl₂ tests) in the combined NaCl and CaCl₂ curve been omitted.

The only obvious explanation to this would be the different experimental methods used. Whereas both Heath et al (1998) and Lye et al (2004) made use of sampling the gas phase in the headspace of a closed vessel, this study made use of direct HCN_(g) measurements by placing a gas sensor inside the headspace of the vessel. It is therefore possible that losses of HCN_(g) might have occurred while sampling the headspace in the previous two studies. However, that does not explain the fact that the zero salinity test of Heath et al (1998) came to approximately the same value for k_H , as determined in this study.

As for the influence of temperature, it was found that k_H increases with temperature, as can be seen from the increasing slopes with temperature depicted in Figure 8.7.

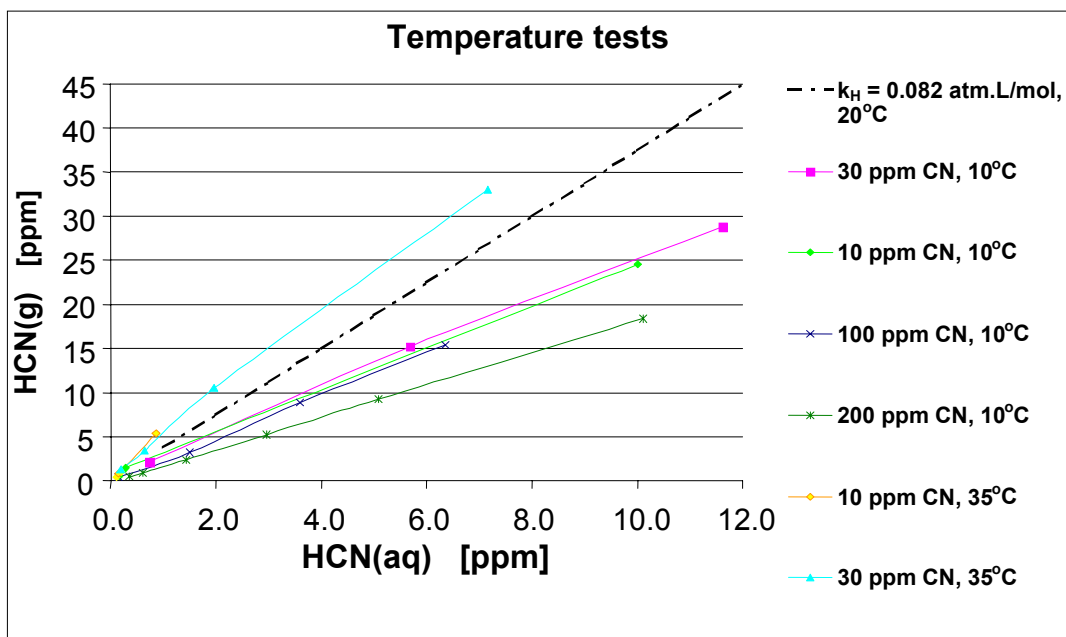


Figure 8.7. Effect of temperature on k_H at various cyanide concentrations (S→0).

8. Results and discussion

A correlation for the temperature dependence of the 10 ppm solution cyanide data set is shown in Figure 8.8, and is compared to the correlation derived from data presented by Dodge and Zabban (1952), as shown in Figure 5.3. The data is presented in a plot of $\ln(k_H)$ vs. $1/T$, according to the Van't Hoff equation for a chemical reaction:

$$\frac{d \ln K}{d(1/T)} = \frac{-\Delta H}{R} \quad [\text{Eq. 8.1}]$$

where K = Equilibrium constant
 T = Temperature (K)
 ΔH = Heat of reaction (J/mol)
 R = Universal gas constant (J/mol.K)

Thus, the gradient of the plot shown in Figure 8.8 represents the heat of reaction for the HCN equilibrium reaction.

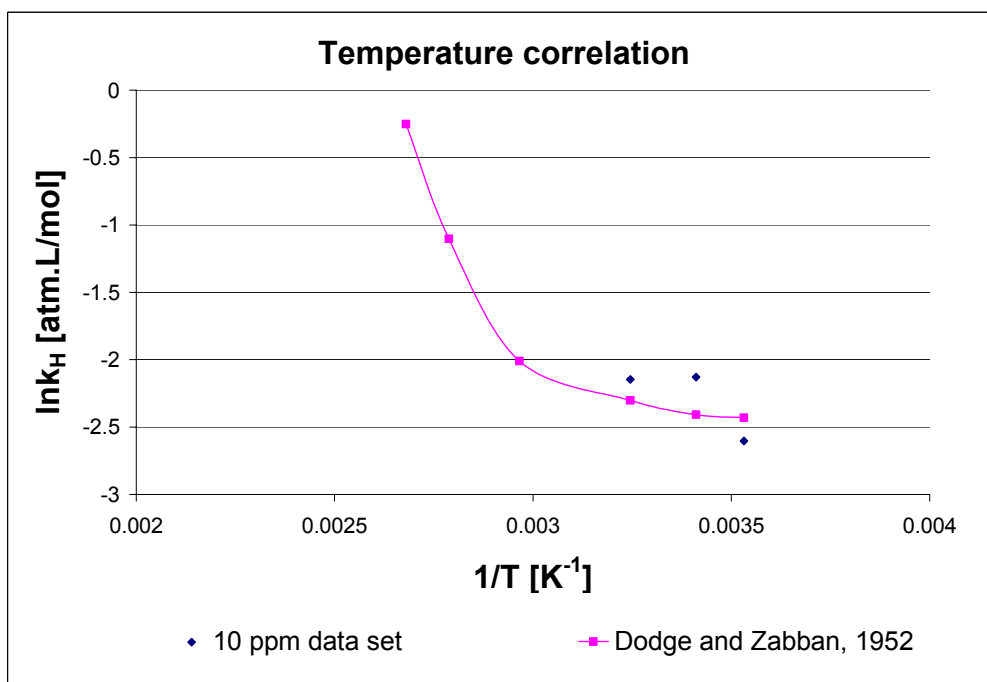


Figure 8.8. Temperature dependence of k_H for 10 ppm aqueous solutions and data from the literature.

8. Results and discussion

The correlations derived from these two data sets seem to be in good agreement. It is evident from this graph that the temperature dependency of k_H is low and typically not significant at ambient conditions, where $1/T$ is equal to 0.003 at 298K. However, at higher temperatures, the heat of reaction increases drastically, indicating that the effect becomes significant at elevated temperatures.

8.2 Wind tunnel test work

Before commencing the wind tunnel test work, the airflow in the duct had to be aligned in order to ensure laminar flow. This was quite a complicated task, and several combinations of air flow straighteners and fans were tested. Finally, it was found that laminar flow could be obtained by using the fan to suck in, rather than blow the air in. This eliminated the influence of the centrifugal action of the fan on the laminarity of the airflow inside the duct. Furthermore, a simple slitted sheet was used at the inlet side of the duct to help align the inflow of air. The fan was fitted with a shutter to facilitate manual adjustment of the airflow rate, and a polystyrene insert was used to achieve increased air velocities in the duct for some tests. The data presented in this section may be viewed in Appendix D.

Figure 8.9 shows the velocity profiles that were measured in the duct using a thermal anemometer, which was relatively sensitive to changes in the linear velocity. Nonetheless, the reproducibility of the measured profiles was found to be good, especially near the surface of the glass plate. No measurements could be taken within 2 cm from the plate, since the length of the anemometer probe tip was 2 cm.

As discussed in section 7.2, the wind tunnel apparatus was used to measure the mass transfer coefficient (K_{OL} , m/h) for both flowing and stagnant solutions. The first set of tests was conducted using a cyanide solution to investigate the influence of cyanide concentration, wind velocity and temperature on K_{OL} .

8. Results and discussion

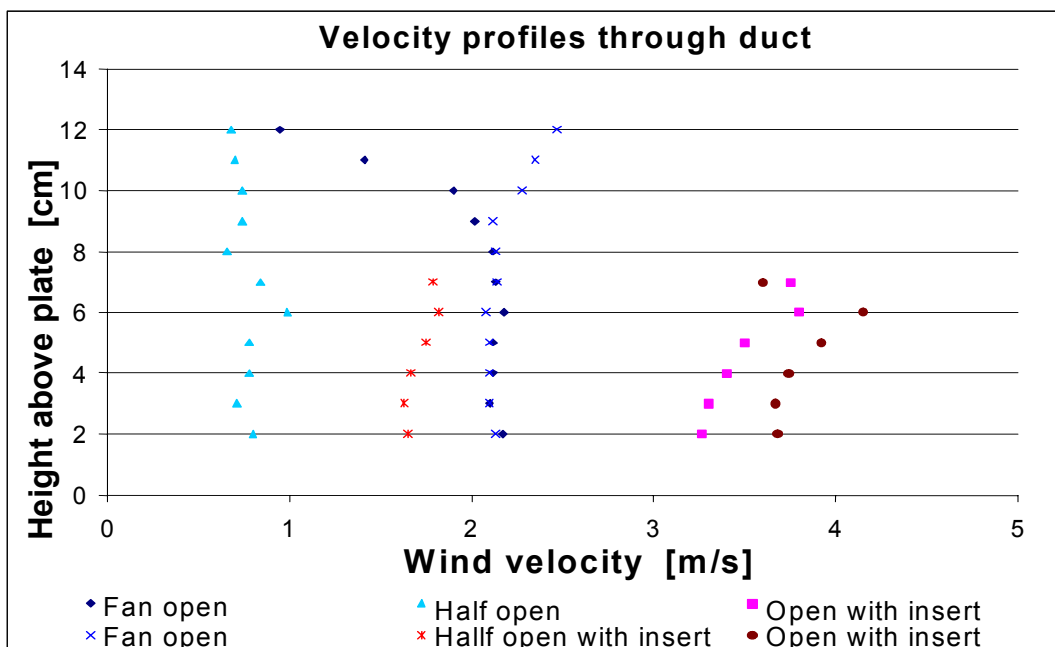


Figure 8.9. Velocity profile measurements inside the wind tunnel.

The results shown in Figure 8.10 indicate that K_{OL} is strongly dependent on the $HCN_{(aq)}$ concentration at low concentrations, but rather insensitive to concentration at higher concentrations. This validates the assumption made in the model hypothesis, discussed in section 6.3, that the $HCN_{(aq)}$ concentration may be used as a starting point for describing the volatilisation mechanism.

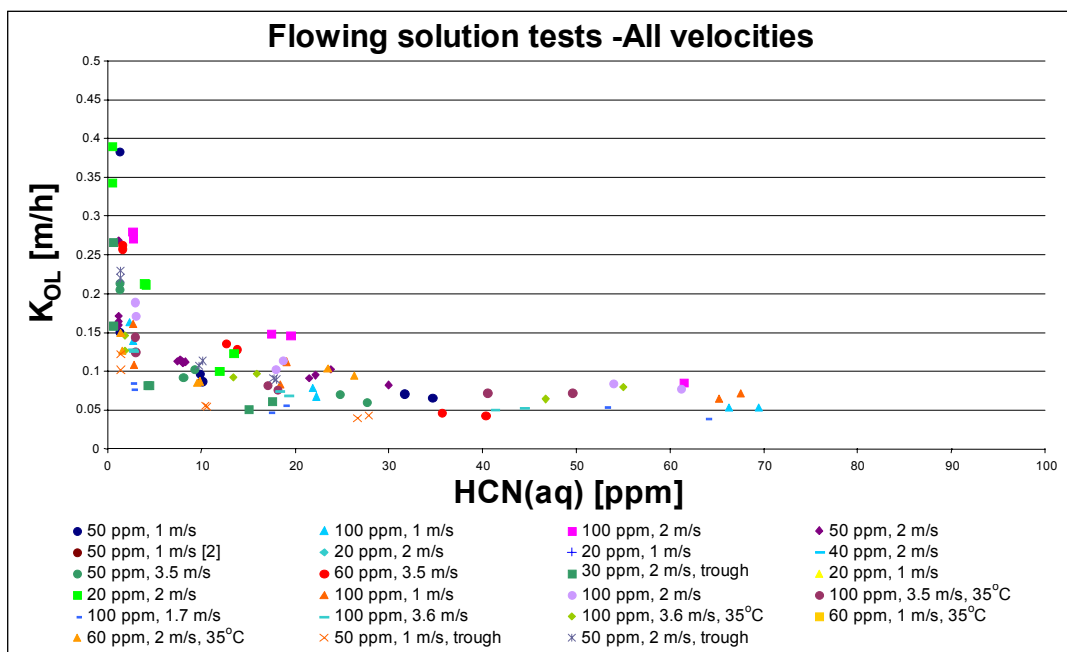


Figure 8.10. Mass transfer coefficient (K_{OL}) as a function of $HCN_{(aq)}$ concentration.

8. Results and discussion

A power curve correlation obtained from the combined data generated by all the flowing solution experiments (different cyanide concentrations, air flow velocities, temperature and solution depths) is shown in Figure 8.11. It follows from this correlation that, in spite of the wide range of experimental conditions covered by this data set, the correlation still fits the entire set relatively well.

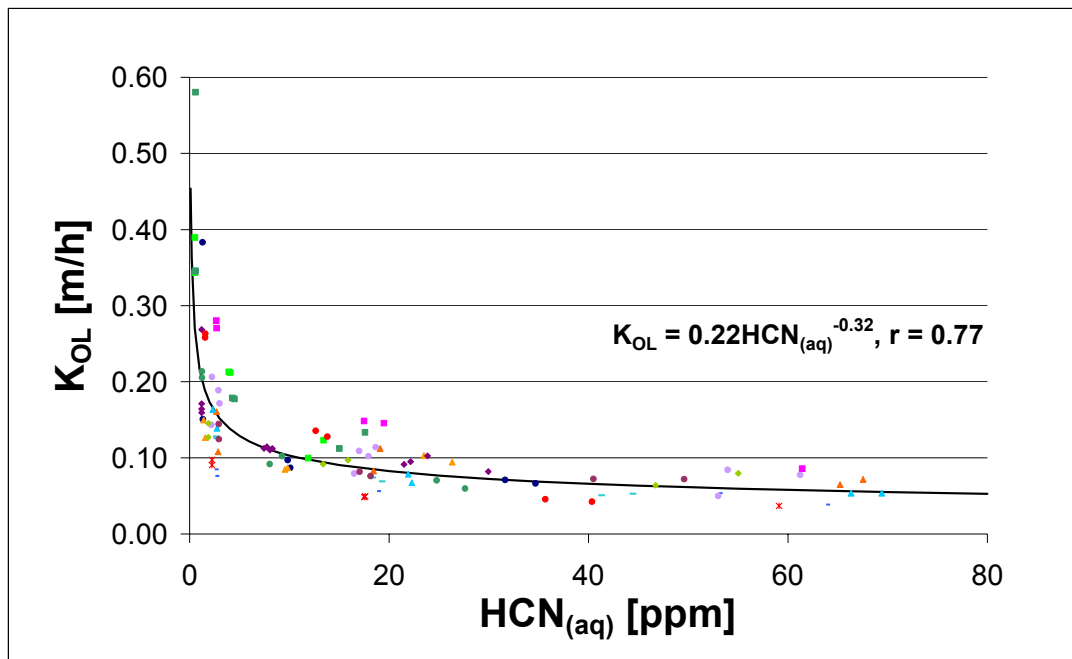


Figure 8.11. Correlation for K_{OL} as a function of $HCN_{(aq)}$ under flow conditions.

The trend observed for K_{OL} with respect to $HCN_{(aq)}$ is interesting, as one would expect that K_{OL} to be a constant value, where the volatilisation rate is a function of $HCN_{(aq)}$ by equation 5.2:

$$N''_{HCN} = k_{OL}(\Delta C) \quad [\text{Eq 8.2}]$$

This observation implies that there is a strong interaction between the HCN molecules, making mass transfer less efficient at higher concentrations. However, at $HCN_{(aq)}$ concentrations above ± 20 ppm, the curve flattens out to a constant K_{OL} value of roughly 0.06-0.07 m/h. A sensitivity analysis was performed to elucidate the role played by both k_g and k_l in the overall determination of K_{OL} , as per the two-film model presented in Figure 5.6. Using the calculation procedure suggested by Thomas (1982) to determine a theoretical K_{OL} value for HCN, k_g and k_l were

8. Results and discussion

calculated as 24.5 and 0.255 m/h, respectively. This returns a K_{OL} value of 0.068 m/h, which is non-specific to $\text{HCN}_{(aq)}$. For a theoretical estimation, this value compares surprisingly well with the experimental constant value (0.06-0.07 m/h) taken from the correlation in Figure 8.11 at $\text{HCN}_{(aq)}$ concentrations above 20 ppm.

Using this correlation, K_{OL} is calculated at 1 ppm (in the $\text{HCN}_{(aq)}$ sensitive region) to be 0.22 m/h. However, K_{OL} may also be calculated from knowledge of k_g , k_l and k_H , according to Equation 5.6. In this case, a value of 0.09 atm.L/mol is assumed for Henry's constant, as the salinity of all the test solutions is low and the temperature effects may be neglected, as discussed in the previous section.

The sensitivity analysis was now performed by assuming k_g to be constant at 24.5 m/h and manipulating the value of k_l to return a value of 0.22 m/h for K_{OL} . The same exercise was then repeated by fixing k_l at 0.255 m/h, and manipulating k_g , to return a K_{OL} value of 0.22 m/h. In this manner, the change necessary for each of these coefficients to reach a K_{OL} value of 0.22 m/h were determined. Table 8.1 shows the outcome of this exercise, indicating that, even if k_l is increased by 26 orders of magnitude, K_{OL} will not reach the required value of 0.22 m/h. Increasing k_g by a factor of 17.4, however, will return the required K_{OL} . This corresponds to a k_g of 427.5 m/h, which implies that mass transfer in the gas layer is more efficient at low $\text{HCN}_{(aq)}$ concentrations.

Table 8.1. Summary of sensitivity analysis of K_{OL} for HCN to k_l and k_g .

Sensitivity analysis of K_{OL} with k_l and k_g						
	K_{OL} [m/h]	k_g [m/h]	k_l [m/h]	Factor increase in k_g	Factor increase in k_l	
Curvefit correlation: $K_{OL}=0.22x^{0.32}$ (Experimental)						
Prediction at 1 ppm $\text{HCN}_{(aq)}$	0.220					
Literature correlation (Thomas)						
Prediction (not $\text{HCN}_{(aq)}$ specific)	0.068	24.5	0.255			
Resistance in layer		0.041	3.922			
Solve for $K_{OL} = 0.22$ by changing k_l	0.092	24.5	1.15E+26	1	4.5E+26	
Resistance in layer		0.041	8.67E-27			
Solve for $K_{OL} = 0.22$ by changing k_g	0.220	427.5	0.255	17.4	1	
Resistance in layer		0.624	3.922			

8. Results and discussion

Relating this finding back to the two film theory, the reader is reminded that this theory views volatilisation across a liquid surface to occur in three steps, assuming that both fluid masses are well mixed. These steps are mass transfer through the liquid boundary layer, followed by mass transfer across the liquid-gas interface, which is assumed to be described by Henry's Law, i.e. at equilibrium, and finally mass transfer through the gas boundary layer. The above finding may therefore be explained by accepting that, at low $\text{HCN}_{(\text{aq})}$ concentrations, the number of HCN molecules residing in the near surface region of the gas boundary layer is low compared to that formed at higher $\text{HCN}_{(\text{aq})}$ concentrations. It is therefore possible, that as these molecules accumulate in the gas boundary layer, the resistance to mass transfer in this region begins to increase due to the strong interaction between these molecules, thus decreasing k_g until a limit is reached.

Furthermore, the general shape of the curve remained unchanged at velocities ranging between 1 and 3.6 m/s. Note that the solution flow rate remained the same throughout (approximately 0.8 L per minute). Figure 8.12 compares the power fit correlation obtained in Figure 8.11, for all the tests conducted under flowing conditions, to individual correlations obtained for the 20°C and 35°C data sets, respectively. It is therefore evident that temperature does not play a significant role in the range studied here.

In addition, Figure 8.12 also shows that a change in solution depth, from a thin flowing liquid film on a smooth glass plate up to a 5 cm deep flowing solution body, may be considered insignificant.

8. Results and discussion

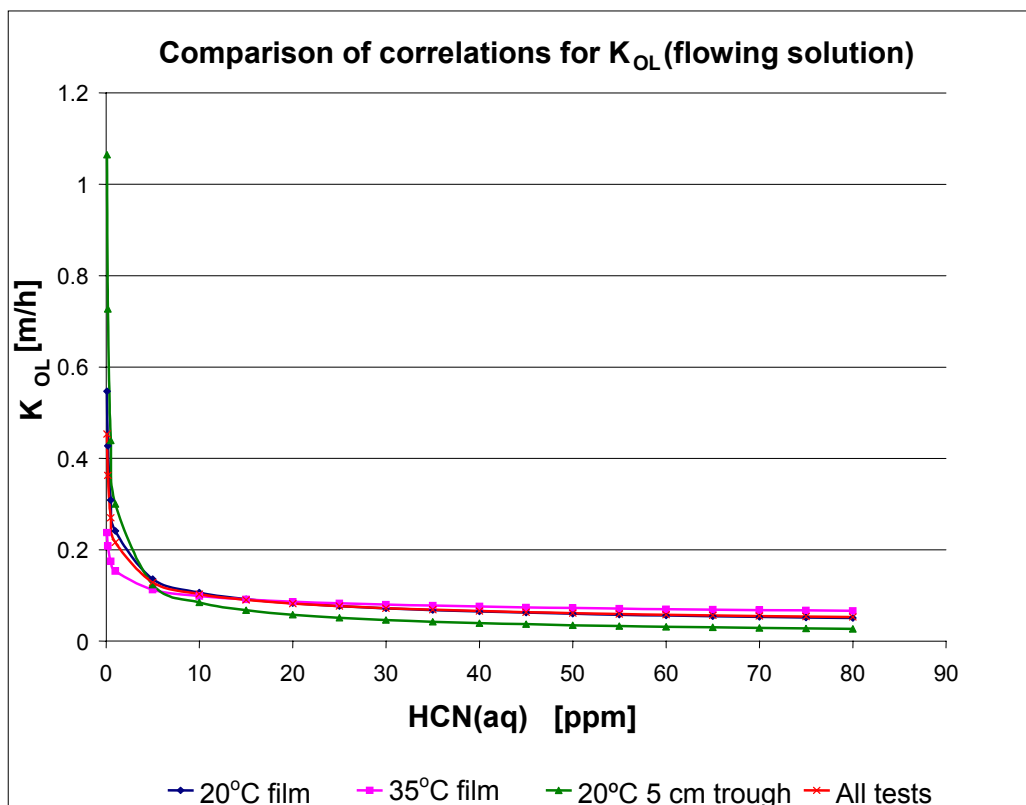


Figure 8.12. Mass transfer coefficient correlations for flowing solutions at 20°C, 35°C and 5 cm depth.

However, experiments that were conducted with stagnant solutions inside the trough, resulted in a notable decrease in K_{OL} , as depicted in Figure 8.13. A new power fit correlation is therefore shown in Figure 8.14 for stagnant solutions.

This observed effect of solution flow might be explained using the two-film theory. The decrease in turbulence, characteristic of stagnant solutions will lead to an increase in the boundary layer film thickness in the solution, leading to an increase in the film resistance, and therefore a decrease in the overall mass transfer coefficient, as was indeed observed.

8. Results and discussion

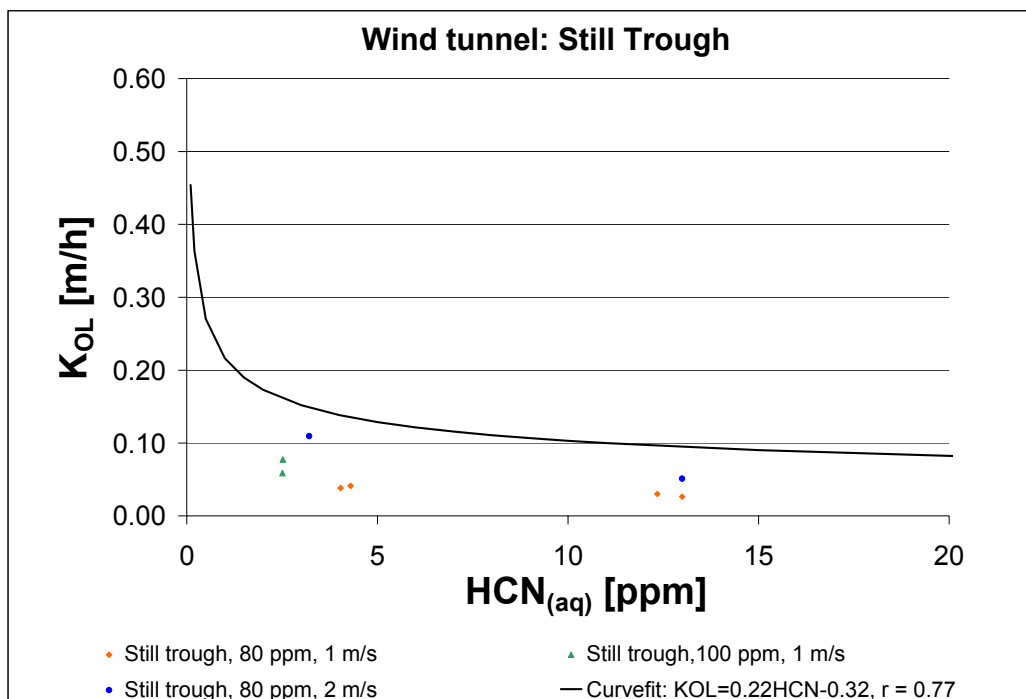


Figure 8.13. Mass transfer coefficient for stagnant trough solutions compared to correlation for flowing solutions.

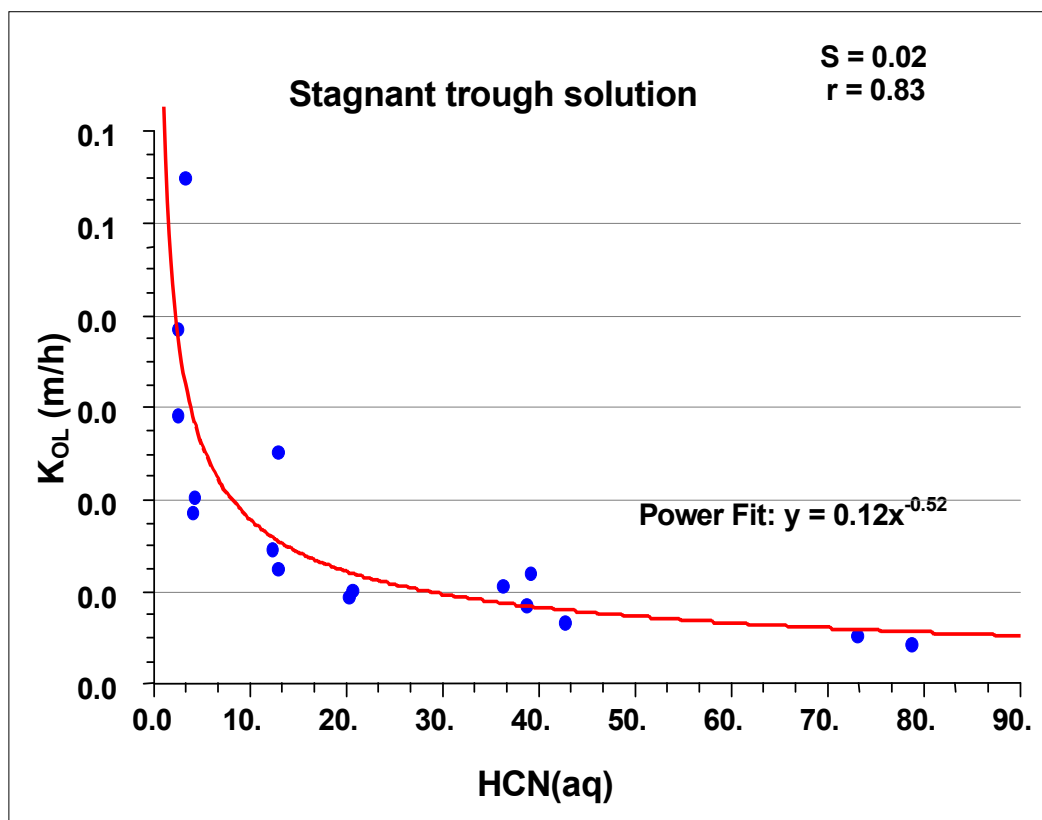


Figure 8.14. Power fit correlation for mass transfer coefficient of stagnant solutions.

8. Results and discussion

Finally, the trough cavity was filled with a synthetic pulp mixture, as described in section 7.2.1. The results are shown in Figure 8.15.

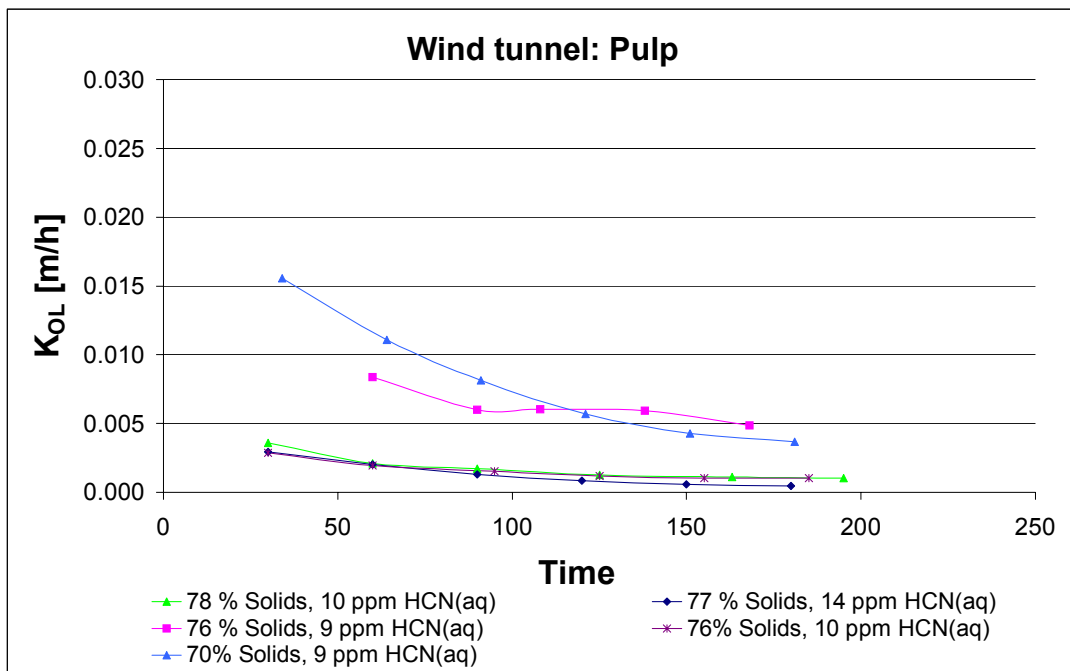


Figure 8.15. Mass transfer coefficient as a function of time for pulp with different solid to liquid ratios.

As can be seen from the above graph, the $\text{HCN}_{(\text{aq})}$ concentrations of all the synthetic pulps were similar, and all fell within the $\text{HCN}_{(\text{aq})}$ sensitive area, as discussed above. However, the cyanide concentration was set in this low bracket because it is relevant to actual tailings pulp, that may contain cyanide of between nearly 0 to 20 ppm $\text{HCN}_{(\text{aq})}$, depending on the pH, age, discharge concentration and site, among other things. It is evident that the mass transfer coefficients measured here, in comparison to those measured from pure solutions are approximately an order of magnitude lower ($\sim 0.002\text{-}0.015$ m/h vs. ~ 0.10 m/h at 10 ppm). This may be as a result of an increased resistance to mass transfer through the bulk of the pulp to the boundary layer at the surface, or to the presence of solid particles in the solution, which will hinder the free movement of species to the surface.

In addition, a general trend was observed whereby K_{OL} decreased with an increase in the solids content of the pulp. In all the experiments, the observed K_{OL} also decreased with time, indicating the development of a thicker boundary layer with time, due to the fact that the pulp mixture was once again stagnant. Furthermore, for

8. Results and discussion

some of the lower solid content tests (higher moisture content), the initial value of K_{OL} was much higher relative to the final value, than was the case for the higher solids content tests. This can be ascribed to a thin, almost clear liquid film that formed on top of the pulp surface because of the settling of the solids. Bearing in mind that the previous data set did indicate that the presence of liquid would lead to a much higher K_{OL} value, this result would be expected.

It is therefore evident that predictions of K_{OL} from actual tailings surfaces may be complicated by the presence of liquid films forming on top of the surface, and then gradually disappearing again, due to evaporation or seepage. It is, however, believed that, although these effects will have to be ignored to an extent, the available data still provide enough information to be used in the first step of predicting K_{OL} based on the parameters that are more easily obtained, such as moisture content, $HCN_{(aq)}$ concentration and wind velocity.

8.3 On-site test work

The results obtained from the on-site test work may be viewed in Appendix E. The tailings storage facility test work was conducted at two different sites, and the leach tank test work was also repeated at two plants.

As described before, the mass transfer coefficient measurements on the tailings surfaces were made at different areas, that were selected based on their appearance as dry tailings that one could easily walk on, thixotropic areas where one would start to sink, when standing in one spot too long, similar to quicksand, and wet sludge where it was not possible to walk or stand. The solid samples taken from these selected areas were later analysed for moisture content and interstitial cyanide. It was found that each type of site could be related to a range of moisture contents, as shown in Table 8.2.

Table 8.2. Moisture content classification of different areas found on talings surfaces.

Category	Moisture content, % H ₂ O
Discharge stream	39-41
Wet sludge	28-38
Thixotropic	24-27
Dry beach	18-23

8. Results and discussion

It is evident here that these categories essentially represent the loss of moisture, with the tailings flowing toward the decant pond, and the gradual decanting of water from the discharged tailings pulp. Furthermore, the thixotropic tailings fall within a very narrow bracket of moisture contents. This was also clearly observed while preparing the synthetic pulp, used in the previous wind tunnel experiments. As the cyanide solution was added to the silica sand, a point was reached where the mixture would change in character from a thixotropic, high viscosity pulp to a wet sludge; and this point was quickly overcome by the addition of very little additional solution.

The K_{OL} values obtained from the tailings surface tests are shown as a function of moisture content in Figure 8.16 below. It is clear from this graph that a strong relationship exists between the moisture content of the tailings and K_{OL} . There also seems to be a drastic increase in K_{OL} at moisture contents of 40% and above. Referring back to Table 8.3, these moisture contents correspond to measurements taken from the discharge stream, which consisted of a very wet sludge covered by a thin film of flowing solution. This confirms the finding, from the laboratory pulp test work, that a solution film forming on top of a pulp surface will result in a significant increase in K_{OL} .

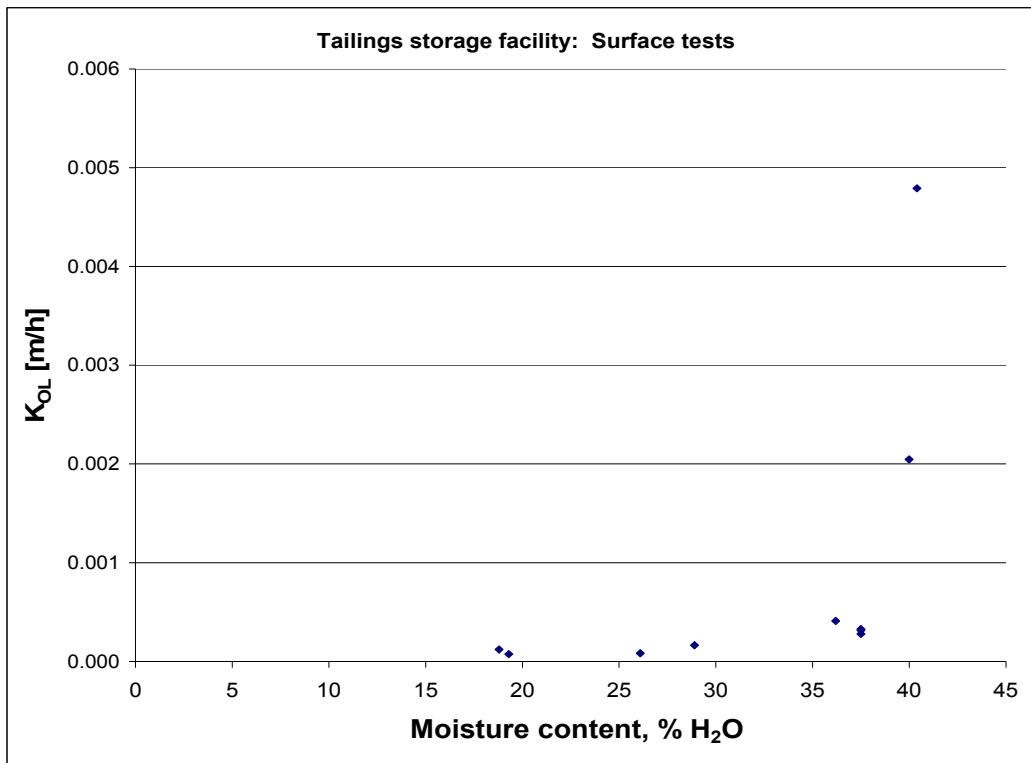


Figure 8.16. Measured effects of moisture content on K_{OL} (tailings storage facilities).

8. Results and discussion

The graph in Figure 8.17 shows the dependency of the same data set shown in Figure 8.16 on the $\text{HCN}_{(\text{aq})}$ concentration of the interstitial solution in the tailings pulp. A similar negative power correlation to that observed from the laboratory test work is once again observed for the on-site test work performed on wet surfaces, where the moisture content was higher than 28% water by mass. However, it was also found that the results of test work performed on surfaces that were classified as thixotropic or dry, shown in the blue data points on the graph, did not follow this trend.

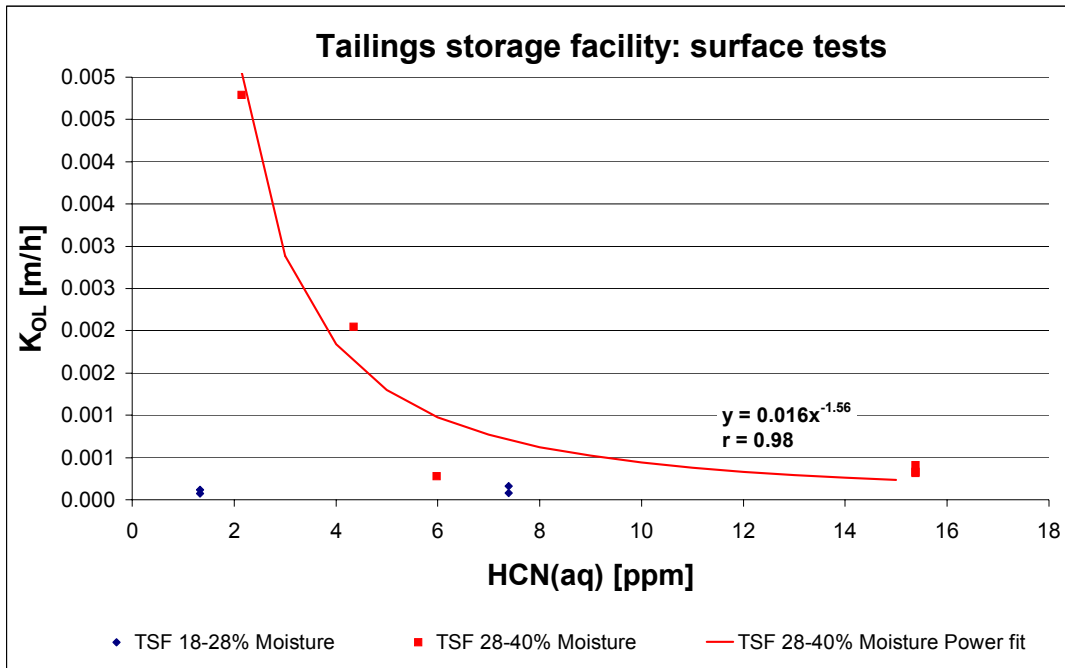


Figure 8.17. Mass transfer coefficients as a function of $\text{HCN}_{(\text{aq})}$ concentration for different tailings surface moisture contents.

This observation therefore confirms the finding in the previous section on pulp laboratory test work that, in the presence of a thin liquid film on top of a pulp mixture surface, the boundary layer in the liquid phase is thinner in comparison to dry surfaces. This led to the higher mass transfer coefficients measured from wet sludge surfaces compared to thixotropic and dry surfaces.

Furthermore, comparison of the on-site measured K_{OL} values to that measured in the laboratory reveals that the latter is approximately an order of magnitude higher than the former, as summarised in Table 8.4. The values listed in this table were inferred from the trends shown by the data in Figure 8.16 and 8.17. Considering that the moisture contents and $\text{HCN}_{(\text{aq})}$ concentrations of all the tests were in the same

8. Results and discussion

region, the difference in K_{OL} values cannot be adequately explained by differences in the moisture content or $HCN_{(aq)}$.

Table 8.3. Comparison of laboratory and on-site K_{OL} measurements with moisture.

Moisture content, % H ₂ O	Laboratory	Site
22	0.0005	0.00007
30	0.005	0.00003

However, it is important to note that different wind speeds, and therefore different roughness Reynolds numbers, Re^* , were applied to the pulp surfaces for both the laboratory and on-site test work, due to the different set-ups used. For the laboratory test work, Re^* may be calculated using Eq. 5.13, returning values between 1.7×10^{-3} and 2.5×10^{-6} , depending on the linear velocity (1-3.6 m/s). For the on-site tests, small monitoring pumps were used to create airflow across the tailings surface of approximately 2 L per minute. This resulted in a linear velocity of 0.0004 m/s inside the dome cover, which is essentially stagnant.

This therefore leads to the conclusion that, in the study of mass transfer coefficients from pulp tailings, the combined effects of moisture content, wind velocity (Re^*) and the $HCN_{(aq)}$ concentration of the interstitial solution in the pulp have to be considered simultaneously in a prediction model.

The leach tank test work was first conducted at Plant A, which treats an average of 120 000 tons per month and uses 10 aerated pachuca tanks in the leach. Measurements were done here from an aerated pachuca tank, where an aeration rate of approximately 40 m³/h per tank was applied. The second set of test work was done at Plant B, treating an average of 300 000 tons per month, which uses a much larger leaching section, i.e. 6 mechanically agitated tanks, followed by a train of thirteen aerated pachucas, with an applied aeration rate of 125 m³/h per tank. In this case, the same tests were repeated at one mechanically stirred tank and one of the pachucas.

As discussed in section 7.3.1, compressed air was used to create airflow at different velocities across the surface of a dome device covering a section of the pulp liquor. The measurements of $HCN_{(g)}$ evolved from the pulp liquor resulting from different airflow rates through the dome cover are shown in Figure 8.18.

8. Results and discussion

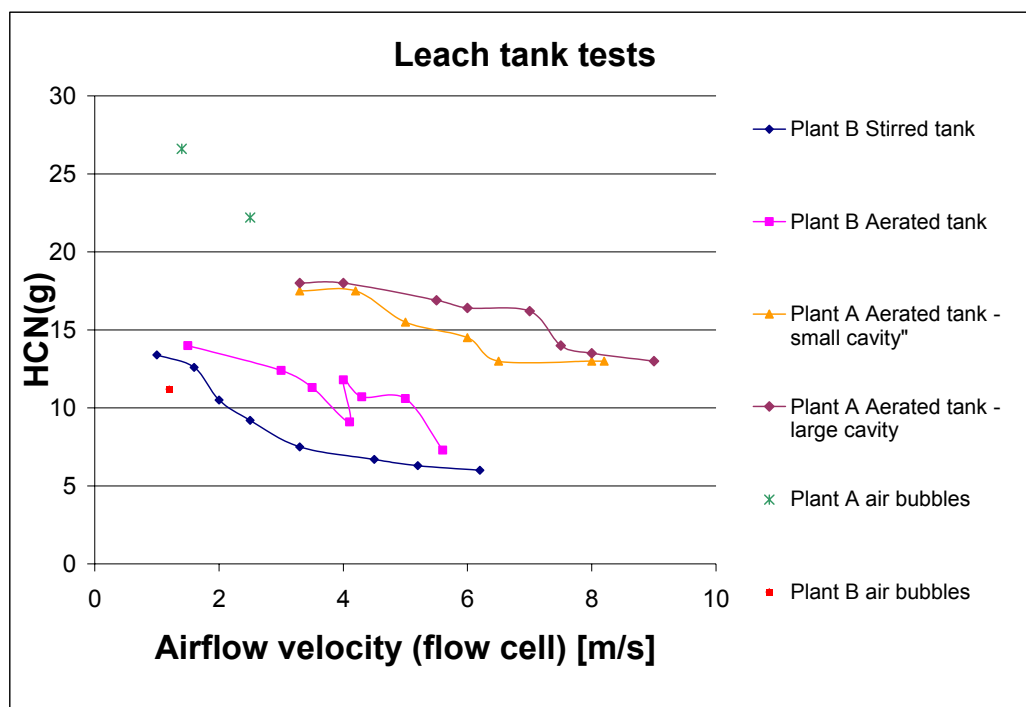


Figure 8.18. Measurements of $\text{HCN}_{(g)}$ evolved from different leach tanks at various airflow velocities.

The results shown in Figure 8.18 indicate that the $\text{HCN}_{(g)}$ concentrations measured above the leach tanks ranged from approximately 5 to 27 ppm. Relating these values to the human exposure limits, as shown in Table 3.1, it is evident that the $\text{HCN}_{(g)}$ concentration levels measured near the surface of the pulp liquor may cause slight symptoms after hours of exposure. However, considering that the $\text{HCN}_{(g)}$ quickly diffuses away from the surface due to wind currents, the levels that plant personnel working in the leach section would normally be exposed to are very low and rarely exceeds 5 ppm, thus rendering this area safe to work in.

It can also be seen from the Figure 8.18 that the $\text{HCN}_{(g)}$ concentration decreased as the airflow velocity increased across the pulp surface. This was due to the increased dilution effect of the increased airflow introduced to the cavity. It is important to note, though, that the $\text{HCN}_{(g)}$ concentrations measured above the pachuca tank at Plant A was approximately 20 ppm higher than that measured from both tanks at Plant B. The speciation data of the leach liquors from both these plants resulted in $\text{HCN}_{(aq)}$ concentrations of approximately 11 and 5 ppm for Plant A and Plant B, respectively. Considering that there was no notable difference in the pulp temperatures, relative

8. Results and discussion

densities or salinities, it is reasonable to ascribe this effect to the difference in $\text{HCN}_{(\text{aq})}$.

In addition, for the aerated tank data points, the compressed airflow feed to the test system was blocked, and the measured airflow velocities in the dome were thus only that resulting from the air bubbles rising to the surface and being released into the gas phase, with a certain pseudo-equilibrium concentration of $\text{HCN}_{(\text{g})}$ accompanying this air volume, as it equilibrated with the cyanide present in the pulp liquor. This is therefore the $\text{HCN}_{(\text{g})}$ that was measured for these data points. Applying a factor of five (see section 8.1) for the nondimensional form of Henry's constant, and ignoring the concentration dependence of k_H at the prevailing free cyanide concentration of roughly 60 ppm, this would translate into an equilibrium $\text{HCN}_{(\text{g})}$ concentration of 55 ppm and 25 ppm for Plant A and Plant B, respectively. This would then lead to the conclusion that the $\text{HCN}_{(\text{g})}$ evolved from the aeration bubbles and captured at the near surface of the pulp liquor was at roughly 50% equilibrium, as the actual $\text{HCN}_{(\text{g})}$ measured was approximately 25 and 12 ppm for Plant A and Plant B, respectively.

It may also be noted from Figure 8.18 that the measurements made from the surface of the mechanically agitated tank were much more stable than those made from aerated tanks. In addition, the stability of the measurements made from the aerated tank at Plant A was in turn much better than that of Plant B, which has a much higher aeration rate. The difficulty experienced in performing measurements from aerated tanks were a result of the sensitivity of the airflow measurements to the smoothness of the pulp surface, or rather, fluctuations in the pulp liquor height, which proved to caused significant fluctuations in the dome cavity volume and therefore the measured airflow rate. The small and large cavities, referred to in the graph, were obtained by decreasing the volume space inside the cavity between the dome cover and the pulp surface.

The calculated volatilisation rates from the data, depicted in Figure 8.18, are shown in Figure 8.19 as a function of Re^* , which was calculated from the drag coefficient and surface air velocity, as shown in section 5.3.2. It is evident that the rates of $\text{HCN}_{(\text{g})}$ volatilisation increased with an increase in Re^* . Comparing the contribution of the $\text{HCN}_{(\text{g})}$ evolved from the air bubbles at Plant A to, for instance, the maximum measured volatilisation rate corresponding to the maximum Re^* number, it can be seen that, at an airflow of 0.2 m/s across the pulp surface, the aeration contribution to the overall $\text{HCN}_{(\text{g})}$ loss was 43%. This value would obviously decrease at higher

8. Results and discussion

surface velocities, since the loss due to aeration is limited by the equilibrium concentration of the air bubble gas volume, while volatilisation from the surface will continue to rise as the wind velocity rises. It was also once again observed that the volatilisation rates from the aerated tank at Plant B were lower than that of Plant A, due to the lower $\text{HCN}_{(\text{aq})}$ concentration present in the pulp liquor. The volatilisation rates measured from the smaller cavity volume were also increased due to the effective increase in airflow velocity, and therefore increased dilution effect in the cavity volume, leading to a higher concentration gradient and therefore higher volatilisation rates.

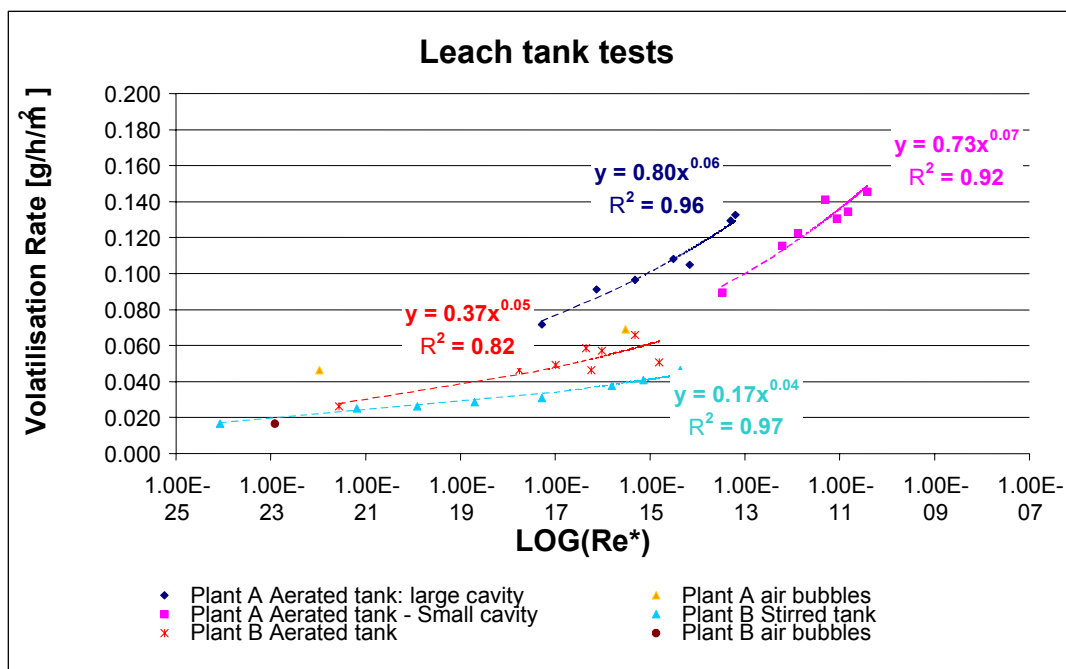


Figure 8.19. Dependence of measured volatilisation rates from leach tanks on Re^* .

Using the correlations obtained from the data, as shown on the graph, to calculate the volatilisation rate at a wind velocity of 1 m/s, the predicted volatilisation rates, as well as the predicted contribution of aeration to the overall volatilisation rate of cyanide from all the leach tanks investigated, are shown in Table 8.5. The calculated percentage contribution of aeration to the overall loss of $\text{HCN}_{(\text{g})}$, assuming that the rate resulting from the air bubbles remains the same, was found to be roughly 20% for Plant A and 10% for Plant B. This may once again be explained in terms of the lower concentration $\text{HCN}_{(\text{aq})}$ available for equilibration with the bubble gas volume in the pulp liquor of Plant B, leading to a lesser effect of aeration on $\text{HCN}_{(\text{g})}$ loss, in spite of the fact that a much higher aeration rate is utilised.

8. Results and discussion

Table 8.4. Prediction of volatilisation rates from leach tanks.

Tank	Predicted rate at 1 m/s [g/h/m ²]	Measured aeration contribution [g/h/m ²] [Fig. 8.24]	% Contribution of aeration to overall rate loss
Plant A – large cavity	0.37	0.06	16.3
Plant A – small cavity	0.29	0.06	20.3
Plant B – aerated tank	0.19	0.02	10.3
Plant B– mechanically agitated tank	0.1	-	-

Finally, the calculated K_{OL} values for the leach tanks investigated are shown in Figure 8.20. It may be seen that K_{OL} is approximately 0.015 m/h, with the exception of the data for the aerated pachuca at Plant B. However, these fluctuations are attributed to the deviations resulting from the abovementioned instability in the pulp liquor level, which was especially problematic in the case of the aerated tank at Plant B, due to the high aeration rates used there.

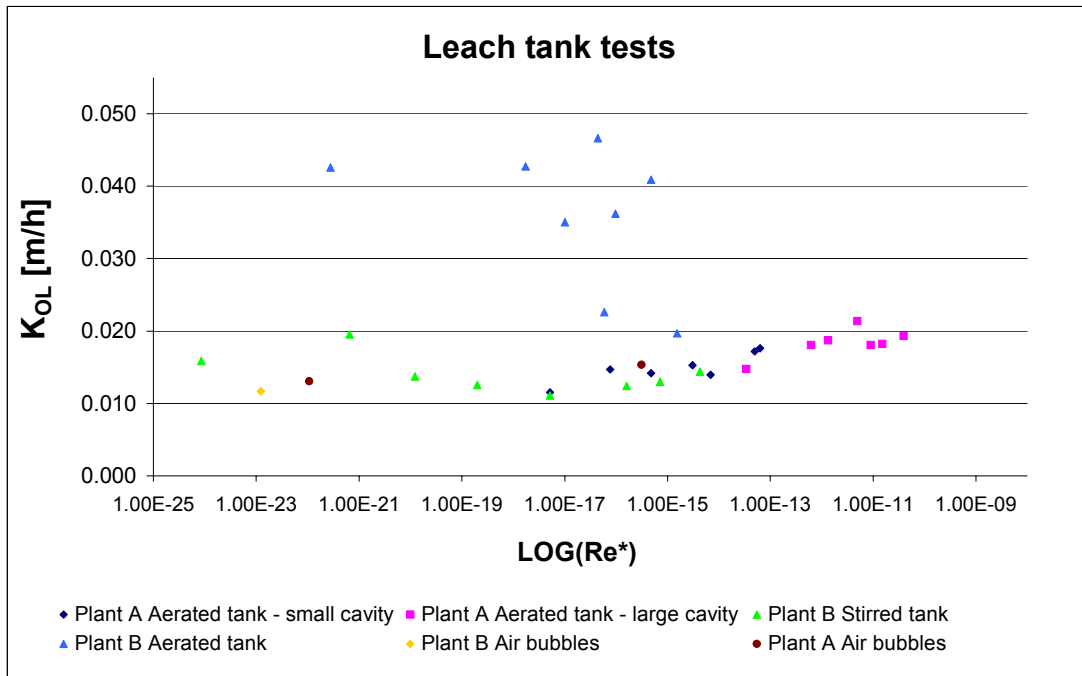


Figure 8.20. Dependence of K_{OL} on Re^* for leach tank tests.

8.4 Model development

The data presented and discussed in the foregoing sections were combined and used as a data set to which an empirical model was fitted. Based on the conclusions drawn from the mass transfer coefficient tests, both laboratory and on-site, the main parameters affecting K_{OL} were prioritised as follows:

- **HCN_(aq) concentration:** As was found in the laboratory experiments and confirmed by the on-site test work, the mass transfer coefficient is dependent on the HCN_(aq) concentration present in the solution phase, i.e. the pulp liquor in the case of leach tanks or discharge streams, the decant pond or return water dam solution or the interstitial solution in the case of tailings solids. This parameter was therefore incorporated into the prediction model.
- **Moisture content:** As was revealed by the laboratory pulp experiments and on-site test work, the moisture content of solid tailings plays an important role in the mass transfer coefficient of HCN from the pulp. This is therefore another factor that was included in the prediction model.
- **Roughness Reynolds number:** As described in section 6.3, the Roughness Reynolds number approach was used to correlate the dependence of K_{OL} on the flow of air across the surface by wind.
- **Solution flow rate:** Another factor that emerged from the experimental work was that of flowing versus stagnant solutions, which would be important at tailings storage facilities, where stagnant solution bodies may be found. In the case of the two sites studied here, it was found that, during the day, residue is constantly discharged, leading to a constant flow of solution toward the decant pond. Even the solution in the decant pond was found to flow constantly due to this constant influx of solution. However, as for the return water dam, this solution body may be considered to be relatively stagnant and concentration gradients may begin to arise during the night. Therefore, the model allowed for two different scenarios of stagnant and flowing solution, and the appropriate data sets were used for each scenario.

8. Results and discussion

Combining the parameters selected as described above, the correlation for K_{OL} may be written as:

$$K_{OL} = a Re^{*b} M^c HCN_{(aq)}^d + e \quad \text{[Eq. 8.3]}$$

where a, b, c, d, and e are modelling coefficients

- K_{OL} = predicted mass transfer coefficient [m/h]
- Re^* = Roughness Reynolds number
- M = Moisture content of pulp [% H₂O]
- $HCN_{(aq)}$ = $HCN_{(aq)}$ concentration determined from cyanide speciation model produced by MINTEK

The MINTEK cyanide speciation model makes use of the analysis of Total, WAD and free cyanide as determined by injection flow analysis, AgCl titrations and ion specific electrode measurements, respectively. The metal speciation is also determined. This is then combined with the known stability constants for metal cyanide complexes, which are found in typical gold mining solutions, to estimate the total amount of the total cyanide that will be consumed by the metals. The remaining amount of cyanide is then compared to the measured free cyanide, determined by titration and ISE, in order to return the best possible fit for the overall cyanide distribution. The $HCN_{(aq)}$ concentration is then calculated, using the pH dependency, from the amount of free cyanide in the sample.

Using the appropriate data sets obtained from the test work presented in this study, the coefficients in the model equation given above was then simultaneously solved by minimising the square of the sum of the errors between the predicted and actual K_{OL} values for each data set. The resulting coefficients are shown below in Figure 8.21.

VOLATILISATION MODEL COEFFICIENTS							
$K_{OL}=a(Re^*)^b(M)^c(HCN_{(aq)})^d+e$							
Data set	Application	a	b	c	d	e	ERROR
Site: Leach tank	Leach tanks	0.196	0.191	0.417	-0.176	0.014	0.00000
Site: TSF	TSF	0.817	0.050	4.358	-1.312	0.000	0.00000
Lab: plate	Flowing solution, TSF	0.109	0.007	0.141	-0.817	0.070	0.21406
Lab: Still trough	Stagnant pond, TSF	0.073	0.250	0.731	-0.756	0.012	0.00011
Lab: Pulp	Solid tailings surface, TSF	0.046	0.002	0.143	-0.048	-0.031	0.00001
SOLVER INPUTS							
<input type="button" value="RESET"/>		<input type="text" value="a"/>	<input type="text" value="0.000"/>	<input type="text" value="c"/>	<input type="text" value="0.000"/>	<input type="text" value="e"/>	<input type="text" value="0.000"/>
		<input type="text" value="b"/>	<input type="text" value="0.000"/>	<input type="text" value="d"/>	<input type="text" value="0.000"/>		

Figure 8.21. Volatilisation prediction model coefficients determined for different scenarios.

8. Results and discussion

The solver input values shown in Figure 8.21 was set to zero before calculating the coefficients for each data set. In order to illustrate the effectiveness of this empirical model, the data fit is illustrated in Figures 8.22 to 8.26, for each scenario in the model application.

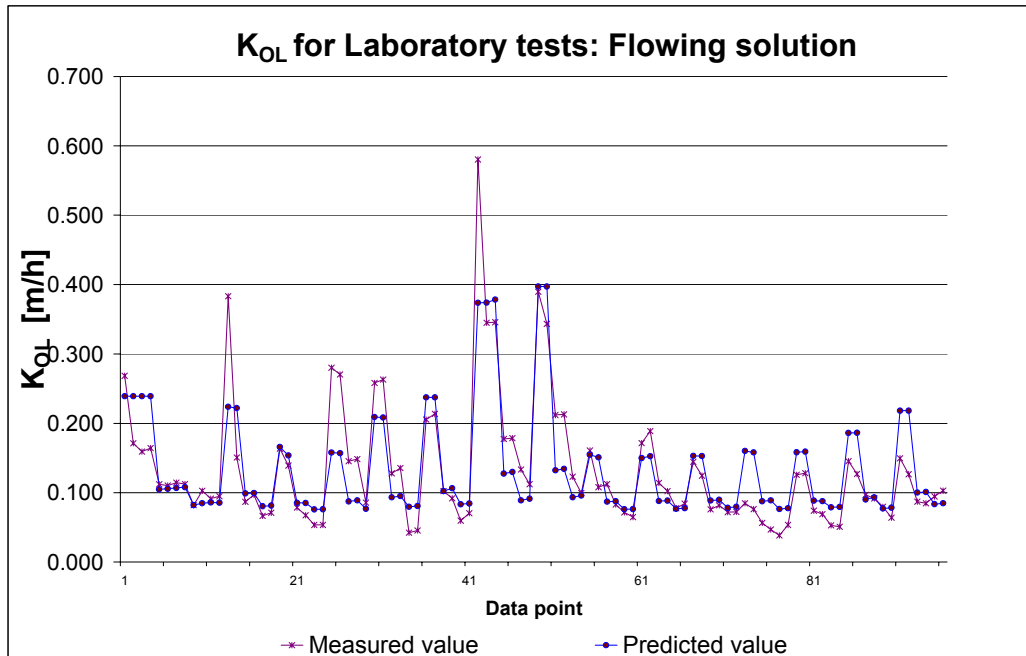


Figure 8.22. Measured mass transfer coefficients vs. empirical model predictions for flowing solution laboratory experiments.

As can be seen, the model predictions for all the laboratory experiments fit very well. As suggested by the model application scenarios shown in Figure 8.21, these correlations may be applied to the TSF surface predictions in the following manner:

- The flowing solution scenario, shown in Figure 8.22, applies to the surface on the TSF that is covered by solution, i.e. the wet beach area as well as the decant pond area during the day.
- The stagnant solution scenario, shown in Figure 8.23, applies to the liquid bodies on the TSF surface that are stagnant, i.e. the decant pond and wet beach during the night, as well as the return water dam.
- The pulp scenario, shown in Figure 8.24, applies to all surfaces on the TSF covered by solids (and not a solution film).

8. Results and discussion

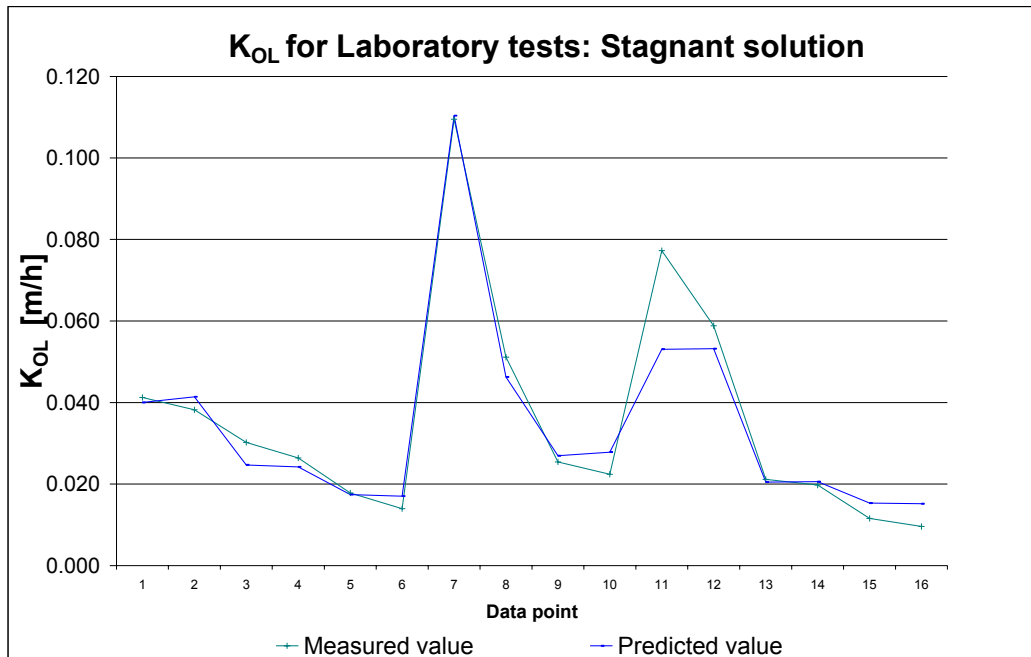


Figure 8.23. Measured mass transfer coefficients vs. empirical model predictions for stagnant solution laboratory experiments.

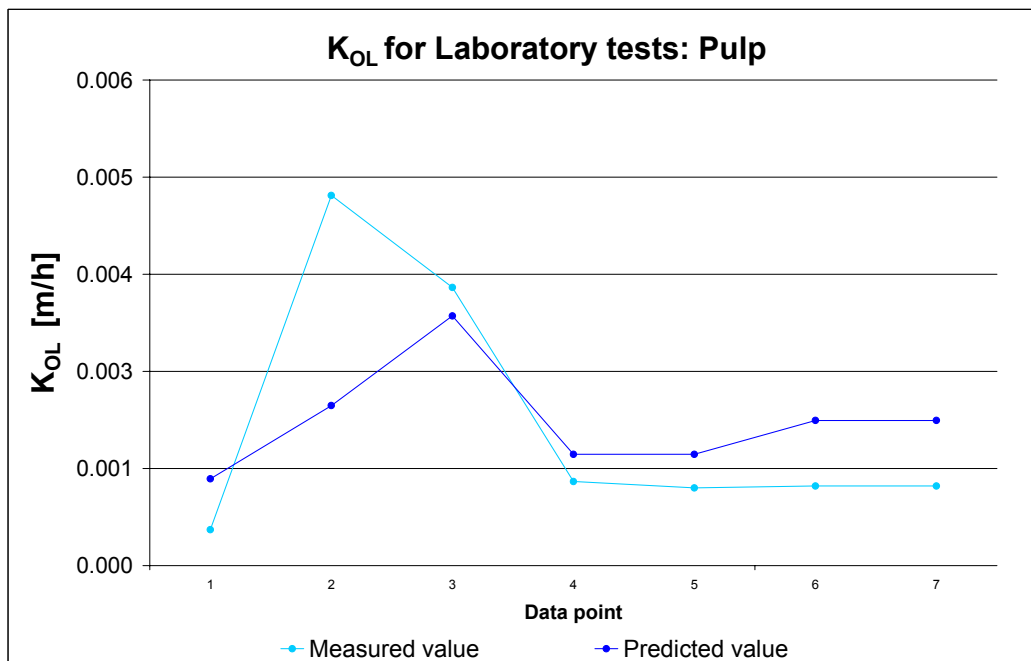


Figure 8.24. Measured mass transfer coefficients vs. empirical model predictions for pulp laboratory experiments.

8. Results and discussion

The model was also used to predict the mass transfer coefficients measured during the on-site test work. The resulting data fit for the leach tank and tailings surface tests are shown in Figures 8.25 and 8.26.

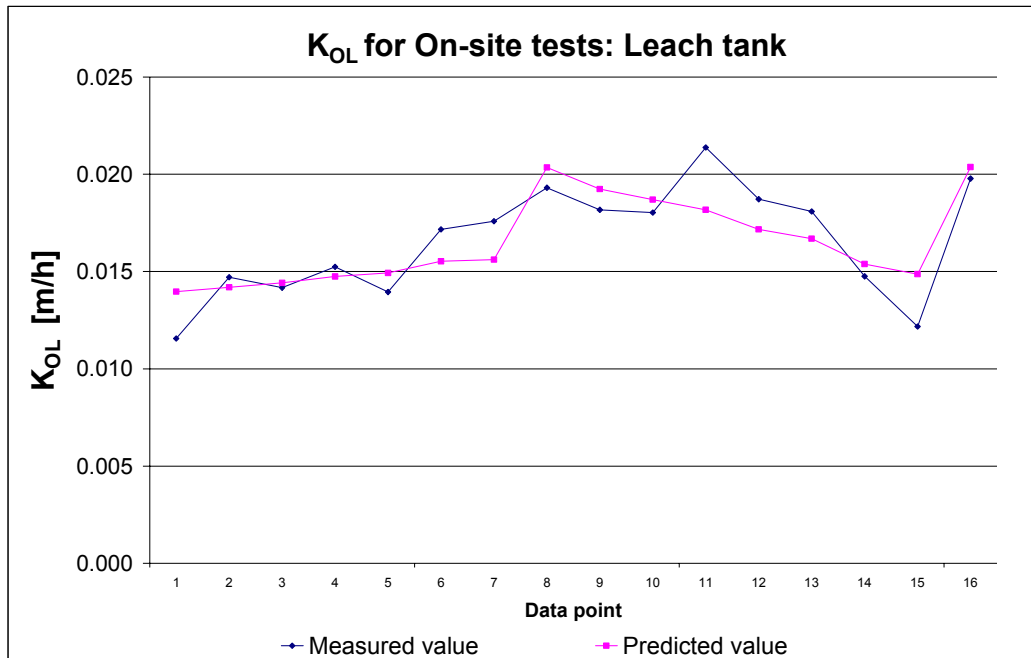


Figure 8.25. Measured mass transfer coefficients vs. empirical model prediction for leach tank tests.

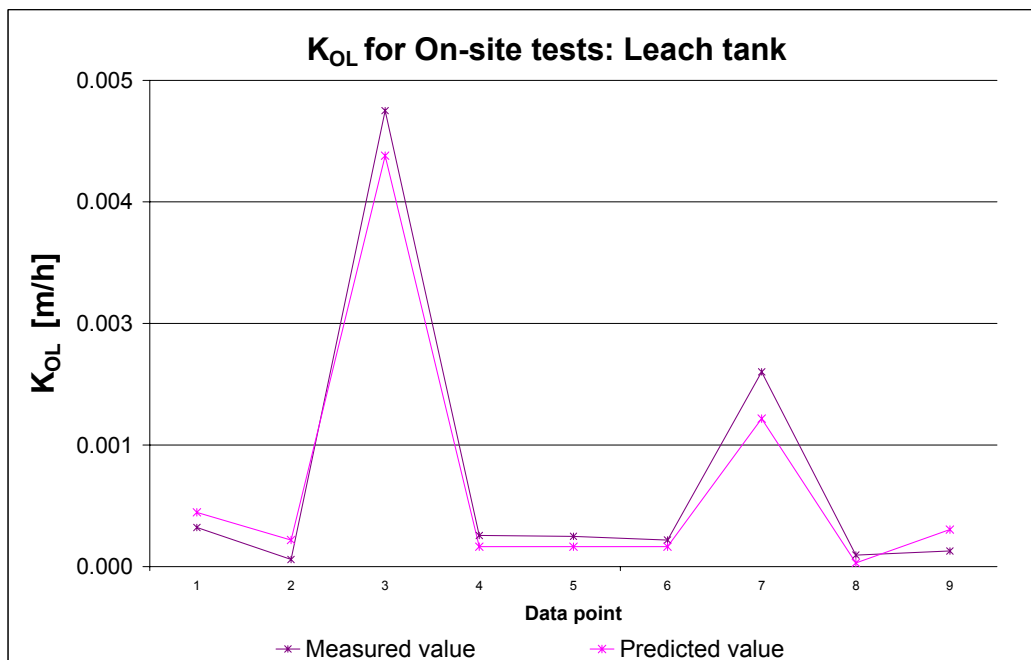


Figure 8.26. Measured mass transfer coefficients vs. empirical model predictions for tailings storage facility surface tests.

8. Results and discussion

The correlations resulting from the on-site tests may be used for leach tank predictions as well as predictions from the TSF surface, including the categories for dry, thixotropic and wet, as used before. As can be seen from these figures, the model, based only on $\text{HCN}_{(\text{aq})}$, moisture content and Re^* , predicts the actual measured K_{OL} values well. The only remaining test necessary to verify this empirical model is a comparison of the mass balance across both the leach section and TSF, which is covered in the next section.

8.5 Model verification

The validity of the model predictions made for the mass transfer coefficients of HCN from leach tanks, as well as tailings surfaces, was tested by comparing predicted volatilisation rates to actual cyanide losses. The volatilisation rates were calculated using equation 8.2, while the actual cyanide losses were determined by performing cyanide mass balances across the leaching and tailings storage facility sections, respectively. The tailings facility areas were determined as described in section 7.3.4, and the geographical points measured on the tailings dam surface, as well as the map of the tailings storage facility, are shown in Appendix F.

The tailings storage facility model was applied to one of the sites that were used for on-site test work in this study in order to validate the predictions. Using the coefficients determined for the laboratory pulp tests and the on-site tailings surface test work, the mass transfer coefficient was calculated using equation 8.3. The loss of cyanide due to volatilisation predicted from the model was then compared to the total cyanide lost from the tailings facility. Some difficulty was experienced during the validation of this model due to the low $\text{HCN}_{(\text{aq})}$ concentrations found in the tailings pulp, especially at the site that was used in this case. As a result, it was found that the sensitivity of the model to the input $\text{HCN}_{(\text{aq})}$ concentration values led to major differences in the model predictions.

The speciation model, developed by MINTEK and described in Appendix B, was used in the determination of the $\text{HCN}_{(\text{aq})}$ concentration, using the stability constants for each of the metal complexes shown in Figure 8.27. However, it is therefore evident that the validity of this model depends on the accuracy of the stability constants used in the calculations. Further work on the effect of very low cyanide

8. Results and discussion

concentrations on these stability constants, as well as interactions of solid particles and other chemical constituents typically found in metallurgical pulp solutions, is ongoing. Nonetheless, it has been found that this model holds in the majority of cases for pulp solutions from various gold plants, and it has subsequently been used successfully for monitoring purposes since 2000.

Stability Constants for complexes:				
	Cu	Zn	Ag	Ni
beta1				1.07E+07
beta2	5.01E+21	1.18E+11	2.41E+20	3.86E+14
beta3	6.31E+26	1.12E+16	2.51E+21	4.31E+22
beta4	7.94E+27	4.17E+19		1.34E+30
beta5				2.67E+29
[Zn(CN)₂OH]⁻		5.13E+14		
[Zn(CN)₃OH]²⁻		1.20E+18		
Zn(OH)⁺		1.10E+05		
Zn(OH)₂		1.26E+11		
Zn(OH)³⁻		3.98E+13		
Zn(OH)₄²⁻		6.31E+14		

Figure 8.27. Stability constants used for metal complexes in the cyanide speciation model developed by MINTEK.

Figure 8.28 and Figure 8.29 illustrates the application of the tailings storage facility model, using two methods for the determination of $\text{HCN}_{(\text{aq})}$, respectively. These were the predictions made by the MINTEK speciation model and direct measurement of the CN^- ion concentration by the use of an ISE electrode. From this CN^- concentration, the $\text{HCN}_{(\text{aq})}$ concentration was calculated at the known pH value of the solution. Prior to analysis, the ISE electrode was calibrated using 0.2, 2, 20 and 200 ppm cyanide standards, which were in turn validated using flow injection analysis. The results obtained from the speciation model are shown in Appendix E.

8. Results and discussion

HCN volatilisation calculation: TSF								
Total TSF top surface area	1,350,000	m ²	WATER BALANCE DATA					
Total TSF wet volume	475,326	m ³	Kopanang feed 161 m ³ /h					
Total TSF wet surface area	139,000	m ²	Noligwa feed 420 m ³ /h					
Return water dam volume	40,000	m ³	Total feed to TSF 581 m ³ /h					
Return water dam surface area	15,088	m ²	Returned stream 317 m ³ /h					
Roughness height, Z ₁₀	10	m						
C _D	0.0011							
Wind velocity, U ₁₀	5	m/s						
Kinematic viscosity	0.000016	m ² /s						
Category	Moisture content [% H ₂ O]	Average moisture, M [% H ₂ O]	HCN(aq) [ppm]	Area coverage [% of total TSF]	Total CN [ppm]	WAD CN [ppm]	Free CN [ppm]	
Discharge in Daywall	39-41	40	0.37	0.4	12	11.8	1.070	
Wet beach	28-38	33	0.46	10.2	11.3	11.2	0.962	
Thixotropic beach	24-27	25	0.00	2.8				
Dry beach	18-23	20	0.00	86.5				
Decant pond	42-100	90	0.46	0.1	11.3	11.2	0.962	
				100.0				
Return water dam	99	99	0.27		5.82	6.01	0.570	
MODEL PREDICTION								
Category	Moisture, M [% H ₂ O]	Re*	HCN(aq) [ppb]	K _{OL} [m/h]	Volatilisation rate [g/h/m ²]	% of Surface	Volatilisation rate [g CN/h]	Volatilisation rate [kg/day]
Daywall	40	0.67	0.37	0.051	0.0189	0.40	98.04	2.353
Wet beach	33	0.67	0.46	0.048	0.0221	10.19	2932.30	70.375
Thixotropic beach	25	0.67	0.00	0.127	0.0000	2.81	0.00	0.000
Dry beach	20	0.67	0.00	0.122	0.0000	86.90	0.01	0.000
Decant pond	90	0.67	0.46	0.060	0.0277	0.10	36.06	0.865
							3,117.1	73.6
Return water dam	99	0.67	0.27	0.013	0.0035	100.00	50.64	1.215
MASS BALANCE								
	HCN(aq)				Total CN			
	Mass in [g CN/h]	Mass out [g CN/h]	Mass lost [g CN/h]	Total % Loss	Mass in [g CN/h]	Mass out [g CN/h]	Mass lost [g CN/h]	Total % Loss
Tailings dam surface	0.21	0.15	0.07	32%	6,972.0	3,582.1	3,389.9	49%
Return water dam	146.5	85.6	60.9	42%	3,582.1	1,905.2	1,676.9	47%
Total CN lost from TSF surface and water return dam					73%		5,066.8	95%
Loss attributed to HCN Volatilisation from TSF surface and return water dam							3,167.69	63%

Figure 8.28. Comparison of predicted HCN loss through volatilisation from tailings storage facilities to the calculated total cyanide loss determined from the mass balance (ISE method).

8. Results and discussion

HCN volatilisation calculation: TSF								
Total TSF top surface area	1,350,000	m ²	WATER BALANCE DATA					
Total TSF wet volume	475,326	m ³	Kopanang feed 161 m ³ /h					
Total TSF wet surface area	139,000	m ²	Noligwa feed 420 m ³ /h					
Return water dam volume	40,000	m ³	Total feed to TSF 581 m ³ /h					
Return water dam surface area	15,088	m ²	Returned stream 317 m ³ /h					
Roughness height, Z ₁₀	10	m						
C _D	0.0011							
Wind velocity, U ₁₀	5	m/s						
Kinematic viscosity, ν _a	0.000016	m ² /s						
Category	Moisture content [% H ₂ O]	Average moisture, M [% H ₂ O]	HCN _(aq) [ppb]	Area coverage [% of total TSF surface]	Total CN [ppm]	WAD CN [ppm]	Free CN [ppm]	
Discharge in Daywall	39-41	40	8.00	0.4	12	11.8	0.007	
Wet beach	28-38	33	14.00	10.2	11.3	11.2	0.001	
Thixotropic beach	24-27	25	0.00	2.8				
Dry beach	18-23	20	0.00	86.5				
Decant pond	42-100	90	14.00	0.1	11.3	11.2	0.001	
				100.0				
Return water dam	99	99	10.00		5.82	6.01	0.001	
MODEL PREDICTION								
Category	Moisture, M [% H ₂ O]	Re*	HCN(aq) [ppb]	K _{OL} [m/h]	Volatilisation rate [g/h/m ²]	% of Surface	Volatilisation rate [g CN/h]	Volatilisation rate [kg/day]
Daywall	40	0.67	8.00	0.067	0.0005	0.40	2.80	0.067
Wet beach	33	0.67	14.00	0.062	0.0009	10.19	115.41	2.770
Thixotropic beach	25	0.67	0.00	0.188	0.0000	2.81	0.00	0.000
Dry beach	20	0.67	0.00	0.181	0.0000	86.90	0.00	0.000
Decant pond	90	0.67	14.00	0.077	0.0011	0.10	1.39	0.033
							122.98	2.871
Return water dam	99	0.67	10.00	0.023	0.0002	100.00	3.37	0.081
MASS BALANCE								
	HCN(aq)				Total CN			
	Mass in [g CN/h]	Mass out [g CN/h]	Mass lost [g CN/h]	Total % Loss	Mass in [g CN/h]	Mass out [g CN/h]	Mass lost [g CN/h]	Total % Loss
Tailings dam surface	4.65	4.44	0.21	5%	6,972.0	3,582.1	3,389.9	49%
Return water dam	4,438.0	3,170.0	1,268.0	29%	3,582.1	1,905.2	1,676.9	47%
Total CN lost from TSF surface and water return dam							5,066.83	95%
Loss attributed to HCN Volatilisation from TSF surface and return water dam							126.35	2%

Figure 8.29. Comparison of predicted HCN loss to volatilisation from tailings storage facilities to the calculated overall cyanide loss determined from the mass balance (MINTEK speciation model method).

It follows from the two tables shown above that the model predictions, resulting from use of the two methods to determine HCN_(aq), vary widely. Using the MINTEK speciation model method, the model predicts that only 2% of the total cyanide lost on the tailings facility is due to volatilisation, whereas the ISE method leads to a prediction of 63% of the total loss. The discrepancy in these model predictions may be attributed to the differences in HCN_(aq) determined by the use of both methods.

8. Results and discussion

Note that the $\text{HCN}_{(\text{aq})}$ concentrations determined using the MINTEK speciation model are roughly 30 to 40 times lower than that determined using direct measurements of CN^- using an ISE electrode. It is difficult in this case to state which of these methods are more accurate, but from the model predictions it would definitely seem that the latter is more reliable, as it would be highly improbable for HCN volatilisation to not account for the majority of cyanide loss from a tailings storage facility, as has been confirmed by all the previous studies discussed in section 5.

Furthermore, accepting the predictions made based on the ISE method to be the more accurate, the model also predicts that the vast majority of the HCN loss through volatilisation occurs on the tailings dam. In addition, 95% of the volatilisation loss on the tailings dam occurred from the wet beach, i.e. the surface covered with a thin film of solution,

It therefore follows from this work that the tailings storage facility model is very sensitive to the $\text{HCN}_{(\text{aq})}$ concentration, and reliable quantification of this parameter is essential to the success of application of the model.

Data generated from a sampling exercise carried out at Plant B was used in the validation of the leach tank model. The coefficients determined for the leach tank scenario, as shown in the previous section, was used to predict the mass transfer coefficient for each leach or adsorption tank, based on the $\text{HCN}_{(\text{aq})}$ concentration and moisture content of the pulp and the prevailing Roughness Reynolds number resulting from the wind velocity measured on the day of sampling. The comparison of the predicted and actual cyanide losses from each section is shown in Figure 8.30.

It follows from the model predictions shown in Figure 8.30 that the HCN volatilised from the new leach section accounted for 72% of the $\text{HCN}_{(\text{aq})}$ that was lost in that section. However, the predicted volatilisation rates were very low compared to the total cyanide loss measured for this section. Upon further inspection of the data, it is clear that this additional loss of cyanide occurred in the last two leach tanks of the new leach section. It is possible that the formation of cyanate at the end of this section, corresponding to a residence time of approximately 10 hours, resulted in the additional loss 8 ppm loss in total cyanide concentration. However, this can unfortunately not be verified in this case, since the cyanate concentrations were not analysed for these samples.

8. Results and discussion

HCN volatilisation calculation - Leach & CIP sections											
SITE: Plant B											
Z ₁₀	1	m	C ₀			0.00050					
U ₁₀	1.00	m/s	Total residence time			55.53	h				
v _a	0.000016	m ² /s	Feed flow rate			229.9	m ³ /h				
Tank diameter	New Leach 8.5 m		Old leach 10.2 m			CIP 9 m					
Tank surface area	56.75 m ²		81.71 m ²			63.62 m ²					
Number of tanks	6		13			8					
Residence time	12.29 h		32.04 h			11.2 h					
Aeration rate	0 m ³ /h		125 m ³ /h			0 m ³ /h					
Input parameters				Model		HCN Volatilised		Cyanide mass balance			AMIRA model prediction
Tank number	Re*	Moisture content [% H ₂ O]	HCN(aq) [ppm]	Aeration rate [m ³ /h]	K _{OL} [m/h]	Total per tank [g CN /h/m ²]	Total per tank [g CN/h]	TCN in tank [ppm]	TCN lost per section [g CN/h]	HCN lost per section [g CN/h]	Total per tank [g CN/h]
New Leach 1	2.38E-05	50	4.98	0	0.11	0.540	30.64	117			28.67
New Leach 2	2.38E-05	50	4.59	0	0.11	0.504	28.58	120			28.40
New Leach 3	2.38E-05	50	4.24	0	0.12	0.471	26.74	112			28.15
New Leach 4	2.38E-05	50	4.86	0	0.11	0.528	29.98	121			28.59
New Leach 5	2.38E-05	50	3.98	0	0.12	0.446	25.33	109			27.96
New Leach 6	2.38E-05	50	3.98	0	0.12	0.447	25.34	109			27.96
CN LOST IN NEW LEACH section						160.43			1839.08	221.78	169.73
Old Leach 1	2.38E-05	50	3.70	125	0.12	0.420	34.29	91.3			39.98
Old Leach 2	2.38E-05	50	3.81	125	0.12	0.430	35.15	90.2			40.09
Old Leach 3	2.38E-05	50	4.01	125	0.12	0.450	36.73	94.8			40.30
Old Leach 4	2.38E-05	50	3.97	125	0.12	0.446	36.42	90.3			40.26
Old Leach 5	2.38E-05	50	4.72	125	0.11	0.516	42.15	97.8			41.02
Old Leach 6	2.38E-05	50	4.16	125	0.12	0.464	37.91	85.7			40.45
Old Leach 7	2.38E-05	50	6.21	125	0.11	0.650	53.12	90.6			42.54
Old Leach 8	2.38E-05	50	5.34	125	0.11	0.573	46.79	101			41.66
Old Leach 9	2.38E-05	50	4.41	125	0.11	0.487	39.83	86.2			40.71
Old Leach 10	2.38E-05	50	4.22	125	0.12	0.469	38.31	84.9			40.51
Old Leach 11	2.38E-05	50	4.22	125	0.12	0.470	38.38	84.8			40.52
Old Leach 12	2.38E-05	50	4.75	125	0.11	0.519	42.41	88			41.06
Old Leach 13	2.38E-05	50	5.00	125	0.11	0.542	44.25	88			41.31
CN LOST IN OLD LEACH section						821.18			758.62	-288.50	530.41
CIP1	2.38E-05	50	6.69	0	0.11	0.692	44.05	97.4			33.51
CIP2	2.38E-05	50	3.72	0	0.12	0.422	26.82	68.5			31.14
CIP3	2.38E-05	50	3.72	0	0.12	0.422	26.84	70.9			31.14
CIP4	2.38E-05	50	3.55	0	0.12	0.405	25.79	65.6			31.01
CIP5	2.38E-05	50	4.30	0	0.12	0.477	30.36	67.2			31.61
CIP6	2.38E-05	50	3.55	0	0.12	0.405	25.78	64.1			31.01
CIP7	2.38E-05	50	2.92	0	0.12	0.344	21.86	56.5			30.50
CIP8	2.38E-05	50	2.48	0	0.13	0.300	19.08	52.4			30.16
CN LOST IN IN CIP section						212.40			10344.83	930.63	250.07
TOTAL CN LOSS DUE TO VOLATILISATION [g CN/h]						1194.01			12942.53	863.91	950.21
% OF TOTAL CN LOSS ATTRIBUTED TO VOLATILISATION						9%					7%

Figure 8.30. Comparison of predicted HCN loss from leach tanks to volatilisation to the calculated overall cyanide loss determined from the mass balance.

In addition, the model predictions obtained from this study was also compared to predictions of the model developed by AMIRA and discussed in section 5.3.4. A comparison of the results from these two models, shown in Figure 8.31, reveals that these two models are in good agreement. The most important difference between their predictions, is that the model presented in this study seems to be more sensitive to fluctuations in HCN_(aq), whereas the AMIRA model predictions are averaged. Nonetheless, both models predict that 160-170 g/h cyanide is lost to volatilisation from the first leach section.

8. Results and discussion

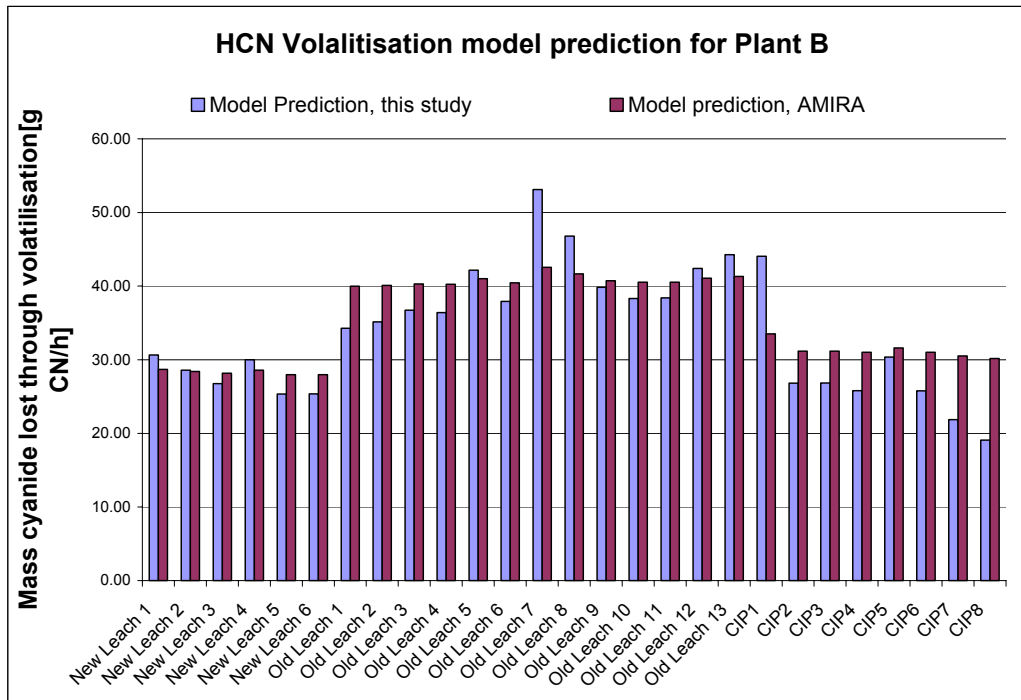


Figure 8.31. Model predictions for HCN volatilisation from leach tanks compared to predictions made using the AMIRA model.

In the case of the second leaching section, where aerated pachuca tanks are used, the model from this study predicts that essentially all the cyanide lost from this section can be ascribed to HCN volatilisation. The AMIRA model, in turn, predicts that approximately 70% of the total cyanide lost from this section is due to volatilisation. As for the carbon-in-pulp section, both models are once again in agreement that roughly 20% of the total cyanide loss can be attributed to volatilisation. The additional cyanide loss was most likely due to adsorption of cyanide onto the carbon in the adsorption tanks, as well as due to further cyanate formation, catalysed by the presence of activated carbon. As mentioned before, these effects were, however, not measured in this study and could be verified in further work.

Finally, the model predictions of the total cyanide lost from all three sections studied indicate volatilisation accounted for 9% of the total cyanide loss. This figure also compares well with the AMIRA model prediction of 7%. It has therefore been shown that, although both models make use of different methods and were developed under

8. Results and discussion

different conditions, they showed good correlation for the conditions found in this study.

9. Conclusions

9. CONCLUSIONS

Based on the preceding sections, the conclusions drawn from this study will now be discussed.

9.1 Laboratory equilibrium test work

- Henry's Law constant (k_H) for HCN was measured and determined to be independent on the total cyanide concentration in a cyanide solution, confirming the findings of previous studies.
- The value for k_H was determined to be 0.082 atm.L/mol, which correlates well with the reviewed literature.
- The effect of the presence of NaCl and CaCl₂ was investigated and it was found that k_H increases with an increase in salinity by approximately 0.15 atm.L/mol for every 1 M increase in NaCl or CaCl₂ concentration. This effect could be ascribed to a "salting-out" effect, which effectively decreased the solubility of HCN in the aqueous phase and therefore increased its partial pressure in the gas phase. This effect was however considered insignificant at the low salinity levels typically found in the local process water.
- The effect of temperature on k_H was also found to be insignificant at ambient temperatures, and it was concluded from the reviewed literature that temperature would only become important at elevated temperatures, that were not applicable to this study.

9.2 Wind tunnel test work

- The mass transfer coefficient for HCN (K_{OL}) was measured in a laboratory set-up and found to be independent of airflow velocities, ranging from 1-3.6 m/s and total cyanide concentrations up to 200 mg/L CN.
- It was also found that solution depth did not have a notable effect on K_{OL} measured from flowing solutions, as tests performed on a thin flowing solution film, compared to a flowing solution body of 5 cm depth, resulted in similar K_{OL} values.
- However, it was found that K_{OL} is dependent on HCN_(aq) at lower concentrations, and becomes rather insensitive to HCN_(aq) at higher concentrations. This was ascribed to the accumulation of HCN molecules in

9. Conclusions

the gas boundary layer at higher $\text{HCN}_{(\text{aq})}$ concentrations, increasing the resistance to mass transfer in the gas boundary layer probably due to a strong interaction between the HCN molecules, and thereby making mass transfer less efficient at higher $\text{HCN}_{(\text{aq})}$ concentrations.

- The measured value for K_{OL} at $\text{HCN}_{(\text{aq})}$ concentrations above approximately 20 ppm was found to reach a constant value of 0.06-0.07 m/h. This value correlates very well to values predicted by theoretical correlations found in literature.
- It was also stagnant solutions led to a notable decrease in K_{OL} , due to an increase in the boundary layer thickness in the absence of efficient mixing of the liquid body.
- Measurements of K_{OL} for pulp mixtures indicated a decrease of K_{OL} of approximately one order of magnitude. This is probably due to either an increase in the boundary layer, or a physical hindrance to the transfer of molecules through the pulp mixture, caused by the solid particles present. This effect was also more pronounced at higher solid to liquid ratios.
- In addition, K_{OL} was found to decrease with time for the pulp tests, probably due to the development of a thicker boundary layer caused by the lack of mixing in the pulp and the subsequent depletion of HCN molecules near the surface of the pulp mixture.
- Finally, the pulp test work showed that K_{OL} was substantially increased in the presence of a thin liquid layer that formed on top of the pulp mixtures with lower solid to liquid ratios.

9.3 On-site test work

- For the purposes of the test work performed on the tailings storage facilities, the different areas found on the tailings surface were classified according to moisture content, as shown in Table 9.1.

Table 9.1. Moisture content classification of different areas found on tailings surfaces.

Category	Moisture content, % H_2O
Discharge stream	39-41
Wet sludge	28-38
Thixotropic	24-27
Dry beach	18-23

9. Conclusions

- The on-site test work showed that K_{OL} increased drastically at moisture contents above 40% water, corresponding to tailings surfaces that were classified as wet sludge or discharge streams. As these surfaces were all covered in a thin solution film, the increase in K_{OL} is probably due to the higher mass transfer coefficients characteristic of solution films, as discussed in the previous section.
- Furthermore, the finding that K_{OL} is sensitive to $HCN_{(aq)}$ in the low $HCN_{(aq)}$ concentration region, was confirmed by the on-site test work performed on the tailings surfaces that were covered by a liquid film. However, the more dry areas, classified as thixotropic and dry surfaces, did not follow this trend, and led to much lower K_{OL} values, indicating once again that surfaces covered with solution films behave differently than dry tailings surfaces.
- The on-site measurements of K_{OL} were found to be approximately an order of magnitude lower than the measurements made from pulp mixtures in the laboratory. This was due to the much lower airflow rates applied across the surfaces of the tailings pulp compared to that of the laboratory pulp tests. This leads to the conclusion that airflow velocity does play a significant role across the ranges studied in the laboratory and on-site test work, respectively.
- In the case of the leach tank test work, it was found that the $HCN_{(g)}$ concentrations encountered on the working level above the leach tanks did not pose a short term exposure health or safety risk.
- The K_{OL} values measured from the leach tanks of two different plants, operating at different $HCN_{(aq)}$ concentrations in the pulp liquor, were found to be directly related to the $HCN_{(aq)}$ concentration, i.e. the $HCN_{(aq)}$ concentration of Plant A was double that of Plant B, leading to double the value for K_{OL} . This is a strange finding in view of the fact that K_{OL} typically decreases with concentration, to a constant value at higher cyanide concentrations.
- It was found that the $HCN_{(g)}$ in the aeration bubbles, captured at the near pulp liquor surfaces of aerated tanks, were at approximately 50% equilibrium, based on the $HCN_{(aq)}$ concentration present in the pulp liquor.
- The contribution of the aeration bubbles to the overall loss of $HCN_{(g)}$ through volatilisation was calculated as 10-20%, depending on the $HCN_{(aq)}$ concentration available for equilibration with the air bubbles in the pulp liquor.
- The measured HCN volatilisation rates increased with increased airflow rates across the pulp surface, and therefore increased Roughness Reynolds numbers.

9. Conclusions

- In addition, the volatilisation rates were also found to increase with an increase in $\text{HCN}_{(\text{aq})}$ concentration, since more HCN was available for volatilisation.

9.4 Model development

- Based on the findings discussed in the previous two sections, an empirical prediction model was developed in order to estimate the mass transfer coefficient based on the identified most important parameters, namely $\text{HCN}_{(\text{aq})}$ concentration, Roughness Reynolds number and moisture content, as shown in equation 9.1.

$$K_{OL} = a \text{Re}^{*b} M^c \text{HCN}_{(\text{aq})}^d + e \quad [\text{Eq. 9.1}]$$

- This empirical model was fitted to the data generated by the laboratory and on-site test work and was showed to be in excellent agreement with the measured data.

9.5 Model verification

- The prediction model for HCN volatilisation from tailings storage facilities was shown to be highly sensitive to the $\text{HCN}_{(\text{aq})}$ concentration input parameter. It is therefore imperative that a reliable quantification method for $\text{HCN}_{(\text{aq})}$ is available to ensure the success of the application of this model, especially to sites containing low levels of cyanide.
- In the case study presented in this work it was concluded that the determination of free cyanide through direct measurement proved to be more reliable than through prediction of the free cyanide using the MINTEK speciation model.
- The tailings storage facility model predicted that 63% of the total cyanide lost on the tailings facility resulted from HCN volatilisation.
- Roughly 95% of the total amount of cyanide lost through volatilisation occurred from the wet beach area, where the tailings surface is covered in a thin liquid layer. It is also interesting to note that the surface covered by this type of area is only 10% of the total tailings storage facility surface area. The majority of the surface therefore does not contribute to the attenuation.

9. Conclusions

- It was also concluded from the leach tank model validation that most of the cyanide lost to volatilisation occurred in the old leach section, where aerated pachuca tanks are used.
- The leach tank model presented in this study compared well to the model previously developed by AMIRA, in spite of the different approaches to modelling and conditions investigated.
- It was found that volatilisation only accounted for 2% of the cyanide lost from adsorption tanks, due to the significant cyanide losses resulting from adsorption and cyanate formation in the presence of activated carbon.
- Finally, it was found that HCN volatilisation accounted for 9% of the total cyanide lost in the two leach sections and one adsorption section. This value agrees well with the expected contribution of volatilisation to overall cyanide loss from leach tanks, as discussed in section 5.

10. RECOMMENDATIONS FOR FUTURE WORK

As a result of the findings presented in this study, the following recommendations for future development are made:

- Henry's Law constant was established at a value of 0.082 atm.L/mol, which applies to solutions of low salinity and temperatures below 35°C. For solutions with higher salinities or temperatures, possible correlations are provided in the discussion of results to compensate for such changes.
- Due to the detected sensitivity of the mass transfer coefficient, and the consequent sensitivity of the volatilisation prediction model presented in this study, to the $\text{HCN}_{(\text{aq})}$ concentration of the pulp, it is recommended that further research be done to improve current methods or develop a new, sensor-based method for determining free cyanide in solutions. It is suggested that a comparative study is launched between ISE, AgCl titration, voltametric and amperometric systems.
- In addition, it is proposed that the model developed in this study be further validated at a variety of sites. For the leach tank model, it would be interesting to investigate the applicability of the model to carbon-in-leach tanks. Furthermore, it would be meaningful to measure the cyanate concentrations in each section, especially in the adsorption tanks where carbon is present, in order to verify whether the additional losses observed in this section may be attributed to cyanate formation.
- As for the tailings storage facility model, it is recommended that the model be validated at sites with different surface areas and free cyanide concentrations, which would correspond to more moderate pH values of around 10. This would simplify the reliable determination of $\text{HCN}_{(\text{aq})}$. In addition, validation of the model across various facilities will provide a better indication as to the generic applicability of the model.
- It is also important to note that the validity of the verification exercise is limited by the accuracy of the water balance information, which have to be obtained from the operations. It is therefore recommended that ongoing work in this area is encouraged, in order to ensure that long-term use of the model will be based on reliable data that is regularly updated to reflect changes made in the water management of the tailings storage facilities.

11. References

11. REFERENCES

- Adams, M.D. 1990a. The chemical behaviour of cyanide in the extraction of gold Part 1: Kinetics of cyanide loss in the presence and absence of activated carbon. *Journal of the South African Institution of Mining and Metallurgy*, Vol. 90, no. 2, p. 37-44.
- Adams, M.D. 1990b. The chemical behaviour of cyanide in the extraction of gold Part 2: Mechanisms of cyanide loss in the carbon-in-pulp process. *Journal of the South African Institute of Mining and Metallurgy*, Vol. 90, no 3, p. 63-73.
- Australian Mineral Industries Research Association (AMIRA). 1997. *Cyanide waste management: Minimising environmental and economic impacts Phase 1 Volume 1*. Prepared by Duffield, J., May, P., Adams, M.D., Australian Mineral Industries Research Association Limited, A.J. Parker Co-operative Research Centre in Hydrometallurgy, Murdoch, Western Australia.
- Broderius, S.J. and Smith, L.L. 1980. *Direct photolysis of hexacyanoferrate complexes: Proposed applications to the aquatic environment*. Department of Entomology, Fisheries and Wildlife, University of Minnesota, St. Paul, Minnesota. p. 12-17.
- Bunce, N. and Hunt, J. 2004. *The science corner: The cyanidation process for gold extraction*. College of Physical Science, University of Guelph. http://www.waihi.co.nz/Gold/science_corner.htm
- Chamber of Mines of South Africa. June 2001. "South African guideline on cyanide management for gold mining".
- Chatwin, T.D. and Trepanowski, J.J. 1987. Utilisation of soils to mitigate cyanide releases. In *Proceedings of Third Western Regional Conference on Precious Metals, Coal and Environment*. Rapid City, South Dakota, September 23-26, p. 201-220.
- Cohen, Y., Choccio, W. and Mackay, D. 1978. Laboratory study of liquid-phase controlled volatilisation rates in the presence of wind waves. *Environment Science and Technology*, Vol. 12, p. 553-558.

11. References

- Devries, F.W. 1996. On the atmospheric non-impact of cyanide releases. Randol Gold Forum, Salt Lake City, Utah, p. 163-166.
- Dicinoski, G., Adams, M.D., Joja, B.M. and Lotz, P. 1997. Investigations into the accuracy and reliability of the most common cyanide determination techniques. Technical memorandum, MINTEK, Randburg, South Africa.
- Dodge, B.F. and Zabban, W. 1952. Disposal of plating room Wastes: IV. Batch volatilisation of hydrogen cyanide from aqueous solutions of cyanides. *Plating and Surface Finishing*, Vol. 29, p. 1133-1139.
- Habashi, F. 1970. *Extractive metallurgy Volume 2: Hydrometallurgy*. Gordon and Breach, Science Publishers, Inc, London.
- Heath, A.R., Rumball, J.A. and Browner, R.E. 1998. A Method for measuring HCN_(g) emission from CIP/CIL tanks. *Minerals Engineering*, Vol. 11, no. 8, p. 749-761.
- Huiatt, J.L., Kerrigan, J.E., Olson, F.A. and Potter, G.L. 1983. *Cyanide from mineral processing: proceedings of a workshop*. Utah Mining and Mineral Industries, Salt Lake City, Utah. Chapter 2-4.
- Kummert, R. and Stumm, W. 1992. *Gewässer als ökosysteme: Grundlagen des Gewässerschutzes*. Printed by Verlag der Fachvereine, Switzerland, p. 80-84.
- Liss, P.S. and Slater, P.G. 1974. Flux of gases across the air-sea interface. *Nature*, Vol. 247, p. 181-184.
- Lorösch, J. 2001. Process and environmental chemistry of cyanidation, Degussa AG, Frankfurt am Main.
- Lye, P. 1999. Cyanide: Legislation and public perceptions. In *Cyanide tailings and management for practitioners*. A.J. Parker Research Centre for Hydrometallurgy, Murdoch University, Western Australia.
- Lye, P. 2001. Current NPI emission estimation techniques for HCN. In *Amira Project P420B, Gold processing technology, Module 3: Cyanide and the environment*. A.J. Parker Research Centre for Hydrometallurgy, Murdoch University, Western Australia.
- Lye, P. 2004. A review: The atmospheric chemistry and fate of hydrogen cyanide. In *Amira Project P420B, Gold processing technology, Module 3: Cyanide*

11. References

- and the environment*. A.J. Parker Research Centre for Hydrometallurgy, Murdoch University, Western Australia.
- Lye, P., Cricelli, R., Corbyn, Z., Hannah, H., Heffer, H and May, P. 2004. Chemical measurements. In *Amira Project P420B, Gold processing technology, Module 3: Cyanide and the environment*. A.J. Parker Research Centre for Hydrometallurgy, Murdoch University, Western Australia.
- Mackay, D. 1977. Volatilisation of pollutants from water. In *Aquatic pollutants: Transformation and biological effects*. Edited by E.O. Hutzinger, I.H. Van Lelyveld and B.C.J.Zoetemans. Proceedings of the Second International Symposium on Aquatic Pollutants, Amsterdam, The Netherlands, p. 175-185.
- Mill, T. 1993. *Environmental chemistry in "Ecological risk assessment"*. Edited by G.W. Suter. Lewis Publishers. P. 91-127.
- Patrick, G. 2000. Studies of hydrogen cyanide volatility from cyanidation slurry - Ergo, Daggafontein and WWO. Technical Memorandum, Process Chemistry Division, MINTEK, Randburg, South Africa.
- Rubo, A., Dickmann, A. and Gos, S. 2000. Laboratory simulation of HCN emissions from tailing ponds. In *Tailings and mine waste '00*, Balkema, Rotterdam, ISBN 90 5809 126 0, p. 307-313.
- Simovec, L, Snodgrass, W.J., Murphy, K.L. and Schmidt, J.W. 1984. Development of a model to describe the natural degradation of cyanide in gold milling, Conference on cyanide and the environment, Tucson, Arizona.
- Simovec, L. and Snodgrass, W.J.. 1985. Natural removal of cyanides in gold mill effluents – evaluation of removal kinetics. *Water Pollution Research Journal Canada*, Volume 2, No. 2., p. 120-133.
- Smith, A. and Mudder, T. 1991. *The chemistry and treatment of cyanidation wastes*. Mining Journal Books Ltd., London.
- Smith, J.H. Bomberger, D.C. and Haynes, D.L. 1980. Prediction of the volatilisation rates of high volatility chemicals from natural water bodies. *Environment Science and Technology*. Volume 14, p. 1332-1337.
- Thomas, R.G. 1982. Volatilisation from water. In *Handbook of chemical estimation methods*. Edited by W.J. Lyman. New York: McGraw Hill Book Company. Chapter 15.

11. References

- Verhoefen, P., Hefter, G. and May, P.M. 1990. Dissociation constant of hydrogen cyanide in saline solutions. *Minerals and Metallurgical Processing*, Vol. 7, No. 4, p. 185-188.
- Wu, J., 1969. Wind stress and roughness at air-sea interface. *Journal of Geophysical Research*, Vol. 74, No. 2, p. 444-455.
- Young, C.A. and Jordan, T.S. 1995. Cyanide remediation: Current and past technologies. In *Proceedings of the 10th annual conference on hazardous waste research*. Department of Metallurgical Engineering, Montana Technicon, Butte. P. 104-128.

Internet references:

www.cyanidecode.org

www.cyantists.com

Mining, minerals and sustainable development. April 2002. "Mining for the future. Appendix A: large volume waste working paper". World business council for sustainable development. <http://www.iiied.org/mmsd/wp/index.html>

National pollutant inventory. June 1999. "Emission estimation technique manual for gold ore processing". <http://www.deh.gov.au/erin/ert/index.html>.

12. Bibliography

12. Bibliography

- Adams, M.D. 2001. A methodology for determining the department of cyanide losses in gold plants. *Minerals Engineering*, January, Vol. 14, No. 4, p. 383-390.
- Australian Government - Department of the Environment and Heritage. 2003. *Cyanide management – Cyanide in gold extraction*. Environment Australia. ISBN 0 642 549 443, p. 1-9.
- Cohen, Y., 1986. Intermedia transport modelling in multimedia systems. In *Pollutants in a multimedia environment*. Edited by Y. Cohen. Plenum press.
- Cohen, Y. and Ryan, P.A., 1985. Theoretical analogy of turbulent mass transfer across sheared gas-liquid interfaces. *International Comm. Heat Transfer*, Vol. 12, p. 139-148.
- Coulson, J.M. and Richardson, J.F. 1999. Fluid flow, heat transfer and mass transfer. In *Chemical Engineering, Volume 1*. 6th Edition. The Bath Press, Bath, Great Britain. ISBN 0 7506 4444 3.
- De Nevers, N. 1991. *Fluid Mechanics for Chemical Engineers*. International edition. Department of Chemical Engineering, University of Utah, McGraw-Hill Book Co, Singapore. ISBN 0 07 100830 6.
- Devries, F.W. 1996. On the atmospheric non-impact of cyanide releases. Randol Gold Forum, Salt Lake City, Utah, p. 163-166.
- Incropera, F.P. and DeWitt, D.P. 1996. *Fundamentals of heat and mass transfer*, School of Mechanical Engineering, Purdue University, 4th edition. John Wiley and Sons, Inc. ISBN 0 471 30460 3.
- International Critical Tables of Numerical Data, Chemistry and Technology*. 1928. Edited by E. W. Washburn et al, National Research Council of the United States of America. McGraw-Hill Book Company, New York and London, Volume 3, 1st edition, p. 365.
- Lye, P. 2002. HCN emission calculator development. In *Amira Project P420B, Gold processing technology, Module 3: Cyanide and the environment*. A.J. Parker Research Centre for Hydrometallurgy, Murdoch University, Western Australia.

12. Bibliography

- Mackay, D. and Shiu, W.Y. 1981. A critical review of Henry's law constants for chemicals of environmental interest. *Journal of Physical and Chemical Reference Data*, Vol. 10, No.4, p. 1175-1199.
- Miltzarek, G.L., Sampaio, C.H. and Cortina, J.L. 2002. Cyanide recovery in hydrometallurgical plants: Use of synthetic solutions constituted by metallic cyanide complexes. *Minerals Engineering*, Vol.15, p. 75-82.
- Perry, R.H., Green, D.W. and Maloney. 1997. *Perry's Chemical Engineer's Handbook*, 7th edition, McGraw-Hill Book Company, Australia. ISBN 0 07 115982 7.
- Sander, R. 1999. "Compilation of Henry's law constants for inorganic and organic species of potential importance in environmental chemistry". <http://www.mpch-mainz.mpg.de/~sander/res/henry.html>.
- Stanley, G.G. 1987. *The extractive metallurgy of gold in South Africa: Volume 1 and 2*. The South African Institute of Mining and Metallurgy Monograph Series, M7, Johannesburg, South Africa.
- Stoyanov, I.J. 2003. Extraction of gold from dump material by agitation. *African Journal of Science and Technology*, Science and Engineering Series Volume 4, No. 1, p. 56-61.
- Tanriverdi, M., Mordogan, H. and İpekoglu, Ü. 1998. Natural degradation behaviour of cyanide leach solution under laboratory conditions, Department of Mining Engineering, Dokuz Eylül University, İzmir, Turkey, p. 865-869.
- U.S Department of Health and Human Services, Public health service, Agency for toxic substances and disease registry. September 1997. "Toxicological profile for cyanide".

APPENDIX A – Gold extraction process summary

Table A.1. Gold extraction process: Comminution.

Process	Unit Operation	Function	Examples of Equipment used in SA	Comments
<u>Comminution</u> The gold particles are liberated from the ore to facilitate separation of minerals from gangue material.	Sizing	Divides ore stream into different size classes.	<ul style="list-style-type: none"> Grizzly screens Vibrating screens 	Static or mechanised grizzly screens are used.
	Crushing	Breaks the rock into smaller sizes by applying compression and/or impact forces to the surfaces.	<ul style="list-style-type: none"> Jaw crushers Roll crushers Gyratory crushers 	Usually applied in two stages, i.e. primary and secondary crushing.
	Grinding	Further size reduction of partially comminuted ore by breaking action of free tumbling bodies, i.e. grinding media such as steel rods, balls or pebbles. In autogenous mills, the grinding media is generated from the run-of-mine ore itself.	<ul style="list-style-type: none"> Rod mills Ball mills Autogenous mills <ul style="list-style-type: none"> Pebble mills Run-of-mine mills 	<ul style="list-style-type: none"> Primary grinding Concentrate regrinding Applied to <ul style="list-style-type: none"> Any grinding stage Primary milling
	Classification	Increase mill grinding efficiency by increasing the relative coarse/fine fraction in the mill and removing the fine fraction to prevent overgrinding.	<ul style="list-style-type: none"> Gravity classifiers (Dorr or Akins) Centrifugal classifiers (hydrocyclone) 	Hydrocyclones have almost completely replaced gravity classifiers over past 30 years.

Appendix

Table A.2. Gold extraction process: De-watering.

Process	Unit Operation	Function	Examples of Equipment used in SA	Comments
<u>De-watering</u> Excess water added during grinding to enhance comminution is removed from the pulp to reduce volume of pulp in downstream processes.	Thickening	Suspended solids are concentrated by gravity settling in a virtually still solution body, resulting in a dilute overflow product and a concentrated underflow product. The overflow is recycled to the milling circuit and the underflow is pumped to the pretreatment circuit or directly to the leaching circuit.	<ul style="list-style-type: none"> • Continuous drag rake thickeners • High rate thickeners 	Flocculants are added to overcome problems with settlement that arise from overloading, low temperatures and ore components that are difficult to settle.

Appendix

Table A.3. Gold extraction process: Concentration.

Process	Unit Operation	Function	Examples of Equipment used in SA	Comments
<u>Concentration</u> Valuable minerals are extracted efficiently from the pulp in one single step, thereby reducing gold lock-up as well as the volume to be pretreated in the case of refractory ore.	Flotation	Air bubbles are passed through the finely milled slurry and the gold bearing sulphides and other minerals attach to the air bubbles to form a froth that is scooped from the surface of the slurry.	<ul style="list-style-type: none"> • Denver flotation cell • Outokumpu flotation cell • Wemco flotation cell 	Modifiers that are used to enhance flotation: <ul style="list-style-type: none"> • Frothers - control bubble stability • Activator / Depressants - improve / reduce floatability of specific mineral.
	Gravity concentration	Utilises the large differences in relative density between high-density gold and pyrites and low-density silica to achieve separation. Only economic where large amounts of gold is locked up in sulphides or for treatment of high grade ores.	<ul style="list-style-type: none"> • Nelson Centrifugal concentrators • Plane tables • Shaking tables • Johnson drums 	Nelson concentrators are most widely used as primary concentrators, and are often followed by shaking tables in the secondary stage.

Appendix

... Table A.4. (continued).

Process	Unit Operation	Function	Examples of Equipment used in SA	Comments
<u>Concentration</u>	Intensive cyanidation	Direct recovery of gold from concentrates with the use of high cyanide strengths and increased oxygen partial pressure.	<ul style="list-style-type: none"> • Gekko Inline leach reactors • Nelson Concentrators • Sealed mechanical agitators 	This process has virtually replaced mercury amalgamation due to the poisoning hazard associated with mercury.

Appendix

Table A.5. Gold extraction process: Pretreatment.

Process	Unit Operation	Function	Examples of Equipment used in SA	Comments
<u>Pretreatment</u> In some cases the characteristics of the ore or pulp necessitate preparation thereof for the downstream process, i.e. leaching	Roasting	Refractory ore concentrates are treated to oxidise sulfides that trap the gold and produce a concentrate where the gold is amenable to cyanide dissolution.	<ul style="list-style-type: none"> • Fluid bed roasters • Rotary kilns • Edwards roasters 	The SO ₂ contained in off-gases during roasting can be converted to sulphuric acid, but this is not normally economic; hence, pressure- or bacterial pre-oxidation is often preferred.
	Pressure oxidation		Pressurised oxygen introduced to autoclave.	High capital cost compared to bio-oxidation.
	Bio-oxidation		Chemolithotropic bacteria in a CSTR	Generally used for pretreatment of refractory sulfidic gold ores or low grade ores.
	Heap oxidation and neutralisation		Heap inoculation with mineral oxidising bacteria and lime.	

Appendix

...Table A.5. (continued).

Process	Unit Operation	Function	Examples of Equipment used in SA	Comments
<u>Pretreatment</u>	Pre-aeration	Some ore mineralogies require pre-aeration of the slurry to enhance gold dissolution during the leach. The slurry is preconditioned for an hour before addition of the lixiviant.	Agitated leach tank	Water is added to make up the required slurry density for the leach and the slurry is mechanically agitated to achieve aeration.
	Agglomeration	The slurry is mixed with lime and cement binder before being fed onto a rotating disk with water spraying nozzles to achieve agglomeration of the fine particles and help prevent poor percolation of the heap.	Rotating disk agglomerators	Poor percolation in a heap may lead to channelling which results in the leaching of only a portion of the heap, or flooding.

Appendix

Table A.6. Gold extraction process: Leaching.

Process	Unit Operation	Function	Examples of Equipment used in SA	Comments
<u>Leaching</u> Gold minerals present in the solid ore is dissolved by means of a cyanide solution.	Agitated leaching	Gold is dissolved into an aqueous solution of a soluble cyanide salt such as sodium or calcium in an air agitated leach tank.	Pachuca tanks	Cyanide, oxygen and calcium or sodium hydroxide are essential components to drive the cyanidation reaction (see) . Heap leaching is generally more economical for low grade ores.
	Heap leaching	Low grade ore is pre-limed, dumped in a heap and sprayed with cyanide solution. The leached solution is collected at the bottom of the heap.	Heaps	

Appendix

Table A.7. Gold extraction process: Solid \ Liquid separation.

Process	Unit Operation	Function	Examples of Equipment used in SA	Comments
<u>Solid \ Liquid separation</u> A selective solid extractant is used to recover the gold from the pregnant liquor. The gold ions are then stripped from the extractant in an elution step, delivering a more concentrated eluate.	Carbon-in-pulp (CIP)	Granular activated carbon is used to extract dissolved gold directly from the pulp, followed by screening of the loaded carbon from the pulp. The equilibrium reaction is reversed during elution in a caustic cyanide at elevated	Adsorption contactors with mechanical mixers and screens between or inside tanks.	Prior to being recycled, the carbon is acid-washed to remove calcium and regenerated at elevated temperatures to remove organic contaminants. The elimination of filtration and clarification stages results in major cost savings.
	Carbon-in-leach (CIL)	Carbon is added during the leach and competes with other gold-adsorbing constituents in the pulp, leading to improved leach efficiency.	Upflow bed contactors	The lower capital costs are offset by operational problems compared to CIP. CIL is often the preferred process for preg-robbing ores.
	Resin-in-pulp (RIP)	Solid organic polymers are contacted with the pulp to facilitate selective adsorption.	Similar to CIP, but with smaller screens.	Resins are less sensitive to organic preg-robbing than carbon, and enables simultaneous recovery of gold and uranium.

Appendix

Table A.8. Gold extraction process: Gold recovery from solution.

Process	Unit Operation	Function	Examples of Equipment used in SA	Comments
<u>Gold Recovery from solution</u> After being dissolved and concentrated, the gold in solution is recovered by a precipitation method before smelting and refining.	Zinc cementation	Zinc dust is used to precipitate the gold from the leachate. The solution is first de-aerated and clarified, the zinc is added in an emulsifier followed by filtration precipitate.	<ul style="list-style-type: none"> • Crowe emulsifiers • Merrill filters • Stellar candle filters • Funda filters 	Lead salts are added to the pregnant liquor to enhance the process and the solution is de-aerated prior to cementation to prevent redissolution of the gold.
	Chemical Precipitation	A non-metallic chemical reducing agent is used to reduce dissolved gold to the metallic state.	Similar to zinc cementation	Borohydride can be used for cyanide eluates, but is often economically unattractive due to its high cost compared to zinc.
	Electrowinning	Gold is electrolytically recovered by applying a potential across two electrodes immersed in the eluate. The the complexed gold is reduced and precipitated onto a cathode surface.	<ul style="list-style-type: none"> • Zadra cell • AARL cell • NIM graphite cell • Mintek steel wool cell • Sludge reactor 	Advanced processes such as intensive cyanidation of gravity concentrates and the use activated carbon resulting in high elution gold tenors has made electrowinning a viable alternative to cementation.

APPENDIX B – MINTEK cyanide speciation approach

Cyanide metal species in aqueous solution are normally present in an equilibrium governed by their parent metal concentration relative to the available free cyanide ion, CN^- , which in turn is dependent on pH and its effect on the protonation of CN^- .

Several speciation programs are available that predict, based on stability constants known from literature, the relative composition of several metals in relation to available cyanide. MINTEQA2, JESS, VIRTUALMINTEQ are examples of such programs, MINTEQA2 being an open domain resource accessible through the US EPA.

MINTEK's calculation program is based on stability constants found in MINTEQA2, but the system has been modified to accommodate difficulties encountered with metallurgical samples. Whereas normally two sets of inputs are made for the total metal concentrations and the total cyanide content, allowing the program to adjust the species composition from the most stable to the very weak complexes in that order, it was found that iron and cobalt are often analysed in solutions to levels that exceed cyanide available for their complex formation (secondary streams mixing, colloids co-analysed). This would lead to results suggesting solutions depleted of weak species, a prediction usually not matched by validating analysis. It was hence decided to exclude the so-called SAD species from the equilibrium calculations and restrict the balancing to the WAD cyanide species (SAD species complexation levels are either assumed or validated through analysis dedicated to specific species). Free cyanide is adjusted to match analysed CN WAD levels supported by the following reasons:

- CN WAD as an analytical method does not suffer from severe interferences (compared to CN Total or the CN free based methods). It is hence the more robust pivot around which to calculate the species distribution.
- CN Total normally accounts for approximately 80% of cyanide bound to cobalt and even more bound to precious metals; this renders the input of CN Total invalid.
- CN Titratable, supposedly quantifying CN free, also co-determines all zinc species as well as portions of the $\text{Cu}(\text{CN})_4^{3-}$ in a concentration dynamic way; input as CN free is hence invalid.

- CN ISE (Ion Selective Electrode), reportedly quantifying CN free, produces results of extreme varying nature, as the activity of the CN^- ion is influenced by many constituents in the solution that are not normally known.
- CN WAD relies on the gap in relative stability between nickel, as the upper limit CN WAD species, and the high stability of the SAD cyanide species, ferro/ferri cyanide and cobalti cyanide.

It should be noted though, that all the stability constants are determined in isolation from other metal species. The presence of unknown levels of other ligands such as thiocyanate, thiosulphate as well as the activity suppression of the CN^- ion could lead to serious shifts in equilibrium conditions, a statement supported by analytical evidence, but not supported by fundamental studies at this point.

The existing calculation program hence represents a compromise between data prediction and data reconciliation.

APPENDIX C – Solid extraction standard operating procedure

Soil analysis: **Water extract on coarse materials for analysis of mobile parameters**

Objective: Process a portion of solids (dry or wet) by means of de-ionised water extraction such that very weak adsorbed or simply entrained species are recovered and quantified from the wet solids and analysis for

- metals
- cyanide species ($CN_{TITRATABLE}$, CN_{WAD} , CN_{TOTAL})
- cyanide derivatives (SCN , CNO , NO_2 , NO_3 , NH_3)
- conductivity, pH, Eh

could be performed on the stabilised extracts. The filtered off residues can be used as feed materials for the base/chelating extraction procedure quantifying solid state cyanide of the Prussian Blue type.

Scope: This procedure can be used on all tailings materials or equivalent material where the matrix is of sand-type particle size. It is only conditionally suitable for top-soil samples or materials with high silt/clay content as the filtration step is drawn out and can lead to deterioration of the liquids.

Resources: De-ion water,
SCHOTT bottles 500 ml,
pressure filtration set-up,
pill vials,
 HNO_3 65 %, NaOH solution 10 %,
laboratory shaker

Procedure:

- Verify solid sample identity carefully
- Transfer number/name onto SCHOTT bottle

-
- Homogenise if necessary or take representative sample quantity to make up 100 g wet/dry pulp or solid and transfer into SCHOTT bottle, record mass (2 digits)
 - Add 150 g of de-ionised water to the bottle and shake for a minimum time (until all solids are homogeneously re-dispersed, 15 to 30 minutes)
 - Vacuum filtrate¹⁾ the solids off and wash with 50 g of de-ionised water (in two portions) adding the water as soon as the surface of the solids appears **without allowing cracks to form**. This step is important as any residual water extract left will interfere with the base extract to follow. Filtrate and wash-water are collected together in the receiving flask. **Do not let air suck through the filter-cake unnecessary (it will dry and the filtrate below will loose constituents)**.
 - Record the damp solid's mass (2 digits)
 - Rebottle the solids if base extract is to follow, label clearly
 - Determine the extract pH if required
 - Determine the extract conductivity if required
 - On a routine basis, take 100 ml filtrate , fill into 100 ml PE bottle and label
 - On a routine basis, discard the rest
- 1) If CN FREE is required as important parameter, vacuum filtration must be replaced by pressure filtration leading into a receiving flask with 1 ml NaOH 1M to keep pH around 11

If more than cyanide-analysis is required, the following additional quantities are needed:

~100 ml solution to be acidified by slow addition of 2 ml HNO₃ 65% to prevent metals from precipitating (perform in the fume cub-cupboard); to be labelled as XW A (water extract, acidic) and send to ASD for sweep on metals as specified in the sample log-sheet. NH₃ analysis is to be done on this sample as well.

~50 ml solution to be rendered basic by addition of a few drops of NaOH 50% (~ pH 12) to stabilise cyanides and species. This portion is to be labelled XW B (water extract basic). The sample goes to the analytical department's Ion Chromatography section for analysis on CN species, SCN, CNO. NO₂, NO₃) if required as well as to the SKALAR SFIA facility for analysis on CN_{WAD}, CN_{total}, CN_{total} plus CN_{SCN}.

Its recommended to keep this samples stored in the fridge right to time of analysis and note any anomalies like color changes, precipitation etc.

**Checks: original solid mass used (g, 2 digits)
 damp solids after water extraction (g, 2 digits)
 dry mass after base extraction (g, 2 digits)**

Draft: revision 3

Soil analysis: Alkaline extract for analysis of precipitated and strongly adsorbed species from coarse materials

Objective: further process the residue from water extraction (SOP 090 – 4-3A) by means of alkaline/chelating extraction such that some adsorbed complexes or most precipitated cyanide species are recovered from the wet cake and analysis for

- complexed metals
- cyanide species

could be performed.

Scope: Secondary samples as obtained from previous procedure. Range of materials currently set tentatively to include tailings, sandy soil solids.

Resources: Extraction liquid: NaOH solution 1M / EDTA 10 g per L, 500 ml SCHOTT bottle, filtration set-up, pill vials, lab shaker

Procedure:

- Obtain the damp residue from water extraction (XW) after filtration, verify the damp mass has been recorded
- place in a 500 ml SCHOTT bottle
- add 200 g extractant (40 g per liter NaOH, 10 g per liter EDTA) to the bottle and close firmly
- place the bottle with the next batch on the laboratory shaker (**horizontally**) and adjust the speed (~110 – 120 rpm) such that all solids are constantly re-suspended
- check for complete re-dispersion of the solids (sulphides etc), turn if necessary. Check also for leaks from time to time (few drops can be ignored, >1ml will have to be repeated)
- shake for 18 h ± 1 h
- filtrate the entire slurry to dryness; do not wash!
- sample 100 ml into a PE bottle, label and store for analysis
- discard the rest of the filtrate
- dry the solids at ~100° C in oven to obtain the dry mass after extractions
- discard the solids after drying

The obtained basic filtrate can be analysed for:

CN_{WAD}, CN_{total}, CN_{total} plus CN_{SCN}
complexed metals as appropriate (Fe, Co and others)

Checks: damp mass (g, 2 digits)
dry mass (g, 2 digits)

Data integration:

Enter the obtained data into the existing spread sheet-or calculate as follows:

Water extracts:

Concentrations of analysed parameters will have to be related to the total mass of liquid. That would be the sum of the added de-ionised water (150 ml + 50 ml = 200 ml) plus the entrained liquid (wet solids – dry final residue).

The mass thus obtained can be calculated back to the entrained liquid (total liquid mass / entrained liquid = dilution factor). Alternatively, if desorption is suspected, the dry final residue mass is used instead of the entrained liquid.

Alkaline EDTA extracts:

Concentrations for these values are related back to mass of extractant added plus the remaining entrained liquid after the water extract has been performed. Masses are then calculated back to dry final residue and expressed in ppm to dry solids.

APPENDIX D – Equilibrium test work summary

Test Description	Test parameters		Aqueous HCN		Gaseous HCN		Henry's Constant		
	Temperature [K]	pH	Solution CN concentration [ppm]	[HCN] _{aq} [ppm]	[HCN] _(g) [ppm]	[HCN] _(g) [g/L]	P _{HCN(g)} [atm]	[HCN] _{aq} [mol/L]	k _H (exp)
	Measured	Measured	Laboratory TCN	Calculated	Drager	Converted	Calculated	Measured	Calculated
183ppm CN	292	12.02	183.0	0.32	1.4	1.27E-06	1.13E-06	1.18E-05	0.096
183ppm CN	292	11.20	183.0	2.08	8.3	7.55E-06	6.70E-06	7.69E-05	0.087
183ppm CN	292	10.75	183.0	5.74	22.4	2.04E-05	1.81E-05	2.12E-04	0.085
183ppm CN	292	10.64	183.0	7.32	28.2	2.56E-05	2.28E-05	2.71E-04	0.084
183ppm CN	293	10.47	183.0	10.63	39.4	3.58E-05	3.19E-05	3.94E-04	0.081
105ppm CN	292	12.15	105.0	0.14	0.6	5.45E-07	4.84E-07	5.00E-06	0.097
105ppm CN	292	11.45	105.0	0.67	2.7	2.47E-06	2.20E-06	2.49E-05	0.088
105ppm CN	292	10.52	105.0	5.47	20.4	1.85E-05	1.65E-05	2.03E-04	0.081
105ppm CN	292	10.22	105.0	10.38	37.3	3.39E-05	3.01E-05	3.84E-04	0.078
180 ppm CN	290	12.14	180.0	0.24	1.0	9.09E-07	8.01E-07	8.78E-06	0.091
180 ppm CN	291	11.52	180.0	0.98	3.7	3.33E-06	2.95E-06	3.64E-05	0.081
180 ppm CN	292	10.71	180.0	6.17	21.6	1.97E-05	1.74E-05	2.28E-04	0.076
188 ppm CN	292	12.18	188.0	0.20	0.6	5.64E-07	5.01E-07	7.45E-06	0.067
183ppm CN	292	11.14	188.0	2.18	8.7	7.88E-06	6.99E-06	8.09E-05	0.086
183ppm CN	292	10.46	188.0	10.01	39.3	3.57E-05	3.17E-05	3.71E-04	0.086
50 ppm CN	293	11.37	50.0	0.39	1.3	1.16E-06	1.04E-06	1.43E-05	0.073
50 ppm CN	292	10.82	50.0	1.34	5.0	4.54E-06	4.03E-06	4.96E-05	0.081
50 ppm CN	292	10.50	50.0	2.72	10.7	9.75E-06	8.66E-06	1.01E-04	0.086
50 ppm CN	295	11.37	50.0	0.34	1.0	9.27E-07	8.31E-07	1.27E-05	0.065
50 ppm CN	292	10.69	50.0	1.60	5.9	5.35E-06	4.74E-06	5.94E-05	0.080
50 ppm CN	292	10.50	50.0	2.44	9.2	8.35E-06	7.41E-06	9.03E-05	0.082
50 ppm CN	292	10.38	50.0	3.17	12.1	1.10E-05	9.79E-06	1.17E-04	0.084
42 ppm CN	294	11.23	42.0	0.40	1.1	9.55E-07	8.54E-07	1.47E-05	0.058
42 ppm CN	293	10.73	42.0	1.23	5.2	4.75E-06	4.23E-06	4.56E-05	0.093
42 ppm CN	293	10.53	42.0	1.92	8.4	7.67E-06	6.84E-06	7.11E-05	0.096
42 ppm CN	294	10.08	42.0	4.99	21.4	1.95E-05	1.74E-05	1.85E-04	0.094
184 ppm CN	290	12.14	186.0	0.24	1.0	9.09E-07	8.01E-07	9.07E-06	0.088
184 ppm CN	291	11.52	186.0	1.02	3.7	3.33E-06	2.95E-06	3.77E-05	0.078
184 ppm CN	292	10.71	186.0	6.37	21.6	1.97E-05	1.74E-05	2.36E-04	0.074
184 ppm CN	292	10.45	186.0	11.28	39.3	3.57E-05	3.17E-05	4.18E-04	0.076
10 ppm CN	290	10.10	10.0	1.26	9.2	8.37E-06	7.37E-06	4.68E-05	0.158
10 ppm CN	290	10.08	10.0	1.31	9.5	8.64E-06	7.60E-06	4.87E-05	0.156
10 ppm CN	290	8.51	10.0	8.49	32.0	2.91E-05	2.56E-05	3.14E-04	0.081
10 ppm CN	290	3.47	10.0	10.00	36.0	3.27E-05	2.88E-05	3.70E-04	0.078
10 ppm CN	292	9.96	9.0	1.50	8.5	7.74E-06	6.87E-06	5.54E-05	0.124
45 ppm CN	292	12.00	45.0	0.08	0.3	2.36E-07	2.10E-07	3.03E-06	0.069
45 ppm CN	292	10.93	45.0	0.94	4.6	4.14E-06	3.67E-06	3.49E-05	0.105
88 ppm CN	292	11.53	88.0	0.47	2.7	2.44E-06	2.16E-06	1.74E-05	0.124
88 ppm CN	292	10.93	88.0	1.84	9.5	8.62E-06	7.65E-06	8.82E-05	0.112
10 ppm CN	295	12.01	10.0	0.02	-	0.00E+00	0.00E+00	6.57E-07	-
10 ppm CN	294	11.88	10.0	0.02	0.2	1.55E-07	1.38E-07	8.86E-07	0.156
10 ppm CN	291	11.80	10.0	0.03	0.2	1.73E-07	1.53E-07	1.07E-06	0.144
10 ppm CN	293	11.10	10.0	0.14	0.6	5.45E-07	4.85E-07	5.28E-06	0.092
10 ppm CN	293	10.88	10.0	0.23	1.0	9.09E-07	8.09E-07	8.68E-06	0.093
10 ppm CN	293	10.73	10.0	0.33	1.4	1.30E-06	1.16E-06	1.21E-05	0.095
20 ppm CN	292	11.85	20.0	0.05	0.3	2.73E-07	2.42E-07	1.90E-06	0.127
20 ppm CN	292	11.38	20.0	0.15	0.8	7.27E-07	6.45E-07	5.58E-06	0.116
20 ppm CN	292	10.33	20.0	1.57	6.3	5.73E-06	5.09E-06	5.81E-05	0.088
20 ppm CN	293	9.98	20.0	3.20	12.6	1.15E-05	1.02E-05	1.19E-04	0.086
50 ppm CN	293	11.91	50.0	0.11	0.6	5.27E-07	4.69E-07	4.14E-06	0.113
50 ppm CN	293	11.59	50.0	0.23	1.2	1.10E-06	9.79E-07	8.62E-06	0.114
50 ppm CN	293	11.35	50.0	0.40	2.1	1.90E-06	1.69E-06	1.49E-05	0.113
50 ppm CN	293	10.95	50.0	1.00	5.1	4.62E-06	4.11E-06	3.71E-05	0.111
50 ppm CN	293	10.49	50.0	2.78	12.5	1.13E-05	1.01E-05	1.03E-04	0.098
50 ppm CN	293	10.11	50.0	6.19	25.0	2.28E-05	2.03E-05	2.29E-04	0.088

APPENBIX D – Wind tunnel test work summary

Table D-1. Glass plate tests at ambient temperature.

Table D- 1: WIND TUNNEL TESTS: Glass Plate @ ambient														
Fan setting	Flow Configuration	Flow rate of solution	Wind velocity		C ₀	Re*	Temperature	pH	WAD CN		ISE CN	HCN(aq)		
			[Lpm]	[m/s]					[m ² /s]	[ppm]		[ppm]	[ppm]	[ppm]
Fully open	Plate	0.77	2.18	0.064	0.01	1.57E-04	18	10.95	50	50	55	1.2	1.2	1.2
Fully open	Plate	0.77	2.18	0.064	0.01	1.57E-04	18	10.97	50	50	55	1.2	1.2	1.2
Fully open	Plate	0.77	2.18	0.064	0.01	1.57E-04	18	10.97	50	50	55	1.2	1.2	1.2
Fully open	Plate	0.77	2.18	0.064	0.01	1.57E-04	18	10.97	50	49	55	1.2	1.2	1.2
Fully open	Plate	0.77	2.18	0.064	0.01	1.57E-04	18	10.05	49	48	55	8.4	8.2	8.3
Fully open	Plate	0.77	2.18	0.064	0.01	1.57E-04	18	10.06	48	47	55	8.2	7.9	8.1
Fully open	Plate	0.77	2.18	0.064	0.01	1.57E-04	18	10.07	47	46	55	7.9	7.6	7.8
Fully open	Plate	0.77	2.18	0.064	0.01	1.57E-04	18	10.08	46	46	55	7.6	7.3	7.5
Fully open	Plate	0.77	2.18	0.064	0.01	1.57E-04	18	8.98	46	40	25	32.1	27.8	30.0
Fully open	Plate	0.77	2.18	0.064	0.01	1.57E-04	18	9.02	40	29	25	27.8	19.9	23.9
Fully open	Plate	0.77	2.18	0.064	0.01	1.57E-04	18	9.05	29	34	25	19.9	23.1	21.5
Fully open	Plate	0.77	2.18	0.064	0.01	1.57E-04	18	9.08	34	32	25	23.1	21.2	22.2
Half open	Plate	0.77	1.00	0.029	0.01	2.49E-06	18	10.98	54	57	45	1.3	1.3	1.3
Half open	Plate	0.77	1.00	0.029	0.01	2.49E-06	18	10.98	57	56	45	1.3	1.3	1.3
Half open	Plate	0.77	1.00	0.029	0.01	2.49E-06	18	10.91	56	55	43	10.2	10.0	10.1
Half open	Plate	0.77	1.00	0.029	0.01	2.49E-06	18	10.02	55	53	43	10.0	9.7	9.8
Half open	Plate	0.77	1.00	0.029	0.01	2.49E-06	18	9.02	53	48	15	36.3	33.0	34.7
Half open	Plate	0.77	1.00	0.029	0.01	2.49E-06	18	9.07	48	46	15	33.0	30.2	31.6
Half open	Plate	0.77	1.00	0.029	0.01	2.49E-06	18	11.08	122	126	93	2.3	2.4	2.3
Half open	Plate	0.77	1.00	0.029	0.01	2.49E-06	18	10.98	117	118	89	2.7	2.7	2.7
Half open	Plate	0.77	1.00	0.029	0.01	2.49E-06	18	10.02	122	122	79	21.9	21.9	21.9
Half open	Plate	0.77	1.00	0.029	0.01	2.49E-06	18	10.04	122	126	79	21.9	22.6	22.3
Half open	Plate	0.77	1.00	0.029	0.01	2.49E-06	18	9.01	102	99	25	70.5	68.3	69.4
Half open	Plate	0.77	1.00	0.029	0.01	2.49E-06	18	9.01	99	93	25	68.3	64.4	66.3
Fully open	Plate	0.77	2.18	0.064	0.01	1.57E-04	18	11.00	118	120	89	2.7	2.7	2.7
Fully open	Plate	0.77	2.18	0.064	0.01	1.57E-04	18	11.01	120	122	89	2.7	2.7	2.7
Fully open	Plate	0.77	2.18	0.064	0.01	1.57E-04	18	10.06	126	108	79	21.0	18.0	19.5
Fully open	Plate	0.77	2.18	0.064	0.01	1.57E-04	18	10.09	108	102	79	18.0	17.0	17.5
Fully open	Plate	0.77	2.18	0.064	0.01	1.57E-04	18	9.03	93	86	25	64.5	58.4	61.4
Fully open-insert	Plate	0.77	3.6	0.043	0.01	1.66E-03	16	11.07	78	84	62	1.5	1.6	1.6
Fully open-insert	Plate	0.77	3.6	0.043	0.01	1.66E-03	16	11.07	84	79	62	1.6	1.5	1.6
Fully open-insert	Plate	0.77	3.6	0.043	0.01	1.66E-03	16	10.00	79	69	55	14.8	12.9	13.8
Fully open-insert	Plate	0.77	3.6	0.043	0.01	1.66E-03	16	10.03	69	67	55	12.9	12.4	12.6
Fully open-insert	Plate	0.77	3.6	0.043	0.01	1.66E-03	16	9.07	67	55	18	44.1	36.6	40.3
Fully open-insert	Plate	0.77	3.6	0.043	0.01	1.66E-03	16	9.10	55	53	18	36.6	34.7	35.7
Fully open-insert	Plate	0.77	3.6	0.043	0.01	1.66E-03	18	10.98	52	53	50	1.2	1.3	1.2
Fully open-insert	Plate	0.77	3.6	0.043	0.01	1.66E-03	18	10.99	53	52	52	1.3	1.2	1.2
Fully open-insert	Plate	0.77	3.6	0.043	0.01	1.66E-03	18	10.01	52	49	50	9.6	9.0	9.3
Fully open-insert	Plate	0.77	3.6	0.043	0.01	1.66E-03	18	10.06	49	48	48	8.2	7.9	8.0
Fully open-insert	Plate	0.77	3.6	0.043	0.01	1.66E-03	18	9.15	48	42	20	29.4	25.9	27.6
Fully open-insert	Plate	0.77	3.6	0.043	0.01	1.66E-03	18	9.20	42	37	19	27.7	21.8	24.8
Fully open	Plate	0.77	2.18	0.064	0.01	1.57E-04	19	11.00	24	24	21	0.5	0.5	0.5
Fully open	Plate	0.77	2.18	0.064	0.01	1.57E-04	19	11.00	24	24	21	0.5	0.5	0.5
Fully open	Plate	0.77	2.18	0.064	0.01	1.57E-04	19	10.00	23	21	21	4.2	4.0	4.1
Fully open	Plate	0.77	2.18	0.064	0.01	1.57E-04	19	10.00	21	21	21	4.0	3.9	3.9
Fully open	Plate	0.77	2.18	0.064	0.01	1.57E-04	19	9.01	21	16	9	14.4	12.4	13.4
Fully open	Plate	0.77	2.18	0.064	0.01	1.57E-04	19	9.03	18	16	9	12.3	11.5	11.9
Fully open	Plate	0.77	1.00	0.029	0.01	2.49E-06	19	10.99	118	118	98	2.7	2.7	2.7
Fully open	Plate	0.77	1.00	0.029	0.01	2.49E-06	19	10.99	118	131	98	2.7	3.0	2.9
Fully open	Plate	0.77	1.00	0.029	0.01	2.49E-06	19	10.07	120	114	98	19.6	18.6	19.1
Fully open	Plate	0.77	1.00	0.029	0.01	2.49E-06	19	10.07	114	112	98	18.6	18.3	18.4
Fully open	Plate	0.77	1.00	0.029	0.01	2.49E-06	19	9.01	98	97	35	68.0	67.1	67.5
Fully open	Plate	0.77	1.00	0.029	0.01	2.49E-06	19	9.03	97	94	35	66.1	64.3	65.2
Fully open	Plate	0.77	2.18	0.064	0.01	1.57E-04	19	10.99	131	131	98	3.0	3.0	3.0
Fully open	Plate	0.77	2.18	0.064	0.01	1.57E-04	19	10.99	131	121	98	3.0	2.8	2.9
Fully open	Plate	0.77	2.18	0.064	0.01	1.57E-04	19	10.08	112	121	98	17.9	19.4	18.6
Fully open	Plate	0.77	2.18	0.064	0.01	1.57E-04	19	10.10	121	107	98	19.4	16.5	17.9
Fully open	Plate	0.77	2.18	0.064	0.01	1.57E-04	19	9.03	94	85	35	64.3	58.1	61.2
Fully open	Plate	0.77	2.18	0.064	0.01	1.57E-04	19	9.06	85	77	35	58.8	51.1	54.0
Fully open-Insert	Plate	0.77	1.70	0.020	0.01	4.47E-05	18	10.99	111	113	109	2.5	2.6	2.6
Fully open-Insert	Plate	0.77	1.70	0.020	0.01	4.47E-05	18	10.99	113	117	109	2.6	2.7	2.6
Fully open-Insert	Plate	0.77	1.70	0.020	0.01	4.47E-05	18	10.07	115	116	80	18.8	18.9	18.9
Fully open-Insert	Plate	0.77	1.70	0.020	0.01	4.47E-05	18	10.07	106	106	80	17.3	17.3	17.3
Fully open-Insert	Plate	0.77	1.70	0.020	0.01	4.47E-05	18	9.08	101	94	55	66.3	61.5	63.9
Fully open-Insert	Plate	0.77	1.70	0.020	0.01	4.47E-05	18	9.15	94	78	55	58.0	48.3	53.1
Fully open-insert	Plate	0.77	3.6	0.043	0.01	1.66E-03	18	10.99	117	120	109	2.7	2.8	2.7
Fully open-insert	Plate	0.77	3.6	0.043	0.01	1.66E-03	18	10.99	120	114	109	2.8	2.6	2.7
Fully open-insert	Plate	0.77	3.6	0.043	0.01	1.66E-03	18	10.07	116	109	80	18.9	17.8	18.4

Appendix

Table D-2. Glass plate tests at 35°C.

Table D - 2: WIND TUNNEL TESTS: Glass Plate @ 35°C																
Fan setting	Flow Configuration	Flow rate of solution	Wind velocity		CD	Re*	Temperature	pH	WAD CN		HCN(aq)			\square_{air}	HCN(g) concentration	Volatilisation rate
			[Lpm]	[m/s]					[m ³ /s]	[°C]	Start [ppm]	Finish [ppm]	Start [ppm]			
Insert	Plate	0.77	3.60	0.043	0.01041	1.53E-03	33.3	10.82	89	86	3.0	2.9	2.9	1.66E-05	0.260	0.412
Insert	Plate	0.77	3.60	0.043	0.01041	1.53E-03	33	10.82	86	89	2.9	3.0	2.9	1.66E-05	0.225	0.357
Insert	Plate	0.77	3.60	0.043	0.01041	1.53E-03	32.2	9.93	89	82	18.9	17.4	18.1	1.66E-05	0.858	1.362
Insert	Plate	0.77	3.60	0.043	0.01041	1.53E-03	31	9.96	82	79	17.4	16.7	17.1	1.66E-05	0.867	1.376
Insert	Plate	0.77	3.60	0.043	0.01041	1.53E-03	32.6	9.02	79	65	54.3	44.9	49.6	1.66E-05	2.225	3.530
Insert	Plate	0.77	3.60	0.043	0.01041	1.53E-03	31.9	9.10	65	60	42.2	38.8	40.5	1.66E-05	1.823	2.893
Insert	Plate	0.77	3.60	0.043	0.01041	1.53E-03	35.4	11.06	95	96	1.9	1.9	1.9	1.66E-05	0.167	0.265
Insert	Plate	0.77	3.60	0.043	0.01041	1.53E-03	34.1	11.08	96	94	1.9	1.8	1.9	1.66E-05	0.146	0.231
Insert	Plate	0.77	3.60	0.043	0.01041	1.53E-03	33.9	10.05	98	89	16.7	15.1	15.9	1.66E-05	0.956	1.518
Insert	Plate	0.77	3.60	0.043	0.01041	1.53E-03	33.1	10.09	89	82	14.0	12.8	13.4	1.66E-05	0.763	1.211
Insert	Plate	0.77	3.60	0.043	0.01041	1.53E-03	32.9	9.02	88	73	60.1	50.0	55.0	1.66E-05	2.727	4.327
Insert	Plate	0.77	3.60	0.043	0.01041	1.53E-03	31.8	9.05	73	66	48.9	44.6	46.7	1.66E-05	1.864	2.959
Fully open	Plate	0.77	2.18	0.064	0.01032	1.44E-04	34.1	10.97	59	59	1.4	1.4	1.4	1.66E-05	0.088	0.207
Fully open	Plate	0.77	2.18	0.064	0.01032	1.44E-04	33.2	10.92	59	58	1.6	1.6	1.6	1.66E-05	0.083	0.195
Fully open	Plate	0.77	2.18	0.064	0.01032	1.44E-04	35.4	10.02	56	54	10.0	9.6	9.8	1.66E-05	0.359	0.846
Fully open	Plate	0.77	2.18	0.064	0.01032	1.44E-04	34.6	10.02	54	53	9.6	9.5	9.6	1.66E-05	0.341	0.803
Fully open	Plate	0.77	2.18	0.064	0.01032	1.44E-04	34.6	9.15	44	41	27.3	25.4	26.3	1.66E-05	1.045	2.460
Fully open	Plate	0.77	2.18	0.064	0.01032	1.44E-04	34.6	9.15	41	35	25.4	21.6	23.5	1.66E-05	1.015	2.390

Appendix

Table D-3. Flowing trough solution tests.

Table D - 3: WIND TUNNEL TESTS: Trough															
Fan setting	Flow Configuration	Flow rate of solution	Wind velocity	CD	Re*	Tempe- rature	pH	ISE CN	HCN(aq)			Air	HCN(g) concentration	Volatilisation rate	
		[Lpm]	[m/s]			[m3/s]			[°C]	Start [ppm]	Finish [ppm]		[ppm]		[m2/s]
Fully open	Flowing Trough	0.77	2.18	0.064	0.00074	1.57E-04	19	11.07	29.30	0.59	0.58	0.59	1.53E-05	0.135	0.319
Fully open	Flowing Trough	0.77	2.18	0.064	0.00074	1.57E-04	19	11.09	29.30	0.58	0.59	0.59	1.53E-05	0.083	0.194
Fully open	Flowing Trough	0.77	2.18	0.064	0.00074	1.57E-04	19	11.06	29.30	0.59	0.56	0.58	1.53E-05	0.081	0.191
Fully open	Flowing Trough	0.77	2.18	0.064	0.00074	1.57E-04	19	10.10	31.50	4.48	4.5	4.49	1.53E-05	0.332	0.781
Fully open	Flowing Trough	0.77	2.18	0.064	0.00074	1.57E-04	19	10.12	31.50	4.31	4.25	4.28	1.53E-05	0.318	0.749
Fully open	Flowing Trough	0.77	2.18	0.064	0.00074	1.57E-04	19	9.10	16.20	18.53	16.65	17.59	1.53E-05	0.982	2.311
Fully open	Flowing Trough	0.77	2.18	0.064	0.00074	1.57E-04	19	9.18	16.20	15.51	14.53	15.02	1.53E-05	0.708	1.666
Half open	Still Trough	0	1.00	0.029	0.00050	2.49E-06	17	10.58	ND	4.3	4.3	4.30	1.53E-05	0.163	0.176
Half open	Still Trough	0	1.00	0.029	0.00050	2.49E-06	17	10.62	ND	3.94	4.13	4.04	1.53E-05	0.141	0.153
Half open	Still Trough	0	1.00	0.029	0.00050	2.49E-06	17	10.10	ND	12.48	12.21	12.35	1.53E-05	0.343	0.370
Half open	Still Trough	0	1.00	0.029	0.00050	2.49E-06	17	10.05	ND	13.14	12.85	13.00	1.53E-05	0.316	0.341
Half open	Still Trough	0	1.00	0.029	0.00050	2.49E-06	17	9.33	ND	40	37.45	38.73	1.53E-05	0.636	0.686
Half open	Still Trough	0	1.00	0.029	0.00050	2.49E-06	17	9.20	ND	42.8	42.8	42.80	1.53E-05	0.550	0.594
Fully open	Still Trough	0	2.18	0.064	0.00074	1.57E-04	17	10.74	ND	3.17	3.25	3.21	1.53E-05	0.147	0.347
Fully open	Still Trough	0	2.18	0.064	0.00074	1.57E-04	17	10.05	ND	12.85	13.14	13.00	1.53E-05	0.280	0.660
Fully open	Still Trough	0	2.18	0.064	0.00074	1.57E-04	17	9.24	ND	41.2	37.24	39.22	1.53E-05	0.422	0.995
Fully open	Still Trough	0	2.18	0.064	0.00074	1.57E-04	17	9.25	ND	37.2	35.36	36.28	1.53E-05	0.344	0.811
Half open	Bird balls	0	1.00	0.029	0.00050	2.29E-06	20	10.97	ND	2.82	2.82	2.82	1.66E-05	0.112	0.121
Half open	Bird balls	0	1.00	0.029	0.00050	2.29E-06	20	10.97	ND	2.82	2.82	2.82	1.66E-05	0.109	0.118
Half open	Bird balls	0	1.00	0.029	0.00050	2.29E-06	20	9.99	ND	21.72	21.72	21.72	1.66E-05	0.318	0.344
Half open	Bird balls	0	1.00	0.029	0.00050	2.29E-06	20	9.98	ND	21.72	20.88	21.30	1.66E-05	0.301	0.326
Half open	Bird balls	0	1.00	0.029	0.00050	2.29E-06	20	9.00	ND	78	74.48	76.24	1.66E-05	0.676	0.730
Half open	Bird balls	0	1.00	0.029	0.00050	2.29E-06	20	9.00	ND	74.48	70.33	72.41	1.66E-05	0.581	0.627
Half open	Still Trough	0	1.00	0.029	0.00050	2.29E-06	20	11.00	ND	2.55	2.49	2.52	1.66E-05	0.177	0.191
Half open	Still Trough	0	1.00	0.029	0.00050	2.29E-06	20	11.00	ND	2.49	2.53	2.51	1.66E-05	0.135	0.146
Half open	Still Trough	0	1.00	0.029	0.00050	2.29E-06	20	10.00	ND	21.08	20.14	20.61	1.66E-05	0.401	0.433
Half open	Still Trough	0	1.00	0.029	0.00050	2.29E-06	20	10.00	ND	20.14	20.31	20.23	1.66E-05	0.368	0.397
Half open	Still Trough	0	1.00	0.029	0.00050	2.29E-06	20	9.02	ND	74.82	71.43	73.13	1.66E-05	0.781	0.843
Half open	Still Trough	0	1.00	0.029	0.00050	2.29E-06	20	9.02	ND	71.43	86.08	78.76	1.66E-05	0.697	0.752
Half open	Flowing Trough	0.77	1.00	0.029	0.00050	2.29E-06	20	11.00	ND	2.23	2.26	2.25	1.66E-05	0.197	0.213
Half open	Flowing Trough	0.77	1.00	0.029	0.00050	2.29E-06	20	11.00	ND	2.26	2.22	2.24	1.66E-05	0.184	0.198
Half open	Flowing Trough	0.77	1.00	0.029	0.00050	2.29E-06	20	10.00	ND	17.7	17.5	17.60	1.66E-05	0.796	0.860
Half open	Flowing Trough	0.77	1.00	0.029	0.00050	2.29E-06	20	10.00	ND	17.5	17.5	17.50	1.66E-05	0.777	0.839
Half open	Flowing Trough	0.77	1.00	0.029	0.00050	2.29E-06	20	9.00	ND	61.7	56.5	59.10	1.66E-05	1.996	2.155
Fully open	Flowing Trough	0.77	2.18	0.064	0.00074	1.44E-04	20	11.00	ND	2.22	2.24	2.23	1.66E-05	0.191	0.450
Fully open	Flowing Trough	0.77	2.18	0.064	0.00074	1.44E-04	20	11.00	ND	2.24	2.12	2.18	1.66E-05	0.131	0.308
Fully open	Flowing Trough	0.77	2.18	0.064	0.00074	1.44E-04	20	10.00	ND	17.5	16.5	17.00	1.66E-05	0.777	1.830
Fully open	Flowing Trough	0.77	2.18	0.064	0.00074	1.43E-04	20	10.00	ND	16.5	16.5	16.50	1.66E-05	0.552	1.300
Fully open	Flowing Trough	0.77	2.18	0.064	0.00074	1.43E-04	20	9.00	ND	56.5	49.5	53.00	1.66E-05	1.121	2.640

Appendix

Table D-4. Pulp laboratory test work.

Table D- 4: WIND TUNNEL TESTS: Pulp															
Fan setting	Flow Configuration	Wind velocity		CD	Re*	Temperature	pH	HCN(aq)			C _{air}	Moisture content	HCN(g) concentration	Volatilisation rate	K _{OL}
		[m/s]	[m ² /s]					Start [ppm]	Finish [ppm]	[ppm]					
Half open	Pulp	1.00	0.029	0.00050	2.29E-06	18	9.60	13.9	13.9	13.94	1.66E-05	23%	0.038	0.041	0.0030
Half open	Pulp	1.00	0.029	0.00050	2.29E-06	18	9.60	13.9	13.9	13.94	1.66E-05	23%	0.026	0.028	0.0020
Half open	Pulp	1.00	0.029	0.00050	2.29E-06	18	9.60	13.9	13.9	13.94	1.66E-05	23%	0.017	0.018	0.0013
Half open	Pulp	1.00	0.029	0.00050	2.29E-06	18	9.60	13.9	13.9	13.94	1.66E-05	23%	0.011	0.012	0.0008
Half open	Pulp	1.00	0.029	0.00050	2.29E-06	18	9.60	13.9	13.9	13.94	1.66E-05	23%	0.008	0.008	0.0006
Half open	Pulp	1.00	0.029	0.00050	2.29E-06	18	9.60	13.9	13.9	13.94	1.66E-05	23%	0.006	0.007	0.0005
Half open	Pulp	1.00	0.029	0.00050	2.29E-06	18	10.08	9.0	9.0	9.00	1.66E-05	24%	0.171	0.184	0.0206
Half open	Pulp	1.00	0.029	0.00050	2.29E-06	18	10.08	9.0	9.0	9.00	1.66E-05	24%	0.070	0.075	0.0084
Half open	Pulp	1.00	0.029	0.00050	2.29E-06	18	10.08	9.0	9.0	9.00	1.66E-05	24%	0.050	0.054	0.0060
Half open	Pulp	1.00	0.029	0.00050	2.29E-06	18	10.08	9.0	9.0	9.00	1.66E-05	24%	0.050	0.054	0.0061
Half open	Pulp	1.00	0.029	0.00050	2.29E-06	18	10.08	9.0	9.0	9.00	1.66E-05	24%	0.049	0.053	0.0059
Half open	Pulp	1.00	0.029	0.00050	2.29E-06	18	10.08	9.0	9.0	9.00	1.66E-05	24%	0.041	0.044	0.0049
Half open	Pulp	1.00	0.029	0.00050	2.29E-06	18	9.97	9.3	9.3	9.30	1.66E-05	31%	0.133	0.144	0.0155
Half open	Pulp	1.00	0.029	0.00050	2.29E-06	18	9.97	9.3	9.3	9.30	1.66E-05	31%	0.095	0.103	0.0111
Half open	Pulp	1.00	0.029	0.00050	2.29E-06	18	9.97	9.3	9.3	9.30	1.66E-05	31%	0.070	0.076	0.0081
Half open	Pulp	1.00	0.029	0.00050	2.29E-06	18	9.97	9.3	9.3	9.30	1.66E-05	31%	0.049	0.053	0.0057
Half open	Pulp	1.00	0.029	0.00050	2.29E-06	18	9.97	9.3	9.3	9.30	1.66E-05	31%	0.037	0.040	0.0043
Half open	Pulp	1.00	0.029	0.00050	2.29E-06	18	9.97	9.3	9.3	9.30	1.66E-05	31%	0.031	0.034	0.0037
Half open	Pulp	1.00	0.029	0.00050	2.29E-06	18	9.70	10.0	10.0	10.00	1.66E-05	22%	0.033	0.036	0.0036
Half open	Pulp	1.00	0.029	0.00050	2.29E-06	18	9.70	10.0	10.0	10.00	1.66E-05	22%	0.019	0.021	0.0021
Half open	Pulp	1.00	0.029	0.00050	2.29E-06	18	9.70	10.0	10.0	10.00	1.66E-05	22%	0.016	0.017	0.0017
Half open	Pulp	1.00	0.029	0.00050	2.29E-06	18	9.70	10.0	10.0	10.00	1.66E-05	22%	0.012	0.012	0.0012
Half open	Pulp	1.00	0.029	0.00050	2.29E-06	18	9.70	10.0	10.0	10.00	1.66E-05	22%	0.010	0.011	0.0011
Half open	Pulp	1.00	0.029	0.00050	2.29E-06	18	9.70	10.0	10.0	10.00	1.66E-05	22%	0.009	0.010	0.0010
Half open	Pulp	1.00	0.029	0.00050	2.29E-06	20	9.42	9.8	9.8	9.75	1.66E-05	24%	0.026	0.028	0.0028
Half open	Pulp	1.00	0.029	0.00050	2.29E-06	20	9.42	9.8	9.8	9.75	1.66E-05	24%	0.018	0.019	0.0019
Half open	Pulp	1.00	0.029	0.00050	2.29E-06	20	9.42	9.8	9.8	9.75	1.66E-05	24%	0.014	0.015	0.0015
Half open	Pulp	1.00	0.029	0.00050	2.29E-06	20	9.42	9.8	9.8	9.75	1.66E-05	24%	0.011	0.012	0.0012
Half open	Pulp	1.00	0.029	0.00050	2.29E-06	20	9.42	9.8	9.8	9.75	1.66E-05	24%	0.009	0.010	0.0010
Half open	Pulp	1.00	0.029	0.00050	2.29E-06	20	9.42	9.8	9.8	9.75	1.66E-05	24%	0.009	0.010	0.0010

Appendix

APPENDIX E – Site test work summary

Table E-1. Tailings storage facility surface tests.

Table E-1: Tailings storage facility surface tests														
Site information		Pump and scrubber info		Water extract				Solid sample	Analysis and calculations			Mass transfer calculations		
Area	Classification	Volume air sampled	Scrubber volume	pH	WAD CN	ISE	HCN (aq)	% Moisture	HCN in scrubber	HCN in air phase	Velocity inside dome	Re*	Volatilisation rate	K _{OL}
		[m ³]	[ml]		[ppb]	[ppm]	[ppm]	[% H ₂ O]	[mg HCN]	[mg HCN/m ³]	[m/s]		[g/h/m ²]	[m/h]
Wet beach	Sludge	0.468	100	9.37	3221	0.10	1.27	41.5	2.43	5.18	0.0004	2.5E-59	0.007	-0.05884
Wet beach	Sludge	0.476	100	9.37	3221	0.10	1.27	41.5	0.15	0.32	0.0004	1.3E-57	0.000	0.00040
Next to river	Wet, thixotropic	0.459	100	10.11	12368	0.08	3.17	36.2	0.78	1.69	0.0004	9.1E-59	0.002	0.00083
Next to river	Wet, thixotropic	0.504	100	10.11	12368	0.08	3.17	36.2	0.07	0.13	0.0004	2.0E-57	0.000	0.00006
Dry beach	Dry	0.436	100	8.22	1464	0.03	1.33	19.3	0.03	0.07	0.0004	1.5E-58	0.000	0.00007
Dry beach	Dry	0.496	100	8.22	1464	0.03	1.33	19.3	0.03	0.05	0.0004	1.6E-56	0.000	0.00006
Dry beach	Dry	0.446	100	8.99	22412	0.24	3.72	26.1	0.40	0.90	0.0004	2.4E-58	0.001	0.00036
Flowing river	Fresh stream	0.457	100	10.41	36139	0.56	2.14	40.4	1.76	3.84	0.0004	3.4E-58	0.005	0.00479
Wet beach top layer	Wet, thixotropic 1st h	0.733	100	9.78	33442	0.42	3.72	37.5	0.29	0.39	0.0004	1.4E-58	0.001	0.00015
Wet beach top layer	Wet, thixotropic 2nd h	0.113	100	9.78	33442	0.42	3.72	37.5	0.39	3.46	0.0004	1.5E-58	0.005	0.00169
Wet beach top layer	Wet, thixotropic 3rd h	0.117	100	9.78	33442	0.42	3.72	37.5	0.39	3.36	0.0004	1.6E-58	0.005	0.00163
Wet beach top layer	Wet, thixotropic 4th h	0.087	100	9.78	33442	0.42	3.72	37.5	0.26	2.98	0.0004	1.6E-58	0.004	0.00139
Wet beach	Thin stagnant liquid film	0.247	100				4.35	40	1.14	4.62	0.0004	2.4E-58	0.006	0.00205
Wet beach bottom layer	Wet, thixotropic	0.184	100	8.53	7490	0.07	6.20	18.8	0.10	0.52	0.0004	3.4E-58	0.001	0.00012
Wet beach lower layer	Wet, thixotropic	0.211	100	9.53	22839	0.23	7.39	28.9	0.15	0.73	0.0004	2.8E-56	0.001	0.00016
Pen stock ambient air	Air above discharge	0.034	100				2.53	100	0.06	1.79	1.0000	2.4E-06	0.002	0.00119
Decant tower	Decant pond solution	0.410	100	8.13	11.2	0.5	0.001	90	0.04	0.11	0.0004	2.8E-56	0.0001	4.4130

REPORT SHEET - CYANIDE SPECIATION & ANALYSIS FOR LIQUID SAMPLE											
Sample no:		SITE B Slurry Discharge		TSF							
Sample description:		0.0		0.0							
Processed by:		P.W. Lotz		Date received:		00-Jan-00					
pH:		9.16		Eh (vs SHE):		353 mV		conductivity:		5.29 mS/cm	
species	detailed speciation				metal based sums						
	CN, ppm individual species		% CN as	% total metal	CN: total per metal in ppm	metal analysis, ppm					
[Au(CN) ₂] ⁻	0.01		0.0	100.00	0.01	0.03					
[Ag(CN) ₂] ⁻	0.		0.0	99.97	0.00	<0.02					
[Ag(CN) ₃] ⁻	0.		0.0	0.03							
[Fe(CN) ₆] ⁴⁻	1.53		5.6	54.85	2.79	1.00					
[Fe(CN) ₆] ³⁻	1.26		4.6	45.15							
[Cu(CN) ₂] ⁻	1.03		3.8	22.78	6.24	5.50					
[Cu(CN) ₃] ²⁻	5.21		19.1	77.20							
[Cu(CN) ₄] ³⁻	0.		0.0	0.03							
[Co(CN) ₆] ³⁻	0.95		3.5	100.00	0.95	2.20					
[Zn(CN) ₂]	1.68		6.2	23.71	9.09	8.90					
[Zn(CN) ₃] ⁻	6.43		23.6	60.55							
[Zn(CN) ₄] ²⁻	0.86		3.2	6.09							
[Zn(CN) ₂ OH] ⁻	0.11		0.4	1.49							
[Zn(CN) ₃ OH] ²⁻	0.01		0.0	0.09							
Zn ²⁺ , ZnOH's etc.	0.		0.0	8.06							
[Ni(CN)] ⁺	0.		0.0	0.00	7.44	4.20					
[Ni(CN) ₂]	0.		0.0	0.00							
[Ni(CN) ₃] ⁻	0.01		0.0	0.12							
[Ni(CN) ₄] ²⁻	7.43		27.3	99.88							
[Ni(CN) ₅] ³⁻	0.		0.0	0.00							
CN⁻	0.33		1.2	Deviation: %	Confirming analysis:						
HCN (aq)	0.37		1.4		ppm CN	method					
Free CN	0.7		2.6	-	0.7	ISE					
Titrateable CN	9.79		36.0	#DIV/0!	0.	AgNO ₃ pot. Tit.					
Gold leachable CN	11.51		42.3								
WAD CN	23.463		86.2	-49.7%	11.8	SFIA					
Total CN	27.217		100.0	-53.1%	12.	SFIA ¹⁾					
Total CN + [S]CN	NC			-	42.4	SFIA					
CN ex SCN only	ND		Ion Chrom.	-	29.64	SFIA ²⁾					
¹⁾ CN Total for comparison with speciation has been corrected for the partial recovery of cyanide from Au(CN) ₂ and Co(CN) ₆ ; the percentage deviation is hence not based on the apparent figures ²⁾ this figure has been corrected for metal cyanide interference on the SFIA channel. If absolute accuracy is crucial, validation by IC is recommended ³⁾ Fe should be complexed preferentially. However to reach this theoretical equilibrium, kinetics and many other factors would have to be taken into consideration. Likewise, iron has a tendency to precipitate out of solution and not be quantified to the full extent in all cases. Trusting analytical data (Eh normally changes upwards from the reducing levels at discharge), the following distribution is most likely (large discrepancies indicate normally the presence of uncomplexed Fe3):											
HCN (g) at equilibrium, pH:		9.16	1.3 ppm max³⁾		-Fe2 0.561	-Fe3 0.462					
³⁾ this value gives an indication of the predicted maximum concentration that can be reached above this particular solution at equilibrium (to be taken as indication only!)											

Figure E-1. Cyanide speciation for tailings discharge stream sample predicted by MINTEK speciation model based on ISE cyanide measurements.

REPORT SHEET - CYANIDE SPECIATION & ANALYSIS FOR LIQUID SAMPLE							
Sample no:		SITE B Slurry Discharge			TSF		
Sample description:		0.0		0.0			
Processed by:		P.W. Lotz		Date received:		00-Jan-00	
pH:		9.16		Eh (vs SHE):		353 mV	
				conductivity:		5.29 mS/cm	
species	detailed speciation			metal based sums			
	CN, ppm individual species	% CN as	% total metal	CN: total per metal in ppm	metal analysis, ppm		
[Au(CN) ₂] ⁻	0.01	0.1	100.00	0.01	0.03		
[Ag(CN) ₂] ⁻	0.	0.0	100.00	0.00	<0.02		
[Ag(CN) ₃] ⁻	0.	0.0	0.00				
[Fe(CN) ₆] ⁴⁻	1.53	9.9	54.85	2.79	1.00		
[Fe(CN) ₆] ³⁻	1.26	8.1	45.15				
[Cu(CN) ₂] ⁻	4.36	28.0	96.83	4.57	5.50		
[Cu(CN) ₃] ²⁻	0.21	1.4	3.17				
[Cu(CN) ₄] ³⁻	0.	0.0	0.00				
[Co(CN) ₆] ³⁻	0.95	6.1	100.00	0.95	2.20		
[Zn(CN) ₂]	0.	0.0	0.03	0.00	8.90		
[Zn(CN) ₃] ⁻	0.	0.0	0.00				
[Zn(CN) ₄] ²⁻	0.	0.0	0.00				
[Zn(CN) ₂ OH] ⁻	0.	0.0	0.00				
[Zn(CN) ₃ OH] ²⁻	0.	0.0	0.00				
Zn ²⁺ , ZnOH's etc.	0.	0.0	99.97				
[Ni(CN)] ⁺	0.	0.0	0.04			7.22	4.20
[Ni(CN) ₂]	0.01	0.1	0.38				
[Ni(CN) ₃] ⁻	0.61	3.9	10.99				
[Ni(CN) ₄] ²⁻	6.59	42.4	88.58				
[Ni(CN) ₅] ³⁻	0.	0.0	0.00				
CN⁻	0.003	0.0	Deviation:	Confirming analysis:			
HCN (aq)	0.004	0.0	%	ppm CN	method		
Free CN	0.007	0.0	-201.0%	0.7	ISE		
Titrateable CN	0.01	0.1	#DIV/0!	0.	AgNO₃ pot. Tit.		
Gold leachable CN	0.08	0.5					
WAD CN	11.8	75.9	0.0%	11.8	SFIA		
Total CN	15.553	100.0	-18.0%	12.	SFIA¹⁾		
Total CN + [S]CN	NC		-	42.4	SFIA		
CN ex SCN only	ND	Ion Chrom.	-	29.64	SFIA²⁾		
¹⁾ CN Total for comparison with speciation has been corrected for the partial recovery of cyanide from Au(CN) ₂ and Co(CN) ₆ ; the percentage deviation is hence not based on the apparent figures ²⁾ this figure has been corrected for metal cyanide interference on the SFIA channel. If absolute accuracy is crucial, validation by IC is recommended ³⁾ Fe should be complexed preferentially. However to reach this theoretical equilibrium, kinetics and many other factors would have to be taken into consideration. Likewise, iron has a tendency to precipitate out of solution and not be quantified to the full extent in all cases. Trusting analytical data (Eh normally changes upwards from the reducing levels at discharge), the following distribution is most likely (large discrepancies indicate normally the presence of uncomplexed Fe3) :							
HCN (g) at equilibrium, pH:		9.16	0.0 ppm max³⁾	-Fe2 0.561	-Fe3 0.462		
³⁾ this value gives an indication of the predicted maximum concentration that can be reached above this particular solution at equilibrium (to be taken as indication only!)							

Figure E-2. Cyanide speciation for tailings discharge stream sample predicted by MINTeK speciation model based on WAD cyanide measurements.

REPORT SHEET - CYANIDE SPECIATION & ANALYSIS FOR LIQUID SAMPLE						
Sample no:		SITE B Decant pond		TSF		
Sample description:		0.0		0.0		
Processed by:		P.W. Lotz		Date received: 00-Jan-00		
pH:		8.13		Eh (vs SHE): 506 mV		
				conductivity: 6.26 mS/cm		
species	detailed speciation			metal based sums		
	CN, ppm individual species	% CN as	% total metal	CN: total per metal in ppm	metal analysis, ppm	
[Au(CN) ₂] ⁻	0.01	<i>0.1</i>	100.00	0.01	0.06	
[Ag(CN) ₂] ⁻	0.	<i>0.0</i>	99.98	0.00	<0.02	
[Ag(CN) ₃] ⁻	0.	<i>0.0</i>	0.02			
[Fe(CN) ₆] ⁴⁻	0.01	<i>0.0</i>	0.31	4.47	1.60	
[Fe(CN) ₆] ³⁻	4.46	<i>15.4</i>	99.69			
[Cu(CN) ₂] ⁻	1.34	<i>4.6</i>	29.23	6.20	5.60	
[Cu(CN) ₃] ²⁻	4.86	<i>16.8</i>	70.76			
[Cu(CN) ₄] ³⁻	0.	<i>0.0</i>	0.02			
[Co(CN) ₆] ³⁻	0.48	<i>1.6</i>	100.00	0.48	2.40	
[Zn(CN) ₂]	2.21	<i>7.6</i>	33.42	8.83	8.30	
[Zn(CN) ₃] ⁻	6.04	<i>20.8</i>	60.95			
[Zn(CN) ₄] ²⁻	0.58	<i>2.0</i>	4.37			
[Zn(CN) ₂ OH] ⁻	0.01	<i>0.0</i>	0.20			
[Zn(CN) ₃ OH] ²⁻	0.	<i>0.0</i>	0.01			
Zn ²⁺ , ZnOH's etc.	0.	<i>0.0</i>	1.06			
[Ni(CN)] ⁺	0.	<i>0.0</i>	0.00	8.50	4.80	
[Ni(CN) ₂]	0.	<i>0.0</i>	0.00			
[Ni(CN) ₃] ⁻	0.01	<i>0.0</i>	0.17			
[Ni(CN) ₄] ²⁻	8.49	<i>29.3</i>	99.83			
[Ni(CN) ₅] ³⁻	0.	<i>0.0</i>	0.00			
CN⁻	0.038	<i>0.1</i>	Deviation:	Confirming analysis:		
HCN (aq)	0.462	<i>1.6</i>	%	ppm CN	method	
Free CN	0.5	<i>1.7</i>	-502727104.8%	0.5	ISE	
Titrateable CN	9.33	<i>32.2</i>	#DIV/0!	0.	AgNO ₃ pot. Tit.	
Gold leachable CN	10.94	37.7				
WAD CN	24.037	<i>82.9</i>	-53.4%	11.2	SFIA	
Total CN	28.997	<i>100.0</i>	-59.7%	11.3	SFIA ¹⁾	
Total CN + [S]CN	NC		-	54.9	SFIA	
CN ex SCN only	ND	Ion Chrom.	-	43.21	SFIA ²⁾	
¹⁾ CN Total for comparison with speciation has been corrected for the partial recovery of cyanide from Au(CN) ₂ and Co(CN) ₆ ; the percentage deviation is hence not based on the apparent figures ²⁾ this figure has been corrected for metal cyanide interference on the SFIA channel. If absolute accuracy is crucial, validation by IC is recommended ³⁾ Fe should be complexed preferentially. However to reach this theoretical equilibrium, kinetics and many other factors would have to be taken into consideration. Likewise, iron has a tendency to precipitate out of solution and not be quantified to the full extent in all cases. Trusting analytical data (Eh normally changes upwards from the reducing levels at discharge), the following distribution is most likely (large discrepancies indicate normally the presence of uncomplexed Fe3):						
HCN (g) at equilibrium, pH:		8.13	1.6 ppm max³⁾	-Fe2 0.004	-Fe3 1.230	
³⁾ this value gives an indication of the predicted maximum concentration that can be reached above this particular solution at equilibrium (to be taken as indication only!)						

Figure E-3. Cyanide speciation for decant pond sample predicted by MINTEK speciation model based on ISE cyanide measurements.

REPORT SHEET - CYANIDE SPECIATION & ANALYSIS FOR LIQUID SAMPLE					
Sample no:		SITE B Decant pond		TSF	
Sample description:		0.0		0.0	
Processed by:		P.W. Lotz	Date received: 00-Jan-00		
pH:		8.13	Eh (vs SHE): 506 mV	conductivity: 6.26 mS/cm	
species	detailed speciation			metal based sums	
	CN, ppm individual species	% CN as	% total metal	CN: total per metal in ppm	metal analysis, ppm
[Au(CN) ₂] ⁻	0.01	0.1	100.00	0.01	0.06
[Ag(CN) ₂] ⁻	0.	0.0	100.00	0.00	<0.02
[Ag(CN) ₃] ⁻	0.	0.0	0.00		
[Fe(CN) ₆] ⁴⁻	0.01	0.1	0.31	4.47	1.60
[Fe(CN) ₆] ³⁻	4.46	27.6	99.69		
[Cu(CN) ₂]	4.56	28.2	99.42	4.60	5.60
[Cu(CN) ₃] ²⁻	0.04	0.2	0.58		
[Cu(CN) ₄] ³⁻	0.	0.0	0.00		
[Co(CN) ₆] ³⁻	0.48	2.9	100.00	0.48	2.40
[Zn(CN) ₂]	0.	0.0	0.02	0.00	8.30
[Zn(CN) ₃] ⁻	0.	0.0	0.00		
[Zn(CN) ₄] ²⁻	0.	0.0	0.00		
[Zn(CN) ₂ OH] ⁻	0.	0.0	0.00		
[Zn(CN) ₃ OH] ²⁻	0.	0.0	0.00		
Zn ²⁺ , ZnOH's etc.	0.	0.0	99.98		
[Ni(CN)] ⁺	0.08	0.5	3.88		
[Ni(CN) ₂]	0.28	1.7	6.48		
[Ni(CN) ₃] ⁻	2.14	13.3	33.58		
[Ni(CN) ₄] ²⁻	4.1	25.4	48.23		
[Ni(CN) ₅] ³⁻	0.	0.0	0.00		
CN⁻	0.	0.0	Deviation:	Confirming analysis:	
HCN (aq)	0.001	0.0	%	ppm CN	method
Free CN	0.001	0.0	-200.2%	0.5	ISE
Titrateable CN	0.	0.0	#DIV/0!	0.	☞ AgNO ₃ pot. Tit.
Gold leachable CN	0.02	0.1			
WAD CN	11.2	69.3	0.0%	11.2	☞ SFIA
Total CN	16.16	100.0	-27.7%	11.3	☞ SFIA ¹⁾
Total CN + [S]CN	NC		-	54.9	☞ SFIA
CN ex SCN only	ND	☞ Ion Chrom.	-	43.21	☞ SFIA ²⁾
¹⁾ CN Total for comparison with speciation has been corrected for the partial recovery of cyanide from Au(CN) ₂ and Co(CN) ₆ ; the percentage deviation is hence not based on the apparent figures ²⁾ this figure has been corrected for metal cyanide interference on the SFIA channel. If absolute accuracy is crucial, validation by IC is recommended ³⁾ Fe should be complexed preferentially. However to reach this theoretical equilibrium, kinetics and many other factors would have to be taken into consideration. Likewise, iron has a tendency to precipitate out of solution and not be quantified to the full extent in all cases. Trusting analytical data (Eh normally changes upwards from the reducing levels at discharge), the following distribution is most likely (large discrepancies indicate normally the presence of uncomplexed Fe3) :					
HCN (g) at equilibrium, pH:		8.13	0.0 ppm max³⁾		
³⁾ this value gives an indication of the predicted maximum concentration that can be reached above this particular solution at equilibrium (to be taken as indication only!)					

Figure E-4. Cyanide speciation for decant pond sample predicted by MINTEK speciation model based on WAD cyanide measurements.

REPORT SHEET - CYANIDE SPECIATION & ANALYSIS FOR LIQUID SAMPLE						
Sample no:		SITE B Return water dam		TSF		
Sample description:		0.0		0.0		
Processed by:		P.W. Lotz		Date received: 00-Jan-00		
pH:		8.25		Eh (vs SHE): 458 mV		
				conductivity: 4.87 mS/cm		
species	detailed speciation			metal based sums		
	CN, ppm individual species	% CN as	% total metal	CN: total per metal in ppm	metal analysis, ppm	
[Au(CN) ₂] ⁻	0.	0.0	100.00	0.00	<0.008	
[Ag(CN) ₂] ⁻	0.	0.0	99.99	0.00	<0.02	
[Ag(CN) ₃] ⁻	0.	0.0	0.01			
[Fe(CN) ₆] ⁴⁻	0.06	0.3	2.00	2.79	1.00	
[Fe(CN) ₆] ³⁻	2.74	14.8	98.00			
[Cu(CN) ₂] ⁻	0.73	4.0	40.77			
[Cu(CN) ₃] ²⁻	1.6	8.6	59.22	2.33	2.20	
[Cu(CN) ₄] ³⁻	0.	0.0	0.01			
[Co(CN) ₆] ³⁻	-0.9	-4.9	100.00	-0.90	1.70	
[Zn(CN) ₂]	2.97	16.0	44.42			
[Zn(CN) ₃] ⁻	4.87	26.3	48.61			
[Zn(CN) ₄] ²⁻	0.28	1.5	2.09	8.14	8.40	
[Zn(CN) ₂ OH] ⁻	0.02	0.1	0.34			
[Zn(CN) ₃ OH] ²⁻	0.	0.0	0.01			
Zn ²⁺ , ZnOH's etc.	0.	0.0	4.51			
[Ni(CN)] ⁺	0.	0.0	0.00			
[Ni(CN) ₂]	0.	0.0	0.00			
[Ni(CN) ₃] ⁻	0.01	0.1	0.28	5.84	3.30	
[Ni(CN) ₄] ²⁻	5.83	31.5	99.72			
[Ni(CN) ₅] ³⁻	0.	0.0	0.00			
CN⁻	0.03	0.2	Deviation:	Confirming analysis:		
HCN (aq)	0.27	1.5	%	ppm CN	method	
Free CN	0.3	1.6	-	0.3	ISE	
Titrateable CN	8.44	45.6	#DIV/0!	0.	≅ AgNO ₃ pot. Tit.	
Gold leachable CN	8.97	48.5				
WAD CN	16.619	89.8	-63.8%	6.01	≅ SFIA	
Total CN	18.508	100.0	-72.4%	5.82	≅ SFIA ¹⁾	
Total CN + [S]CN	NC		-	25.	≅ SFIA	
CN ex SCN only	ND	≅ Ion Chrom.	-	19.895	≅ SFIA ²⁾	
¹⁾ CN Total for comparison with speciation has been corrected for the partial recovery of cyanide from Au(CN) ₂ and Co(CN) ₆ ; the percentage deviation is hence not based on the apparent figures ²⁾ this figure has been corrected for metal cyanide interference on the SFIA channel. If absolute accuracy is crucial, validation by IC is recommended ³⁾ Fe should be complexed preferentially. However to reach this theoretical equilibrium, kinetics and many other factors would have to be taken into consideration. Likewise, iron has a tendency to precipitate out of solution and not be quantified to the full extent in all cases. Trusting analytical data (Eh normally changes upwards from the reducing levels at discharge), the following distribution is most likely (large discrepancies indicate normally the presence of uncomplexed Fe3) :						
HCN (g) at equilibrium, pH:		8.25	0.9 ppm max³⁾	-Fe2 0.023	-Fe3 1.112	
³⁾ this value gives an indication of the predicted maximum concentration that can be reached above this particular solution at equilibrium (to be taken as indication only!)						

Figure E-5. Cyanide speciation for return water dam sample predicted by MINTEK speciation model based on ISE cyanide measurements.

REPORT SHEET - CYANIDE SPECIATION & ANALYSIS FOR LIQUID SAMPLE					
Sample no:		SITE B Return water dam		TSF	
Sample description:		0.0		0.0	
Processed by:		P.W. Lotz	Date received: 00-Jan-00		
pH:		8.25	Eh (vs SHE): 458 mV	conductivity: 4.87 mS/cm	
species	detailed speciation			metal based sums	
	CN, ppm individual species	% CN as	% total metal	CN: total per metal in ppm	metal analysis, ppm
[Au(CN) ₂] ⁻	0.	0.0	100.00	0.00	<0.008
[Ag(CN) ₂] ⁻	0.	0.0	100.00	0.00	<0.02
[Ag(CN) ₃] ⁻	0.	0.0	0.00		
[Fe(CN) ₆] ⁴⁻	0.06	0.7	2.00	2.79	1.00
[Fe(CN) ₆] ³⁻	2.74	34.7	98.00		
[Cu(CN) ₂]	1.79	22.7	99.50	1.80	2.20
[Cu(CN) ₃] ²⁻	0.01	0.2	0.50		
[Cu(CN) ₄] ³⁻	0.	0.0	0.00		
[Co(CN) ₆] ³⁻	-0.9	-11.5	100.00	-0.90	1.70
[Zn(CN) ₂]	0.	0.0	0.01	0.00	8.40
[Zn(CN) ₃] ⁻	0.	0.0	0.00		
[Zn(CN) ₄] ²⁻	0.	0.0	0.00		
[Zn(CN) ₂ OH] ⁻	0.	0.0	0.00		
[Zn(CN) ₃ OH] ²⁻	0.	0.0	0.00		
Zn ²⁺ , ZnOH's etc.	0.	0.0	99.99		
[Ni(CN)] ⁺	0.08	1.0	5.19		
[Ni(CN) ₂]	0.22	2.8	7.49		
[Ni(CN) ₃] ⁻	1.47	18.6	33.56		
[Ni(CN) ₄] ²⁻	2.44	30.9	41.68		
[Ni(CN) ₅] ³⁻	0.	0.0	0.00		
CN⁻	0.	0.0	Deviation:	Confirming analysis:	
HCN (aq)	0.001	0.0	%	ppm CN	method
Free CN	0.001	0.0	-200.3%	0.3	ISE
Titrateable CN	0.	0.0	#DIV/0!	0.	AgNO ₃ pot. Tit.
Gold leachable CN	0.01	0.1			
WAD CN	6.01	76.1	0.0%	6.01	SFIA
Total CN	7.898	100.0	-35.4%	5.82	SFIA ¹⁾
Total CN + [S]CN	NC		-	25.	SFIA
CN ex SCN only	ND	Ion Chrom.	-	19.895	SFIA ²⁾
¹⁾ CN Total for comparison with speciation has been corrected for the partial recovery of cyanide from Au(CN) ₂ and Co(CN) ₆ ; the percentage deviation is hence not based on the apparent figures					
²⁾ this figure has been corrected for metal cyanide interference on the SFIA channel. If absolute accuracy is crucial, validation by IC is recommended					
³⁾ Fe should be complexed preferentially. However to reach this theoretical equilibrium, kinetics and many other factors would have to be taken into consideration. Likewise, iron has a tendency to precipitate out of solution and not be quantified to the full extend in all cases. Trusting analytical data (Eh normally changes upwards from the reducing levels at discharge), the following distribution is most likely (large discrepancies indicate normally the presence of uncomplexed Fe3) :				-Fe2 0.023	-Fe3 1.112
HCN (g) at equilibrium, pH:		8.25	0.0 ppm max³⁾		
³⁾ this value gives an indication of the predicted maximum concentration that can be reached above this particular solution at equilibrium (to be taken as indication only!)					

Figure E-6. Cyanide speciation for return water dam sample predicted by MINTEK speciation model based on WAD cyanide measurements.

Appendix

Table E-2: Leach tank tests

Table E-2: Leach tank on-site tests														
Dome cavity dimensions		Length	370	Volume	10212	5328	cm ³							
		Width	240											
Date/ Site	Tank	Measurement point	Flow configuration	Wind velocity [m/s]	Vol flow [m ³ /s]	Cavity area [cm ²]	Wind velocity [m/s]	Vol flow [m ³ /s]	HCN	HCN DRA	HCN(aq)	Volatilisation rate	KOL	CD
				meas	meas	dome	dome	dome	DRA	[mg/m ³]	[ppm]	[g/h/m ²]	[m/h]	
2005/07/06	Pachuca 4	flow cell	bubble	1.4	0.00044	276	0.0159	0.0004	26.6	29.26	11.39	0.046	0.013	0.00006
Plant A	Pachuca 4	flow cell	compr air	3.3	0.00104	276	0.0375	0.0010	17.5	19.25	11.39	0.072	0.011	0.00010
	Pachuca 4	flow cell	compr air	4.2	0.00132	276	0.0478	0.0013	17.5	19.25	11.39	0.091	0.015	0.00011
	Pachuca 4	flow cell	compr air	5	0.00157	276	0.0569	0.0016	15.5	17.05	11.39	0.096	0.014	0.00012
	Pachuca 4	flow cell	compr air	6	0.00188	276	0.0683	0.0019	14.5	15.95	11.39	0.108	0.015	0.00013
	Pachuca 4	flow cell	compr air	6.5	0.00204	276	0.0739	0.0020	13	14.3	11.39	0.105	0.014	0.00014
	Pachuca 4	flow cell	compr air	8	0.00251	276	0.0910	0.0025	13	14.3	11.39	0.129	0.017	0.00015
	Pachuca 4	flow cell	compr air	8.2	0.00257	276	0.0933	0.0026	13	14.3	11.39	0.133	0.017	0.00015
	Pachuca 4	flow cell	compr air	9	0.00283	144	0.1963	0.0028	13	14.3	11.39	0.145	0.019	0.00022
	Pachuca 4	flow cell	compr air	8	0.00251	144	0.1744	0.0025	13.5	14.85	11.39	0.134	0.018	0.00021
	Pachuca 4	flow cell	compr air	7.5	0.00236	144	0.1635	0.0024	14	15.4	11.39	0.131	0.018	0.00020
	Pachuca 4	flow cell	compr air	7	0.00220	144	0.1526	0.0022	16.2	17.82	11.39	0.141	0.021	0.00020
	Pachuca 4	flow cell	compr air	6	0.00188	144	0.1308	0.0019	16.4	18.04	11.39	0.122	0.019	0.00018
	Pachuca 4	flow cell	compr air	5.5	0.00173	144	0.1199	0.0017	16.9	18.59	11.39	0.116	0.018	0.00017
	Pachuca 4	flow cell	compr air	4	0.00126	144	0.0872	0.0013	18	19.8	11.39	0.090	0.015	0.00015
	Pachuca 4		bubble	2.5	0.00079	144	0.0545	0.0008	22.2	24.42	11.00	0.069	0.015	0.00012
15/09/05	Mechanical 1	flow cell	no flow	0	0.00000	276	0.0000	0.0000	0.6	0.66	4.98	0.000	0.000	0.00000
Plant B	Mechanical 2	flow cell	comp air	6.2	0.00195	276	0.0705	0.0019	6	6.6	4.98	0.046	0.014	0.00013
	Mechanical 3	flow cell	comp air	5.2	0.00163	276	0.0592	0.0016	6.3	6.93	4.98	0.041	0.013	0.00012
	Mechanical 4	flow cell	comp air	4.5	0.00141	276	0.0512	0.0014	6.7	7.37	4.98	0.037	0.012	0.00011
	Mechanical 5	flow cell	comp air	3.3	0.00104	276	0.0375	0.0010	7.5	8.25	4.98	0.031	0.011	0.00010
	Mechanical 6	flow cell	comp air	2.5	0.00079	276	0.0284	0.0008	9.2	10.12	4.98	0.029	0.013	0.00008
	Mechanical 7	flow cell	comp air	2	0.00063	276	0.0228	0.0006	10.5	11.55	4.98	0.026	0.014	0.00008
	Mechanical 8	flow cell	comp air	1.6	0.00050	276	0.0182	0.0005	12.6	13.86	4.98	0.025	0.020	0.00007
	Mechanical 9	flow cell	comp air	1	0.00031	276	0.0114	0.0003	13.4	14.74	4.98	0.017	0.016	0.00005
		Pachuca 5	flow cell	comp air	5.6	0.00176	276	0.0637	0.0018	7.3	8.03	4.72	0.051	0.020
	Pachuca 6	flow cell	comp air	5	0.00157	276	0.0569	0.0016	10.6	11.66	4.72	0.066	0.041	0.00012
	Pachuca 7	flow cell	comp air	4.3	0.00135	276	0.0489	0.0014	10.7	11.77	4.72	0.057	0.036	0.00011
	Pachuca 8	flow cell	comp air	4	0.00126	276	0.0455	0.0013	11.8	12.98	4.72	0.059	0.047	0.00011
	Pachuca 9	flow cell	comp air	4.1	0.00129	276	0.0466	0.0013	9.1	10.01	4.72	0.046	0.023	0.00011
	Pachuca 10	flow cell	comp air	3.5	0.00110	276	0.0398	0.0011	11.3	12.43	4.72	0.049	0.035	0.00010
	Pachuca 11	flow cell	comp air	3	0.00094	276	0.0341	0.0009	12.4	13.64	4.72	0.046	0.043	0.00009
	Pachuca 12	flow cell	comp air	1.5	0.00047	276	0.0171	0.0005	14	15.4	4.72	0.026	0.043	0.00007
	Pachuca 13	flow cell	bubble	1.2	0.00038	276	0.0137	0.0004	11.2	12.32	4.72	0.017	0.012	0.00006

Appendix

APPENDIX F – Tailings storage facility geographical information and data

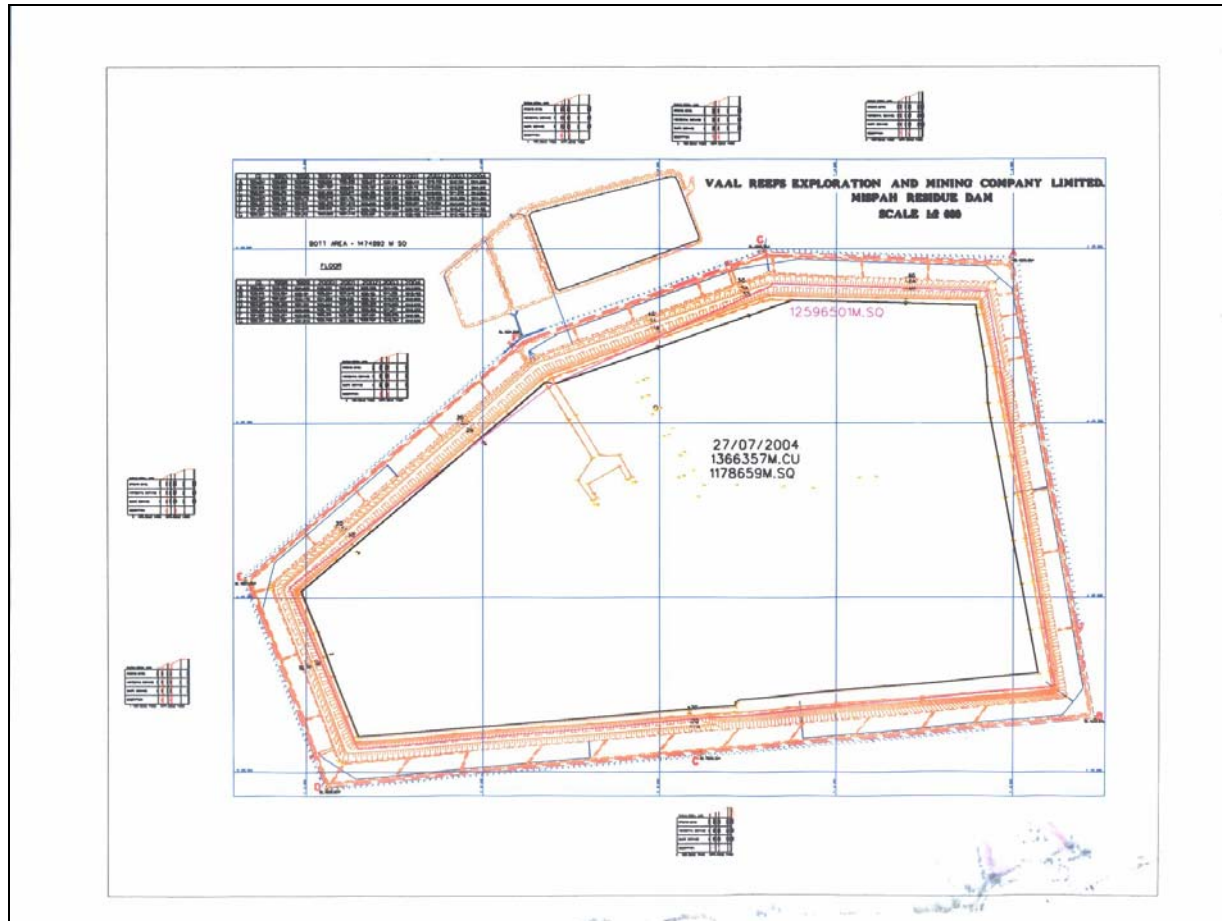


Figure F-1. Map of tailings storage facility used in TSF model validation.

Appendix

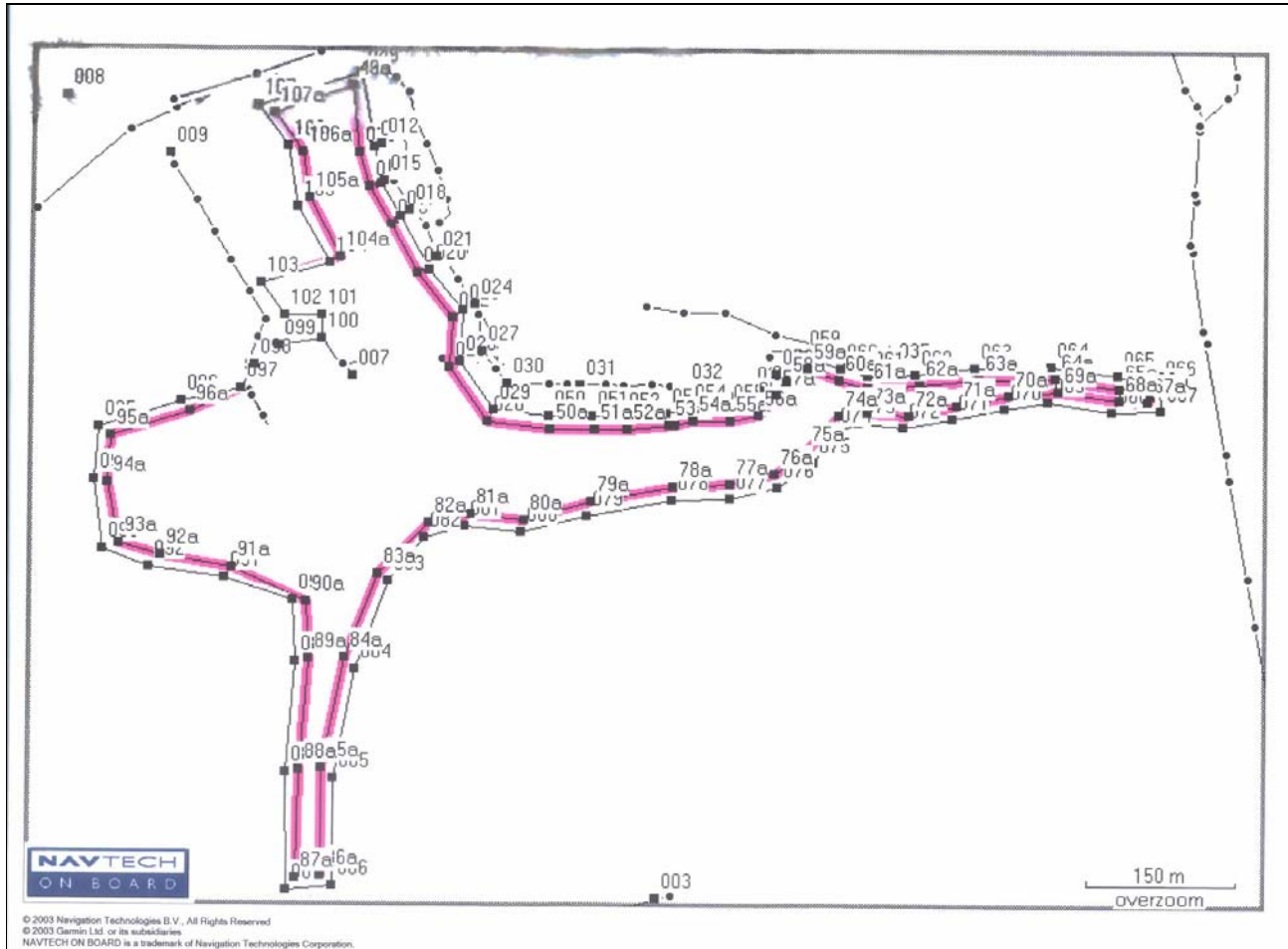


Figure F-2. Location of global positioning system data points on TSF map.

Appendix
